FACULTY OF INFORMATION TECHNOLOGY AND ELECTRICAL ENGINEERING

DEGREE PROGRAMME IN ELECTRONICS AND COMMUNICATIONS ENGINEERING

MASTER'S THESIS

UWB implementation and utilization in mPOS device

Author	Niko Juopperi
Supervisor	Marko E. Leinonen
Second Examiner	Tuomo Hänninen
Technical Advisor	Sami Kolanen

December 2022

Juopperi N. (2022) UWB implementation and utilization in mPOS device. University of Oulu, Faculty of Information Technology and Electrical Engineering, Degree Programme in Electronics and Communications Engineering. Master's Thesis, 77 p.

ABSTRACT

This thesis investigates the possible implementation and utilization of ultra-wideband (UWB) technology in a handheld device that serves as a sales system. The basic information of UWB technology based on theory is introduced, such as history, benefits and challenges, current standards, and the most common use cases. The general requirements and the planned use cases for UWB technology are presented to narrow the scope of the thesis. The thesis covers status of the current suppliers of UWB components and reasonings of the selection of a UWB chip and antennas for this thesis. Measurements are performed with the UWB chip, the UWB antennas and the entire UWB system implementation to verify that the requirements are met, and the technology works as designed. Based on theory and measurement results, it is demonstrated that both the implementation and utilization of UWB in the handheld device with the desired characteristics can be done.

Key words: Ultra-wideband, UWB, IEEE 802.15.4z, accurate positioning, Time-of-Flight, Angle-of-Arrival, Phase-Difference-of-Arrival

Juopperi N. (2022) UWB toteutus ja hyödyntäminen mPOS-laitteessa. Oulun yliopisto, tieto- ja sähkötekniikan tiedekunta, elektroniikan ja tietoliikennetekniikan tutkinto-ohjelma. Diplomityö, 77 s.

TIIVISTELMÄ

Tässä työssä tutkitaan ultra-wideband (UWB) teknologian mahdollista toteutusta ja hyödyntämistä kannettavassa laitteessa, joka toimii myyntijärjestelmänä. Esitellään UWB teknologian perustiedot teorian pohjalta, kuten historia, hyödyt ja haasteet, nykyiset standardit ja yleisimmät käyttötapaukset. Työn laajuuden kaventamiseksi esitellään yleiset vaatimukset ja suunnitellut käyttötapaukset, joissa UWB teknologiaa tullaan käyttämään. Työssä käsitellään UWB-komponenttien nykyisten toimittajien tilannetta ja perusteita UWB-sirun ja antennien valinnalle tätä työtä varten. Mittaukset suoritetaan UWB-sirulle, UWB antenneille ja koko UWB järjestelmän toteutukselle, jotta varmistetaan vaatimusten täyttyminen ja teknologian toimivuus suunnitellusti. Teorian ja mittaustulosten perusteella voidaan osoittaa, että UWB:n toteutus ja hyödyntäminen kannettavassa laitteessa halutuilla ominaisuuksilla on mahdollista.

Avainsanat: Ultra-laajakaista, UWB, IEEE 802.15.4z, tarkka paikantaminen, lentoaika, saapumiskulma, saapumisen vaihe-ero

TABLE OF CONTENTS

FOREWORD

This master's thesis was done for Aava Mobile Oy at the Oulu office, and it explains the current situation of UWB technology in terms of standard and component supply, as well as the possibility of using the technology in the desired application. I would like to thank Aava Mobile for this opportunity and the interesting topic they offered for the thesis. Special thanks to my supervisor Sami Kolanen from Aava Mobile, whose advice and knowledge of RF technology have been helpful during my thesis. Many thanks to Hannu Heiskanen from Aava for his help with the antenna measurement arrangements and the construction of the measurement platform. I would also like to thank all other friendly employees of Aava Mobile for the professional and pleasant working atmosphere at Aava.

I would especially like to thank my supervisor Marko Leinonen from the University of Oulu, whose expertise in UWB technology and helpfulness towards the success of my thesis have been important. And in addition, many thanks to him for allowing the antenna measurement arrangements at the radio technology laboratory of the University of Oulu, which without this would have remained unexamined. I would also like to thank Tuomo Hänninen, the second examiner of my thesis.

I would like to thank my family for their support and encouragement both during my thesis and throughout my studies. Thanks to Kuura for the grammatical advice and help with proofreading. Thanks to my girlfriend Riina for her support and understanding when sometimes the days stretched into the night while working on the thesis.

Oulu, 19 December, 2022

Niko Juopperi

LIST OF ABBREVIATIONS AND SYMBOLS

AoA	angle of arrival
API	application programming interface
BLE	Bluetooth Low Energy
BPM	burst position modulation
BPRF	base pulse repetition frequency
bps	bits per second
BPSK	binary phase shift keying
CCC	Car Connectivity Consortium
CRCE	cyclic redundancy check error
CSML	common service and management layer
DAA	detect and avoid
DRBG	deterministic random bit generator
DS	direct sequence
DSSS	direct sequence spread spectrum
DS-TWR	double-sided two-way ranging
DUT	device under test
EIRP	equivalent isotropic radiated power
ERDEV	enhanced ranging device
ETSI	European Telecommunications Standard Institute
FCC	Federal Communication Commission
FFT	fast Fourier transform
FiRa	Fine Ranging Consortium
FPC	flexible printed circuit
GPS	global positioning system
HPRF	higher pulse repetition frequency
HRP	high-rate pulse
IC	integrated circuit
IEEE	Institute of Electrical and Electronics Engineering
IoT	internet of things
IR-UWB	impulse radio ultra-wideband
ISED	Innovation, Science and Economic Development
LDC	low duty cycle
LLC	logical link control
LOS	line-of-sight
LRP	low-rate pulse
MAC	medium access control
MB-OFDM	multi-band orthogonal frequency-division multiplexing
MIC	Ministry of Internal Affairs and Communications
MIIT	Ministry of Industry and Information Technology
mPOS	mobile point-of-sale
NFC	near-field communication
NLOS	non-line-of-sight
NRMSE	normal root mean square error
OOB	out-of-band
OSI	open system interconnection
OWR	one-way ranging

PCB	printed circuit board
PCS	personal communication service
PDoA	phase difference of arrival
PHR	PHY header
PHY	physical layer
POS	point-of-sale
PRF	pulse repetition frequency
PSD	power spectral density
QPSK	quadrature phase-shift keying
RF	radio frequency
RFID	radio frequency identification
RSE	Reed-Solomon error
RSSI	received signal strength indicator
RTLS	real-time location system
RX	receive
SECDEC	single error correction double error detect
SFD	start-of-frame delimiter
SNR	signal-to-noise ratio
SRC	secure remote commerce
SS-TWR	single-sided two-way ranging
STS	scrambled timestamp sequence
SYNC	synchronization
TDoA	time-difference-of-arrival
ToF	time-of-flight
TR	temporal resolution
TWR	two-way ranging
TX	transmit
UCI	UWB command interface
UWB	ultra-wideband
VR	virtual reality
WPAN	wireless personal area network

B	bandwidth
B_f	fractional bandwidth
C	channel capacity
c	speed of light
d	distance/separation
f	frequency
f_c	center frequency
f_H	highest cut-off frequency
f_L	lowest cut-off frequency
g_0^n	position of the burst of pulses
g_1^n	polarity of the burst of pulses
G_r	gain of the receiving antenna
G_t	gain of the transmitting antenna
N_{burst}	number of bursts per symbol
$p(t)$	pulse shape
P_r	power at the receiving antenna

P_t	power of the transmitting antenna
$r(t)$	root-raised-cosine pulse
T_{BPM}	duration of the BPM sequence
T_{burst}	duration of the burst
T_{dsym}	symbol duration
T_p	duration of the pulse
T_{prop}	estimate of time-of-flight
T_{reply}	duration of the reply
T_{round}	duration of the round
T_w	duration of the main lobe width
α	angle of arrival to the antenna A
β	angle of arrival to the antenna B
λ	wavelength
$\Delta\varphi$	phase difference

1 INTRODUCTION

The need for wireless networks and their rapid technological growth can be seen in our everyday life. Mobile phones, computers and other portable devices allow us to share and receive information wherever we are in the world. This communication between devices is based on well-known wireless networks such as 4G, 5G, Wi-Fi and Bluetooth. However, there is a need to offer consumers increasingly faster, larger capacity and more secure ways to transfer information, and therefore new technologies are being researched. The challenge with new radio technologies is, among other things, finding a space in a narrow and precisely defined radio band where it could operate without interfering with already existing technologies. [1]

Ultra-wideband (UWB) technology offers a promising solution for this because it enables operation with radio frequencies on top of existing radio systems. This coexistence also brings the benefit of avoiding the expensive license fees that must be paid for other radio services [1]. The growing interest in UWB technology, especially location-based services, can be seen in the increase of new UWB devices and the availability of the technology such as chips and antennas. Many well-known phone manufacturers have already adopted UWB technology in their devices and increasing number of other fields of technology have also noticed the unique features offered by UWB.

In this thesis, the characteristics, history, benefits, and possible challenges of UWB from a theoretical point of view are introduced. Then, the review of the most important requirements and standards regarding the use of UWB are done, as well as a brief comparison with other technologies and alternative use cases. After that, the project, which utilizes and implements the UWB technology into a handheld device based on the selected use cases, is presented. In addition, the availability of UWB components is covered, and a suitable UWB chip and antennas are studied for the project. Finally, the verification measurements are performed for the UWB device with the selected antennas and for the entire UWB system implementation. The measurement results are studied and analysed and based on those, improvements and challenges of the implementation are discussed.

2 THE BASICS OF UWB

In this section, the basics, history, possible advantages and challenges, regulations and standards, the most common use cases, comparisons with other technologies and future trends of ultra-wideband technology are presented.

2.1 History and Concept of UWB

Ultra-wideband radio communication is not a new invention: it has been around for over hundred years. Over time, it has been used in many different ways, developing into its current form as a location-enabling technology. In the beginning, UWB was used to carry telegraph signals over long distances. It was first used by Italian inventor Guglielmo Marconi in 1901 to transmit the Morse code across the Atlantic Ocean using spark gap radio transmitter [1]. As we know, early telecommunications were based on Morse code to send information in the form of short and long bursts of electrical current.

However, the advantage of a large bandwidth and the ability of implement multi-user systems were not yet understood. The U.S. Military adopted UWB technology in the 1960s for high-security communications and impulse radars. Because of this, from the 1960s to the 1990s, the UWB applications were strictly limited to military use only. During that time, the development of UWB achieved at least a few patents, such as the UWB ground penetrating radar, designed by scientist Morey in 1974. In the 1990s, Robert Scholtz and Moe Win demonstrated the superiority of UWB in a multipath environment and laid the foundation for wireless UWB networks [2]. [1]

At the turn of the 1990s and 2000s, interest in UWB increased and developers demanded approval of UWB for commercial use from the U.S. Federal Communication Commission (FCC). In February 2002, the FCC approved the First Report and Order for commercial use of UWB technology within strict power emission limits [1]. This allowed unlicensed use of the UWB systems in radar, public safety, and data communication applications. Many different parties also wanted the technology for themselves when the awareness and possibilities of using UWB began to spread. The strict rules of allowed frequencies, power limits and disagreements between parties delayed the standardization of the UWB technology. Today, the term UWB often refers to Impulse Radio Ultra-Wideband (IR-UWB), i.e., a system that uses short pulses and high bandwidth, close to or greater than 500 MHz, to communicate [2]. In recent years, UWB systems have also received a lot of attention when large companies such as Apple, Samsung, Google, Audi, and BMW have added the technology to their products [3][4].

According to the FCC, the UWB signals must have a fractional bandwidth larger than 20% at all times of the transmission. The fractional bandwidth B_f is a factor used to define signals as: narrowband (B_f < 1%), wideband (1% < B_f < 20%) or ultra-wideband (B_f > 20%). As shown in equation (1), its defined by the ratio of bandwidth at -10 dB points to center frequency f_c.

$$B_f = \frac{B}{f_c} \times 100\% = \frac{f_H - f_L}{(f_H + f_L)/2} \times 100\% = \frac{2(f_H - f_L)}{f_H + f_L} \times 100\%, \quad (1)$$

where f_H is the highest cut-off frequency at the -10 dB and f_L is the lowest cut-off frequency at the -10 dB point. [1]

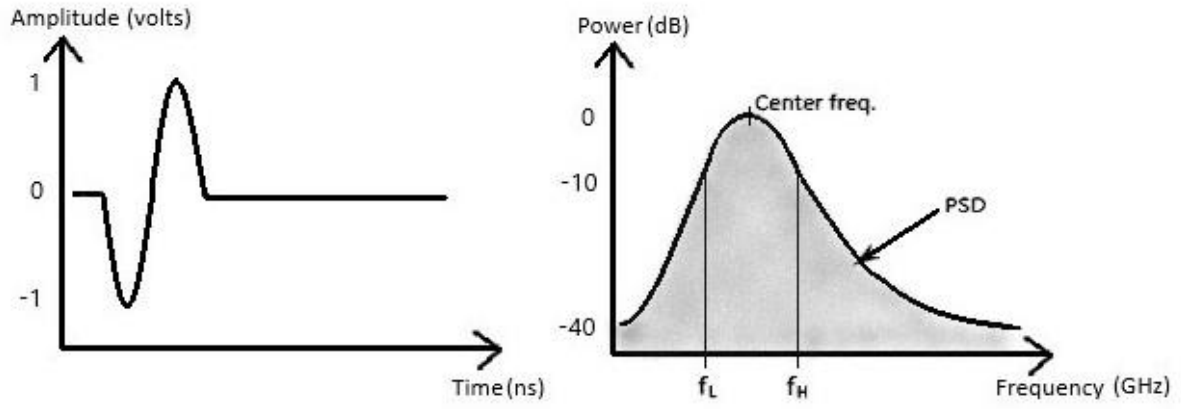

Figure 1. Illustration of a UWB pulse in the time domain on the left and in the frequency domain on the right based on [1].

An example of a UWB pulse is shown in Figure 1, short pulses in range of nano or picoseconds forms large bandwidths in the frequency domain. The duration of the pulse determines the bandwidth, and the shape of the pulse can be used to determine the lowest and highest cut-off frequencies at -10dB points, which determines the center frequency.

The UWB communications works very differently from other traditional carrier wave-based techniques. Rather than using a continuous waveform signal on a specific carrier frequency, UWB uses extremely short-duration time domain pulses to transmit and receive information. Continuous waveform radio frequency (RF)-signals are more vulnerable to detection and jamming due to their continuous nature, and the well-defined signal concentrates the energy to narrow frequency band. An example of a narrowband signal in the time and frequency domains is illustrated in Figure 2. [1]

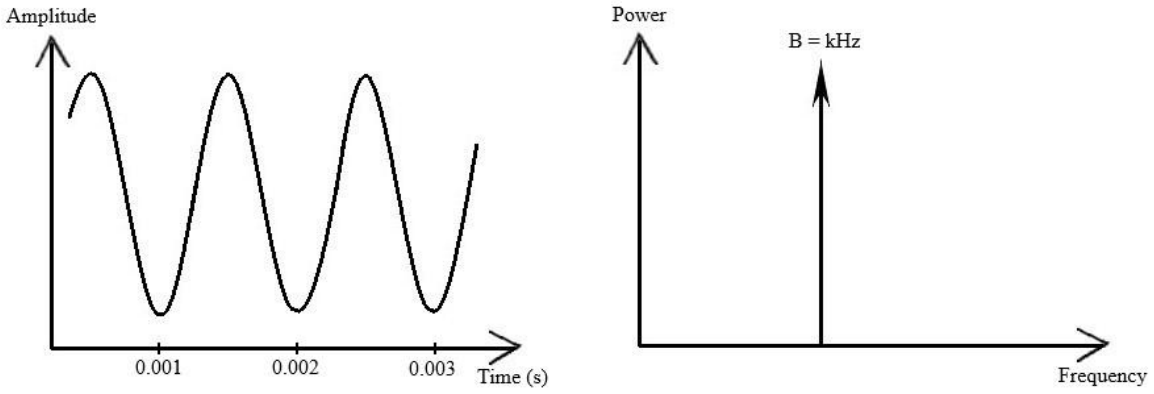

Figure 2. Example of narrowband signal in the time and frequency domain. [1]

These short-duration time domain pulses also have a very low duty cycle for transmission and reception of the information. A simple definition of the duty cycle is the ratio of the time that the pulse is present to the total transmission time. In the UWB systems a low duty cycle, usually less than 0.5%, offers an exceptionally low average transmission power, which is also an important advantage. This can offer a long battery life for handheld devices even if the peak or instantaneous power of the individual UWB pulses can be relatively large. The short-duration pulses spreads RF energy across a wide range of frequencies with low power spectral density (PSD), as illustrated in Figure 1. [1]

2.2 Advantages and Benefits

The UWB technology offers several advantages and benefits due to its wide bandwidth and short pulses. The UWB technology can coexist with other wireless technologies on top of each other due to transmission (TX) power spectrum density level. The maximum allowed transmission PSD for UWB systems is limited to -41.3 dBm/MHz, i.e., 75 nW/MHz by regulators such as the FCC. Tight emission restrictions of TX power ensure that UWB signals do not significantly rise over the background thermal noise level known as the thermal noise floor. This enables UWB systems to coexist with current RF technologies without or with minimal interference. And as already mentioned earlier, this coexistence brings another benefit, namely the avoidance of expensive spectrum license fees. The UWB operates higher frequencies than the busy licence free 2.4 GHz band. Figure 3 illustrates the idea of coexistence of UWB transmission in US with other wireless technologies, such as Wi-Fi 6, Wi-Fi 6E 802.11ax, Bluetooth, ZigBee 802.15.4, Citizens Broadband Radio Service (CBRS) and Personal Communications Service (PCS) aka GSM1900. [1]

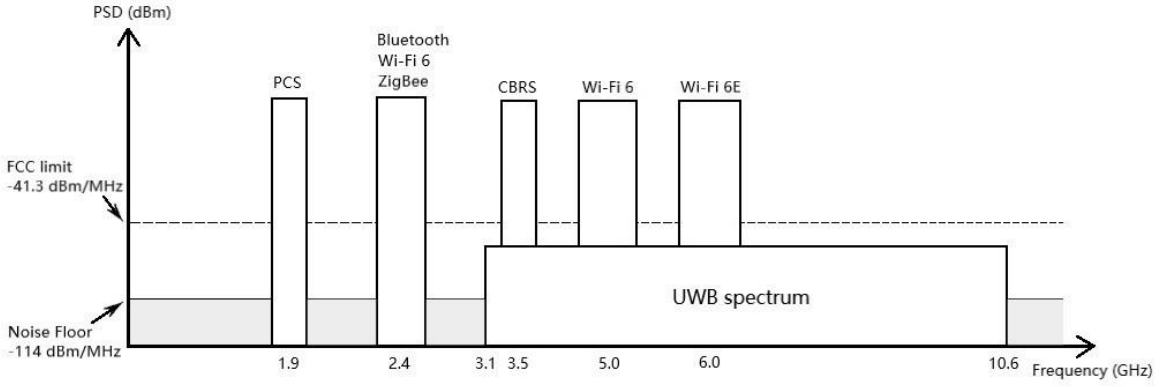

Figure 3. Coexistence of UWB with other wireless technologies in US. [5][6]

The wide bandwidth offered by UWB pulses brings another important advantage: a high channel capacity. The channel capacity is the maximum data transfer rate that the channel can transmit in bits per second (bps). However, it should be noted that the value is only a rough estimate, because the definition does not consider the quality of communication, but only the total amount of data transferred. The Shannon-Hartley theorem can be used to demonstrate high data transfer rate of UWB system:

$$C = B \log_2(1 + SNR), \tag{2}$$

where C is the channel capacity in bits per second, B is the bandwidth and SNR is the signal to noise ratio. The equation (2) shows that the channel capacity increases linearly as the bandwidth increases. The high data rate is, however, limited to short distances due to the FCC's strict TX power requirement. This allows UWB systems to be used in areas where high data rates over short distances are desired, such as wireless personal area networks (WPANs) for streaming high-quality video, for example. The trade-off between distance and data rate makes UWB technology an interesting alternative for many high data rate use cases, as well. [1]

Another aspect of the Hartley-Shannon theorem is that the signal-to-noise ratio affects the channel capacity on logarithm manner. Therefore, it can be assumed that due to the large bandwidth, UWB systems can operate even under demanding conditions with low SNRs and still produce high channel capacity. [1]

The UWB systems have a low average transmission power, which gives them inherent protection against detection and interception. In addition, the extremely short UWB pulses are time-modulated with unique codes for each pair of devices, and it is almost impossible to detect these nano-picosecond pulses without knowing the exact arrival time of signal, which improves communication security significantly. [1]

Unlike many other communication technologies, UWB is also resistant to relay attacks. In a relay attack, an attacker intercepts communication between two host equipment, and then forwards it to another device without viewing or manipulating it. For example, a thief can capture a radio signal from a vehicle's key fob, and transmit it to an accomplice, who could use it to open the vehicle's doors. This has led to numerous thefts of vehicles with keyless entry and keyless start. With additional security layer introduced in the IEEE 802.15.4z standard, and especially the Time-of-Flight (ToF) measurements, the UWB systems can detect the difference between the actual distance and time-of-flight, and thus prevent the theft. [7][8]

The UWB technology is reliable and resistant for multipath environments, because the UWB pulses are easily identifiable and distinguishable. The UWB signals are quite immune to intentional and unintentional jamming due to the wide frequency spectrum. Compared to narrowband technologies that have specific operational frequencies, the UWB can cover or operate a wide range of frequencies if certain frequencies are jammed. The multipath is a radio communication propagation phenomenon, which results in the signals arriving at the receiving antenna via several paths. It is caused by the diffraction and reflections of the transmitted signal from different surfaces, such as walls or people, and can cause signal interference and phase shifting. Multipath fading causes delays and distortions when the signal from indirect paths, called non-line-of-sight (NLOS), interferes with the required signal, called line-of-sight (LOS), in both amplitude and phase. [1]

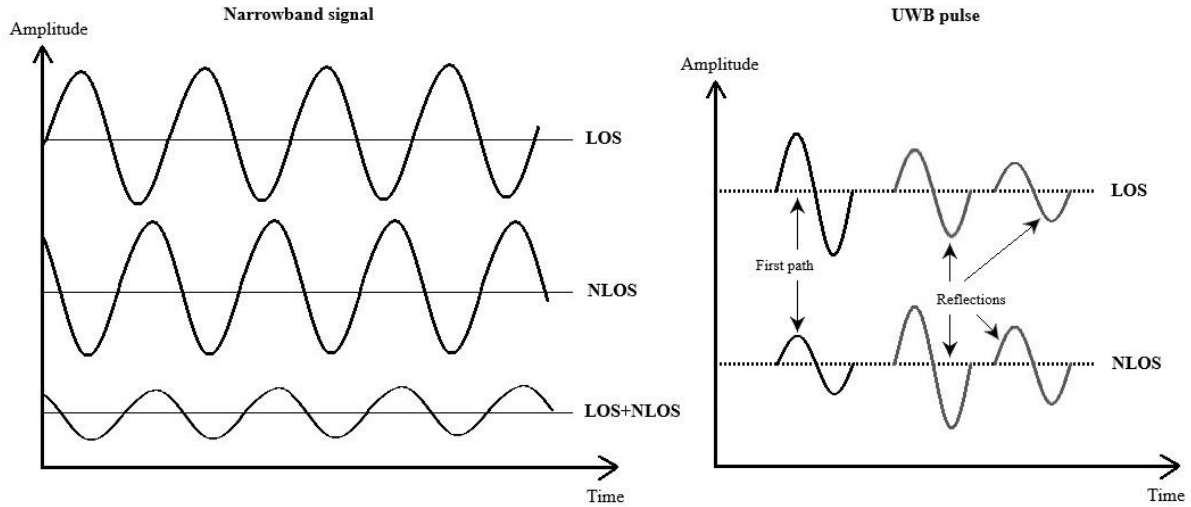

Figure 4. The multipath effects in radio communication, on the left a narrowband signal and on the right a UWB pulse. [1][2]

Figure 4 shows the effects of multipath on both the narrowband signal and the UWB pulse. It can be noted that narrowband signals can be attenuated a lot due to the sum of continuous

LOS and NLOS waveforms and make the RF-signal so weak that it cannot be received sufficiently. Short time-duration UWB pulses, on the other hand, are less sensitive to these multipath effects. The reflected pulses have a very short time frame to combine with the first path pulse and thus cause signal degradation. The incoming pulses can also be separated and filtered, but a high dynamic range is required from the receiver to identify the correct first path. This is important so that reliable ranging data can be collected, because in the NLOS situations the first path is not necessarily the strongest signal [2]. [1]

Due to the large bandwidth, UWB pulses are only nanoseconds long, so they offer remarkably high precision. Instead of relying on incoming signal strength, UWB uses techniques such as Time-of-Flight, Two-Way Ranging (TWR) and Time-Difference-of-Arrival (TDoA) to determine the distance to another device. The high temporal resolution (TR) allows much more precise timing and with these techniques, the receiver can accurately measure the time of the incoming signal and thus calculate the exact distance at the centimeter level. By adding two antennas, the UWB device can also calculate the angle of the incoming signal, this is called Angle of Arrival (AoA) technique. It is possible to obtain AoA using several different methods, such as calculating the ToF difference of the received signal in the two antennas, comparing the TDoA of the same frame in the two antennas or the Phase Difference of Arrival (PDoA) of the received signal in the two antennas. Combining a precise angle with a precise distance means that it is possible to pinpoint the exact location of the device. Figure 5 illustrates the differences in ranging and positioning accuracy when comparing Received Signal Strength Indicator (RSSI) technique used by Bluetooth to ToF and AoA techniques used by UWB. It can be noted that ToF is by far more accurate for ranging than the currently widely used RSSI technique, without forgetting the precise positioning allowed by AoA technique. [3][6][7]

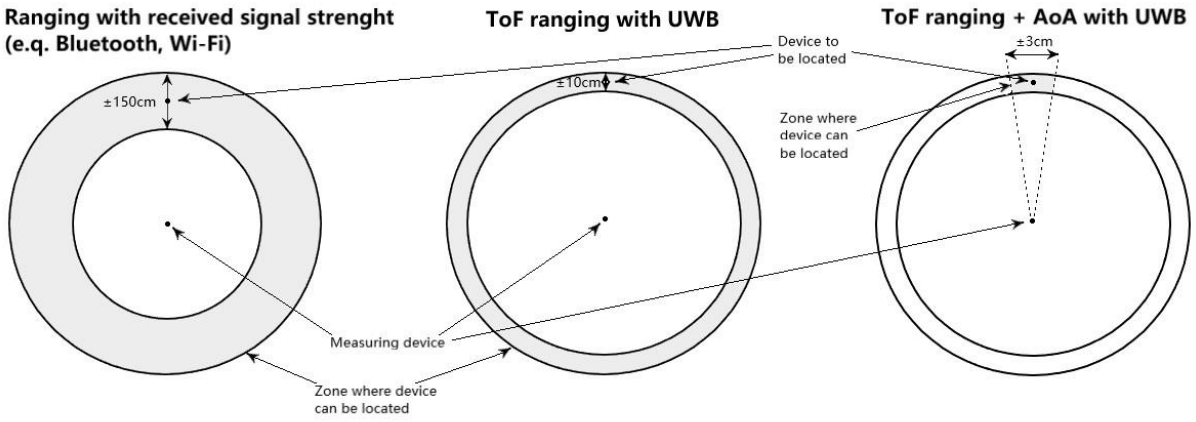

Figure 5. Examples of ranging/positioning accuracies using different techniques. [7]

Finally, since UWB uses carrierless transmission, it does not need data modulation, unlike narrowband technologies where a continuous waveform operates at a specific carrier frequency. The advantage of transmitting without a carrier frequency is that neither transmitters nor receivers need mixers or local oscillators to generate a carrier wave. Because of this, the architecture of the UWB transceiver is simpler and requires fewer RF components, which means a cheaper and less power consuming implementation. A power amplifier, which is the most power-consuming part of an RF transmitter, is not needed to transmit low-power UWB pulses either. [1]

2.3 Challenges

Since the UWB technology for location purposes is still under development, there are possible compatibility problems between device manufacturers [3], and these challenges are addressed by the chip manufacturers and the institutes driving the UWB technology.

The correct pulse shape is essential for accurate operation. The transmission characteristics of weak and low-power UWB pulses are more difficult to implement than those of continuous narrowband sine waves. It is possible for the pulse shape to be significantly distorted during transmission, thus affecting to the radio performance. The received signal power attenuates in free space according to well-known Friis transmission equation:

$$P_r = P_t G_r G_t \left(\frac{c}{4\pi d f}\right)^2, \tag{3}$$

where P_r is received signal power, P_t is transmitted signal power, G_r is antenna gain of the receiver, G_t is antenna gain of the transmitter, c is speed of light, d is the distance between the receiver and the transmitter, and f is the frequency of the signal. [1]

It can be seen from the equation (3) that as the frequency increases, the power of the received signal decreases quadratically. Due to the wide frequency range of UWB, the reception power can change a lot and thus distort the pulse shape [1]. Even slight differences in pulse width can lead to an error of dozens of centimeters in the ranging accuracy due to the very fast pulses, and this is critical, as centimeter-level accuracy is expected from UWB technology. The pulse shape can differ slightly between UWB chip manufacturers, even though the same standardized pulse shape restrictions are used, which can cause a decrease in accuracy. However, adjusting the signal timing delay parameters, this challenge can be avoided in the state-of-the-art UWB ranging systems. [3]

Synchronization and accurate channel estimation are critical for successful operation in a UWB system [1]. Since timing error even of a nanosecond significantly affects the accuracy of the result, the synchronization must be very precise. Time synchronization in wireless communication usually depends on the correlation of the template signal and the received signal. In order to define the shape of the template signal, it is necessary to know in advance some of the channel parameters. When using a system of several UWB tags, for example with the TDoA method, it is important that everyone is synchronized with each other so that the result is accurate. However, there are several different techniques that can also be used to solve these challenges, such as TWR, which eliminates the need for synchronization between two UWB devices [2].

In addition, possible interference towards new radio technologies must be considered. Now, UWB has been allowed to operate at the frequency band defined by the FCC and other regulatory bodies. However, this does not mean that new technologies cannot appear in the frequency band used by UWB. With the IEEE 802.11ax standard, in addition to the already commonly used 2.4 GHz and 5.0 GHz, Wi-Fi 6E was granted a much wider 6 GHz band (5.925–7.125 GHz in the US). The research shows that strong Wi-Fi 6E interference decreases the performance of the UWB device, but the research also shows that by changing some of the UWB configurations, the effects of Wi-Fi traffic can be mitigated. Interference can be avoided with Wi-Fi 6E by moving operation to the higher UWB channels like 8 or 9 as well. [9][10]

2.4 Regulations

As already mentioned earlier, the first regulations regarding the use of UWB were announced by the FCC in 2002. It specified the guidelines that the bandwidth of the UWB signal should be greater than or close to 500 MHz. The power spectral density for indoor use was limited to -41.3 dBm/MHz, and it was assigned to the regulated unlicensed frequency band from 3.1 GHz to 10.6 GHz in US.

The commissions and associations in other geographical regions have defined the regulation of UWB use based on FCC guidelines. Since UWB signals mainly overlap with the licensed frequency spectrum, it is important to ensure that the device operates according to the regulations of that specific country. Figure 6 shows the power limits in the United States, Europe and Japan expressed as the maximum mean equivalent isotropic radiated power (EIRP) level and that emission limits vary between these countries.

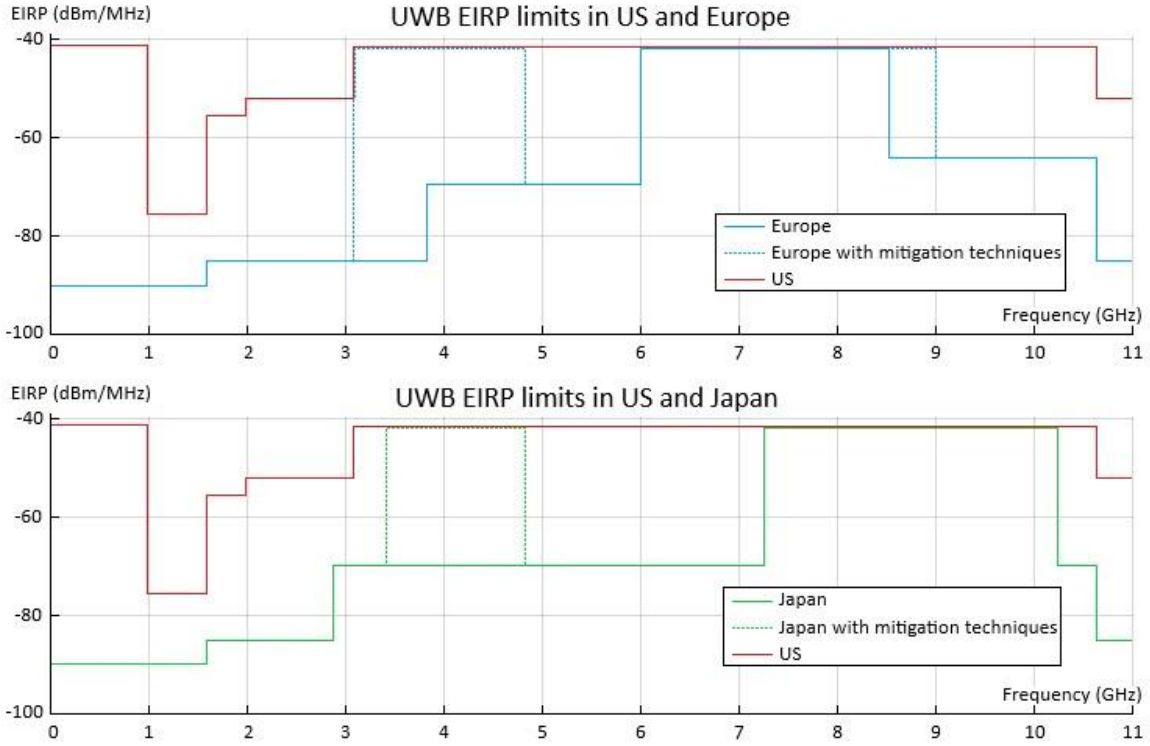

Figure 6. EIRP limits of US, Europe and Japan for UWB transmission. [11]

In Europe, the FCC regulations were followed, but with stricter requirements. The European Telecommunications Standard Institute (ETSI) classified two operational RF bands for UWB instead of one: the lower band covers frequencies from 3.1 to 4.8 GHz and the upper band from 6.0 to 9.0 GHz. At the lower EU UWB band and between 8.5 to 9.0 GHz, the system should use Detect and Avoid (DAA) mitigation technique [12]. DAA means that the UWB device must first examine the band used for transmission and ensure that no other signals are present. If other transmissions are detected, the device must not operate. Another mitigation technique is called low duty cycle (LDC). In an ideal situation the UWB device is active only when transmitting or receiving data and is otherwise in sleep mode. [13]

In Japan, the Ministry of Internal Affairs and Communications (MIC) recommends the usage of two bands: 3.4 GHz to 4.8 GHz, where the use of DAA is mandatory, and 7.25 GHz to 10.25 GHz [12]. Initially the higher band was targeted for indoor use only, but due to

growing demand, the ministry also approved the band 7.25 GHz to 9.0 GHz for UWB outdoor use [14]. In addition to Japan, the ARIB STD-191 standard has been followed in South Korea, as well.

Similarly, in China, the Ministry of Industry and Information Technology (MIIT) defined the frequency band 6.0 to 9.0 GHz for the UWB. The Innovation, Science and Economic Development (ISED) in Canada had their own specifications for UWB outlined in the RSS-220 specification. It is similar to the FCC including one operational band of 4.75 to 10.6 GHz. [13]

A summary of the permitted frequency ranges for UWB usage are shown in Table 1. The table includes regulatory bodies of different continents and countries, as well as the maximum allowed mean EIRP for transmission. The common UWB frequency allocation for most regulatory bodies is from 6.0 GHz to 8.5 GHz without mitigation techniques, and with a maximum EIRP of -41.3 dBm/MHz based on information of Table 1. If the UWB allocation of 6.0 GHz to 8.5 GHz is compared to the channels defined by the IEEE 802.15.4z standard in Table 2, it can be seen that the UWB channels 5, 6, 8 and 9 fit into range globally.

Table 1. Permitted frequency range and maximum mean EIRP values by continent/country. [13]

Continent/Country	**Permitted frequency range (GHz) without mitigation techniques**	**Additionally permitted freq. ranges (GHz) with mitigation techniques**	**Max mean EIRP (dBm/MHz)**
Europe	6.0 – 8.5	3.1 – 4.8 and 8.5 – 9.0	-41.3
UAE, Qatar	6.0 – 8.5	3.1 – 4.8 and 8.5 – 9.0	-41.3
Australia	3.4 – 4.8 and 6.0 – 8.4		-41.3
China	6.0 – 9.0		-41.0
Japan	7.25 – 10.25	3.4 – 4.8	-41.3
South Korea	7.25 – 10.25	3.735 – 4.8	-41.3
New Zealand	6.0 – 8.5	2.7 – 4.8	-41.3
Singapore	4.2 – 4.8 and 6.0 – 8.5	3.4 – 4.2	-41.3
Canada	4.75 – 10.6		-41.3
USA	3.1 – 10.6		-41.3
Brazil	3.1 – 10.6		-41.3

2.5 Standards

When UWB was approved for commercial use in 2002, it was designed to be used as a high-speed data transmission technology over short distance. Although at the time UWB was an excellent alternative to IEEE 802.15.3 wireless personal area networks (WPANs) thanks to its unique features, it was never released due to disagreements between two alliances [15]. UWB technology was divided into two branches, single-band technique supported by the UWB Forum, and multi-band technique supported by the WiMedia Alliance.

The single-band proposal was direct-sequence UWB (DS-UWB), which uses short pulses and time domain signal processing combined with the direct sequence spread spectrum (DSSS) technique to transmit and receive information. The multi-band orthogonal frequency-division multiplexing (MB-OFDM), on the other hand, divided the available 7.5 GHz band into smaller sub bands, each with a bandwidth of 500 MHz, to meet the FCC's requirements of a UWB signal. Both techniques received support from the technology industry, but the

marketing of UWB was problematic due to conflicts and incompatibilities between these two techniques. [1]

The year 2006 can be considered the starting point of the current UWB standards, when the IEEE 802.15.4 standard defined the media access control (MAC) and four different physical layers (PHYs), three using the DSSS technique and one using the offset quadrature phase-shift keying (QPSK) technique. In 2007, UWB localization technology received its first standardization when the IEEE 802.15.4a amendment was published with an additional PHY using DS-UWB. With this standard, the PHY layer of UWB was changed from OFDM-based data communication to an impulse radio technology (IR-UWB), focusing above all on high-precision ranging and low data rate communication. [3][16]

Over the years, numerous improvements have been made to the UWB standards, with the aim of improving ranging accuracy, reducing interference, and ensuring safety. In 2015, an enhanced version of the IEEE 802.15.4 standard was introduced, and it defined two different UWB PHY modes: High-rate Pulse (HRP), which, as the name suggests, transmit pulses at a higher rate, and Low-rate Pulse (LRP), which correspondingly transmit slower but stronger pulses. The HRP was directed for ranging use and the LRP for data transfer. [3]

The enhanced IEEE 802.15.4z standard was released and the UWB PHY received improvements in the accuracy of ranging measurements in 2020, and it is the current de facto UWB standard [17]. At the same time, integrity has been improved, thus ensuring the best possible compatibility between all devices that support UWB technology.

Other organizations that provide standards for the upper layers of UWB are Omlox, Digital Key 3.0 and Apple Nearby Interaction as well as FIRa, which is covered in own chapter.

Omlox is an open standard for real-time location services (RTLS) that provides a standardized open user interface for the products from different device manufacturers, ensuring their compatibility and enabling the acquisition of location data from a wide range of location technologies such as UWB, Wi-Fi, GPS, 5G, RFID and BLE. [18]

The Car Connectivity Consortium (CCC) is an organization that includes many vehicle and phone manufacturers. CCC aims to make it possible to use the phone as a fully digital car key, with an option to share access in the application with family or friends if desired. The purpose of the Digital Key Release 3.0 open standard is to enable secure hands-free operation and location-aware keyless access using UWB technology. [19]

Apple Nearby Interaction is a framework that allows one to locate and interact with nearby devices that contain Apple's U1 chip. Apple has also shared some resources and details for other accessory manufacturers looking to add Apple Nearby Interaction to their UWB-enabled hardware. [20]

An IEEE 802.15.4ab task group has been established in 2022 for the next-generation UWB development. It aims to further enhance the UWB PHY layers, MAC sublayer and ranging techniques, while maintaining backward compatibility with the IEEE 802.15.4z standard. Other areas of development include, among other things, additional channels and operating frequencies, interference mitigation techniques for higher traffic use cases, definitions for hybrid operation using narrowband signalling to assist UWB, improved native discovery and connection setup mechanisms. The purpose is also to create protocols that support peer-to-peer and peer-to-multi-peer operation. In addition, this amendment contains safeguards, so low duty-cycle use cases for ranging do not face too much interference from high throughput use cases for data transmission. [21]

For the future of UWB, it is important that all technology manufacturers and suppliers adhere to the same regulations and standards in order to achieve comprehensive and universal compatibility the way Wi-Fi and Bluetooth have done.

2.5.1 IEEE 802.15.4z

The IEEE 802.15.4z standard is currently the main standard on which most chip and device manufacturers base their products and development. In addition to the update, the standard maintains full compatibility with the previous IEEE 802.15.4 standard. One of the main goals in the IEEE 802.15.4z standard was to improve ranging accuracy, and that requires reliable and robust timestamps since all ranging measurements are based on the signal's time-of-flight. For this, reliable detection of the first path is important, which in addition to ToF accuracy affects security, and thus possible false transmissions containing a delay can be identified. New methods have been introduced in the IEEE 802.15.4z standard to guarantee security of wireless transmissions. Security did not play a significant role in the earlier IEEE 802.15.4 standards for UWB, as the technology was new and thought to be difficult to detect and distinguish from noise anyway due to low transmission power. However, as UWB has started to be adopted in many different fields of technology, such as the vehicle and mobile industry, security has become an increasingly important matter. [3]

Like mentioned earlier, the IEEE standards include two modes for the UWB PHY: High-Rate Pulse and Low-Rate Pulse. Improvements in the IEEE 802.15.4z standard have been made mainly to the HRP UWB PHY, which is the more commonly used mode for localization due to the previous IEEE 802.15.4 standard, which defined the HRP for ranging operation [3]. Support for ranging features has also been added to the LRP UWB PHY in this standard, but not nearly as comprehensively as for the HRP UWB PHY. Therefore, only the HRP UWB PHY requirements for channels, pulse shape, frame structure, coding, modulation, and the methods provided by this standard for ranging, will be discussed. [17][22]

2.5.1.1 Channel

The IEEE 802.15.4z standard defines 16 channels for the HRP UWB PHY, each with its own center frequency and maximum bandwidth. Two UWB devices must operate using the same UWB channel to establish a connection. Although the standard defines several UWB channels, it is not mandatory to support all of them. The requirement is that channel 3 is the mandatory channel for the low-band operation, and channel 9 is mandatory for the high-band operation [17]. Table 2 presents 16 different UWB channels, and it can be observed that the same center frequency with a different bandwidth has been defined for some of these channels.

Table 2. Allocation of the HRP UWB PHY channels. [22]

Channel number	**Center freq. (MHz)**	**Bandwidth (MHz)**	**Channel number**	**Center freq. (MHz)**	**Bandwidth (MHz)**
0	499.2	499.2	8	7448.0	499.2
1	3494.4	499.2	9	7987.2	499.2
2	3993.6	499.2	10	8486.4	499.2
3	4992.8	499.2	11	7987.2	1331.2
4	3993.6	1331.2	12	8985.6	499.2
5	6489.6	499.2	13	9494.8	499.2
6	6988.8	499.2	14	9984.0	499.2
7	6489.6	1081.6	15	9484.8	1354.97

2.5.1.2 Pulse shape

The pulse shape is another requirement in order to achieve the best possible ranging accuracy and interoperability between the ranging devices. In the IEEE 802.15.4z standard, the pulse shape requirements have remained the same as in the previous IEEE 802.15.4 standard. The transmitted pulse shape *p(t)* shall be limited by the shape of its cross-correlation function with the reference root-raised-cosine pulse *r(t)* with a roll-off factor of 0.45 or 0.5. The total duration of the pulse T_p and the duration of the main lobe width T_w are defined depending on the bandwidth of the UWB channel. The main lobe amplitude of the transmitted pulse *p(t)* must be greater than or equal to 0.8 of the duration T_w, and the amplitudes of all sidelobes must also be less than ±0.3. As can be seen from Table 2, most channels operate with a bandwidth of 499.2 MHz, in which case the total pulse duration T_p should be 1/499.2 MHz = 2.0 ns, and the main lobe width duration T_w should be 0.50 ns. [17]

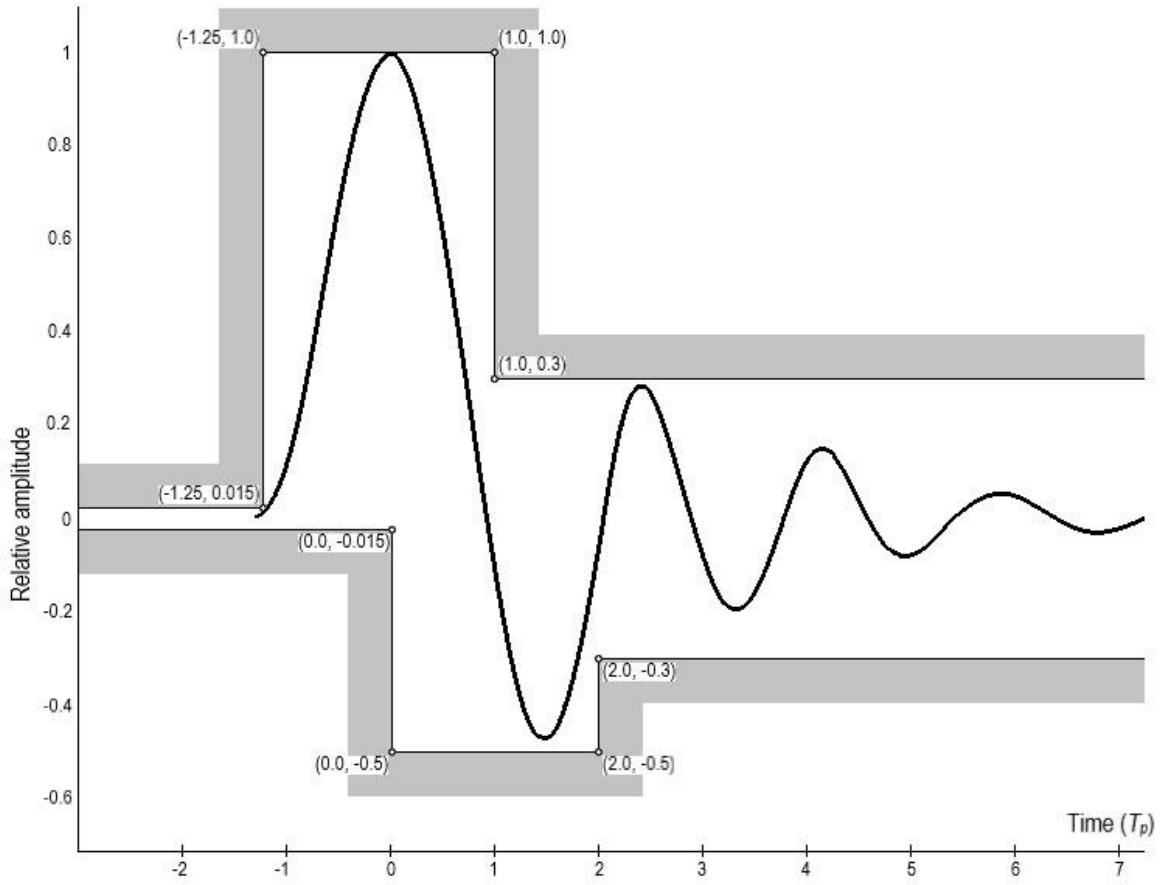

Figure 7. Example time domain mask for the IEEE 802.15.4z approved pulse. [17]

The mask of the IEEE 802.15.4z approved UWB pulse in the time domain is shown in Figure 7, where the time unit is relative to the pulse duration T_p and the peak amplitude is scaled to one [17]. It shows the limits within which the pulse must be in order to meet the requirements of the standard. These limits also meet the UWB pulse restrictions set by the FCC and other regulatory bodies.

2.5.1.3 Frame structure

The IEEE 802.15.4z standard defines four different frame structures, shown in Figure 8. The first frame is compatible with the previous standard IEEE 802.15.4 and therefore does not contain the new scrambled timestamp sequence (STS) field. In the second frame, the STS field is added between the Start-of-Frame Delimiter (SFD) field and the PHY Header (PHR) field, and in the third frame, the STS is placed after the PHY Payload field. The fourth frame, on the other hand, contains only the STS field after the SFD field, and is intended for applications where only location information is required. The standard defines support for frame structures 1, 2 and 4 as mandatory and 3 as optional. [17]

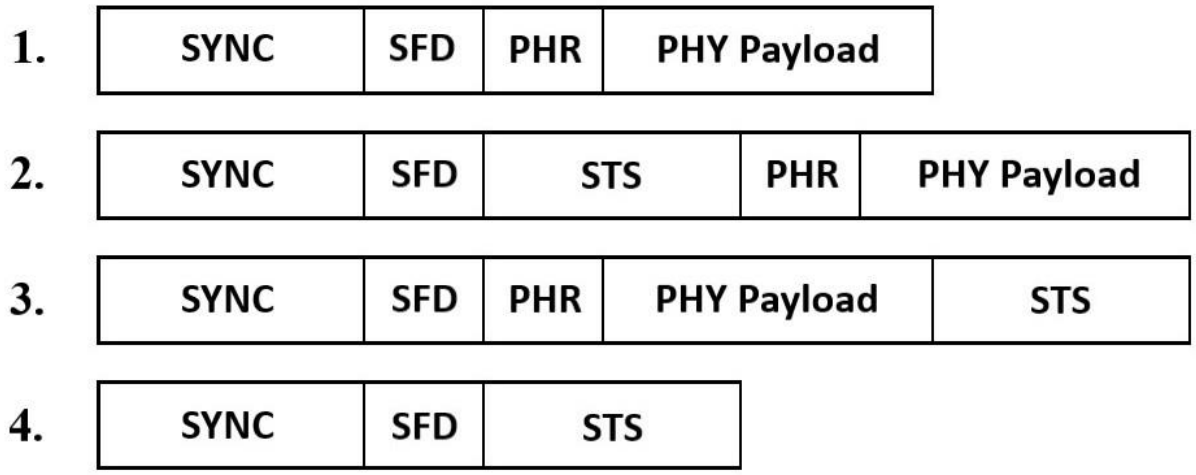

Figure 8. Four UWB PHY frame structures defined in the IEEE 802.15.4z standard. [17]

Frame structures must be the same between UWB devices for communication to be possible. The purpose of the Synchronization (SYNC) field is to synchronize the sender and receiver, and this field contains the preamble code defined in the standard. The preamble consists of a ternary code (-1,0,1) and when the receiver recognizes it, the receiver can then synchronize with the transmitter. In the ternary code, -1 represents a negative pulse, 0 represents no pulse and 1 represents a positive pulse. For several devices to work on the same channel simultaneously without interference, the channel codes are chosen in such a way that the cross-correlation factor with each other is as low as possible. According to the IEEE 802.15.4z standard, the length of the ternary codes is either 91 or 127 pulses, the latter of which is compatible with the previous IEEE 802.15.4 standard. In the UWB PHY, correlation achieves a high dynamic range and can be improved if fewer zeros are selected in the ternary code, i.e., when no pulse is sent. Therefore, these new ternary codes allow higher accuracy because more pulses are sent, but the receiver must have a high dynamic range to successfully detect the first path. The IEEE 802.15.4z standard presents 32 of predefined ternary codes of length 91 that contain less zeros, and these codes must be supported by High-Rate Pulse - Enhanced Ranging Devices (HRP-ERDEVs). If the ternary codes do not match between the sender and the receiver, communication cannot be completed. [3][17][22]

The Start-of-Frame Delimiter field defines the end of the SYNC field and the exact starting point of the PHR field. The SFD field is important for performance as it is also used for timestamping. The IEEE 802.15.4z standard defines four new sequences of length 4, 8 or 16 and 32, which is optional for the SFD, and one sequence of length 8, which is compatible with

the previous IEEE 802.15.4 standard. The new sequences are binary, so there is no situation where a pulse is not sent, which achieves better accuracy. In addition, the SFD configurations must be the same on the sender and receiver to enable communication. [3][17][22]

The PHY field contains the actual data to be transferred and it can be divided into two parts: the PHY Header (PHR), whose task is to provide the receiver with information about the incoming packet, and the PHY Payload, which contains the data [3]. The IEEE 802.15.4z standard includes the previous PHR format for the Base Pulse Repetition Frequency (BPRF) mode and a new format developed for the Higher Pulse Repetition Frequency (HPRF) mode, both of which are 19 bits in length and presented in Figure 9. [17][22]

BPRF

Bits: 0 - 1	2 - 8	9	10	11 - 12	13 - 18
Data Rate	Frame Lenght	Ranging	Reserved	Preamble Duration	SECDEC

HPRF

Bits: 0	1	2 - 11	12	13 - 18
A1	A0	PHY Payload Lenght	Ranging	SECDEC

Figure 9. PHY Header formats for BPRF and HPRF modes. [17][22]

Figure 9 shows that the PHY Payload length has been increased to 10 bits in the HPRF mode, and it is possible to use bits A1 and A0 to determine the length, thus reaching a maximum length of 12 bits. With this, sending 4096 bytes in one packet can be achieved, while with the BPRF mode the maximum is 128 bytes. However, supporting the increased payload length format is not mandatory, nor compatible with the previous standard, so the BPRF mode is only mandatory in this standard. In both, the ranging bit is used to indicate whether the frame is used for a ranging operation and the SECDEC (Single Error Correct Double Error Detect) bits are used for error detection and correction. [17]

The Scrambled Timestamp Sequence is a new field introduced in the IEEE 802.15.4z standard to improve security. In the previous standard, security was based on repeating the preamble code in the SYNC field, but since there are a limited number of possible codes, they are very vulnerable to attacks [3]. The STS, on the other hand, does not repeat itself and consists of a sequence of pseudo-randomized pulses. These sequences are generated using a Deterministic Random Bit Generator (DRBG) based on the AES-128 encryption method. Since there is no periodicity due to the pseudo-randomness and as each bit produces a pulse (0 for a positive pulse and 1 for a negative pulse), it is possible for the receiver to produce reliable and accurate channel estimates. The length of the STS can also vary, for BPRF it is mandatory to support at least one STS segment of length 64 and for HPRF it is mandatory to support one or two STS segments of length 32, 64 or 128. For the receiver to decode the STS, it must have a corresponding copy of the sequence available before reception. The receiver and the sender must therefore know the keys and the cryptographic structure for the STS, otherwise communication cannot be carried out. It can be seen from Figure 8 that the STS can be located either before or after the PHR, but always only after the SFD field. Devices conforming to the IEEE 802.15.4z standard must support the use of STS to meet security requirements against both unintentional and intentional interference. The IEEE 802.15.4z standard describes in detail how to create the STS. [3][17]

2.5.1.4 Modulation and Convolutional Encoding

The data-containing fields PHR and PHY payload need encoding and modulation before transmission. The payload is coded with a systematic Reed-Solomon block code and the last six bits of the PHR are SECDEC coded. They are then encoded together using a convolutional encoder. The IEEE 802.15.4z standard defines two half-rate convolutional encoders with K value of 3, which is compatible with the previous IEEE 802.15.4 standard and 7, which is optional. [3][17]

In UWB transmissions, bits are produced as pulse trains at the rate of pulse repetition frequency (PRF). By increasing the PRF larger dynamic range can be achieved, and therefore the IEEE 802.15.4z standard introduces two new PRFs, 128 MHz and 256 MHz, and the 64 MHz PRF of the previous IEEE 802.15.4 standard is supported as well. The operation at the lower 64 MHz PRF is called the BPRF mode, and it uses a Burst Position Modulation and Binary Phase-Shift Keying (BPM-BPSK) modulation technique introduced in the IEEE 802.15.4 standard. The operation at the higher PRFs is called the HPRF mode and the Binary Phase-Shift Keying (BPSK) modulation technique is slightly modified for it. The pulse bursts are sent in both halves of the symbol, and time hopping is not used. Likewise, the polarities of those bursts are determined by both bits g_0^n and g_1^n, according to the table presented in the IEEE 802.15.4z standard. [3][17]

Figure 10 shows a block diagram of the coding and modulation of the BPRF method, as well as the symbol structure of the HRP UWB PHY. After convolutional coding, two bits (g_0^n and g_1^n) are obtained, which are used in the BPM-BPSK modulation to form a symbol. Each symbol is divided into two halves with a duration of T_{BPM}, allowing for BPM. The first bit g_0^n determines the position of the burst of pulses (at 1st or 2nd T_{BPM} interval), the second bit g_1^n determines the polarity (+ or -) of the same burst. In addition to this, T_{BPM} is divided into two halves, a possible burst position and a guard interval, which limits interference with other transmissions and must not contain bursts. The advantage brought by time hopping in the BPRF also brings some resistance against multi-user access interference. The duration of one burst T_{burst} is the symbol duration T_{dsym} divided by the possible number of bursts per symbol N_{burst}, and a single burst must be sent in each symbol interval. [22]

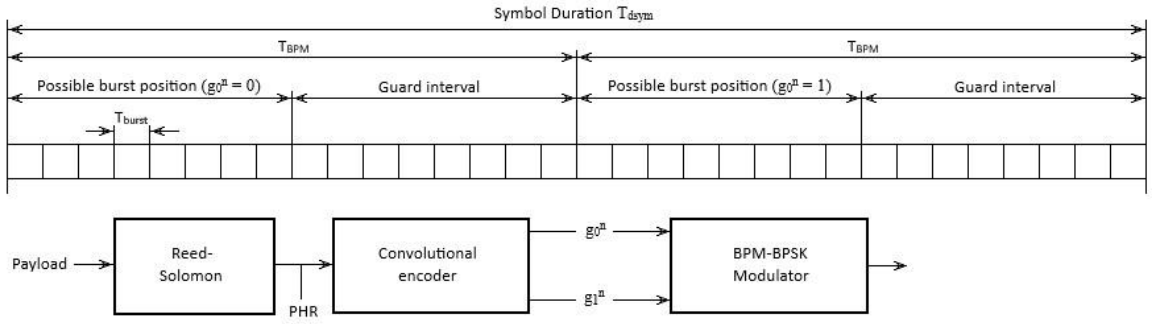

Figure 10. Symbol structure, modulation and coding process for BPRF presented in the IEEE 802.15.4 standard [22].

Those IEEE 802.15.4z standard devices that support the HPRF mode and HRP UWB PHY frame structures including the STS, are called the HRP-ERDEVs, and thus device meeting the requirements of the previous IEEE 802.15.4 standard are called the non-HRP-ERDEV. The IEEE 802.15.4z standard defines a bit rate of 6.81 Mbit/s (128MHz PRF) and 27.24 Mbit/s (256 MHz PRF) for the HPRF modes when mandatory Reed-Solomon coding is used. For the

receiver to decode the transmission and successfully start communication, it must use the same encoding scheme, modulation, PRF and bit rate as the sender. [3][17]

2.5.1.5 MAC layer

Another layer defined in the IEEE 802.15.4z standard is the media access control (MAC). The MAC layer is a sublayer that, together with the logical link control (LLC) sublayer, forms the data link layer or layer 2 in the OSI model (The Open Systems Interconnection model). Its task is to provide unique address recognition in compliance with the MAC protocols, and with the channel access control it allows the use of different UWB devices on the same UWB channel. The MAC frame resides in the UWB PHY payload frame and consists of a MAC header, MAC payload and MAC footer. The MAC Header contains information to identify the frame, such as the frame type and whether the sender has more data for the receiver. The function of the MAC footer is to report possible errors in the transmission. The specifications of the MAC frame have not changed from the previous IEEE 802.15.4 standard, so compatibility is ensured in this respect. [3][22]

2.5.1.6 Ranging and Localization methods

The IEEE 802.15.4z standard introduces three time-based techniques for ranging and localization measurements, which can be used to calculate the distance or relative position between two UWB devices. These techniques are Single-Sided Two-Way Ranging (SS-TWR), Double-Sided Two-Way Ranging (DS-TWR) and Time Difference of Arrival (TDoA). [17]

Time-of-Flight is the method used by UWB devices to measure the distance, and as the name suggests, it counts the time from when a signal is sent to when it arrives, and thus the distance can be calculated by multiplying ToF by the speed of light. The problem is that synchronization between the sender and the receiver cannot be achieved with a single message, so without a common clock it is impossible to calculate the exact distance. When only the ToF method is used for positioning with multiple UWB anchors, it is extremely important that each anchor has the common clock synchronization. [3]

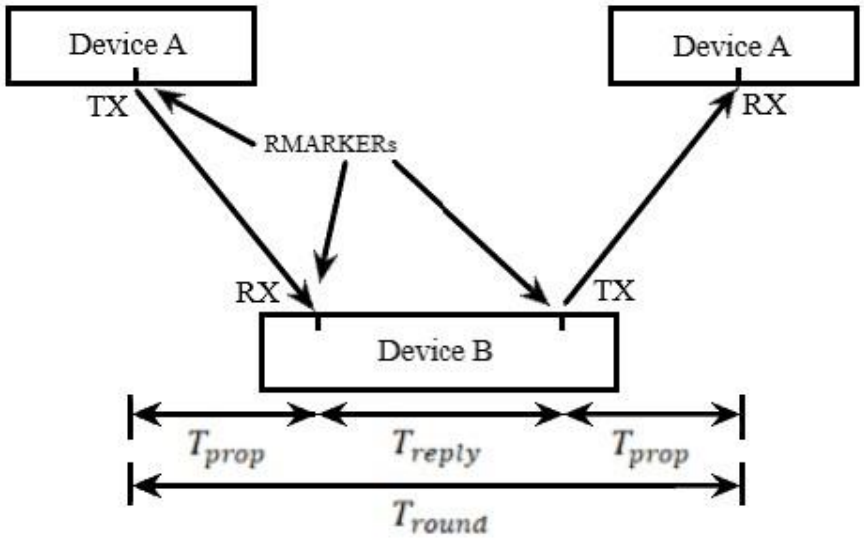

Figure 11. SS-TWR technique for ranging. [17]

SS-TWR is an improved technique that sends two messages to determine the distance and thus synchronization between devices is not required. Figure 11 shows the SS-TWR technique, where device A starts the operation and device B responds. A ranging marker (RMARKER) is a reference point in the ranging measurements, and it is always located immediately after the SFD field. Device A counts how long it takes for the message to arrive back from device B. Once the time for the entire round T_{round} and another device's respond time T_{reply}, is known, the estimate of ToF or T_{prop} can be calculated:

$$T_{prop} = {}^{1}/_{2}\left(T_{round} - T_{reply}\right). \tag{4}$$

However, if the devices are not synchronized, the error of the clock frequency offset has not been considered in the equation (4). The offset error increases as the response time grows. There are a few ways to determine T_{reply} from device B. The first option is for device A to define the duration of T_{reply} in its first message, in which case it is enough for device B to implement that duration. The second option is for device B to estimate its transmission time and include it in the return message. The third option is that device B calculates T_{reply} after answering and sends the value with an additional message. [17]

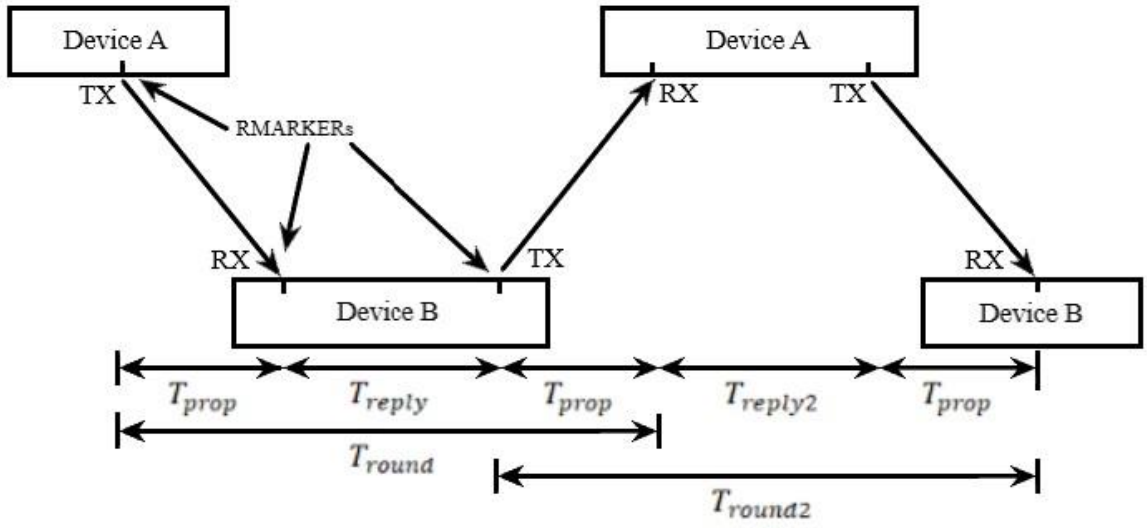

Figure 12. DS-TWR technique with three messages. [17]

The DS-TWR technique is basically two SS-TWRs executed back-to-back and can be performed with either three or four messages. Performed with four messages, device B, after the response time of the first round T_{reply1}, sends a second message and starts counting the duration of the second round T_{round2}. Figure 12 shows DS-TWR performed with three messages, where device B, after sending the response time of the first round T_{reply1}, simultaneously starts counting the duration of the second round T_{round2}. After the response time of the second round T_{reply2} is received back from device A, the estimate of ToF or T_{prop} can be calculated in device B by:

$$T_{prop} = \frac{\left(T_{round1} \times T_{round2} - T_{reply1} \times T_{reply2}\right)}{\left(T_{round1} + T_{reply1} + T_{round2} + T_{reply2}\right)}. \tag{5}$$

This is a more secure and more accurate technique than SS-TWR but consumes more power due to longer transmission time. However, the DS-TWR technique is a better option for use cases that require more reliable accuracy and security, and in this way both devices also get the ranging information. [3][17]

The TDoA method is based on One-Way Ranging (OWR) technique and is intended for anchor operation. In this method, a UWB device (for example, a mobile phone or a key fob) sends a message to several fixed anchor points located in different known locations. Due to this, the signal arrives at the anchors at various times and a hyperbola can be calculated from this time difference between the anchor pair. When there are at least three anchors, three anchor pairs can be formed, and thus, three hyperbolas can be calculated. The UWB device would be located at the intersection of these hyperbolas. Figure 13 shows the positioning methods, both TDoA using hyperbolas and the ToF-based method, where the device is located at the intersection of the ranging circles. [17]

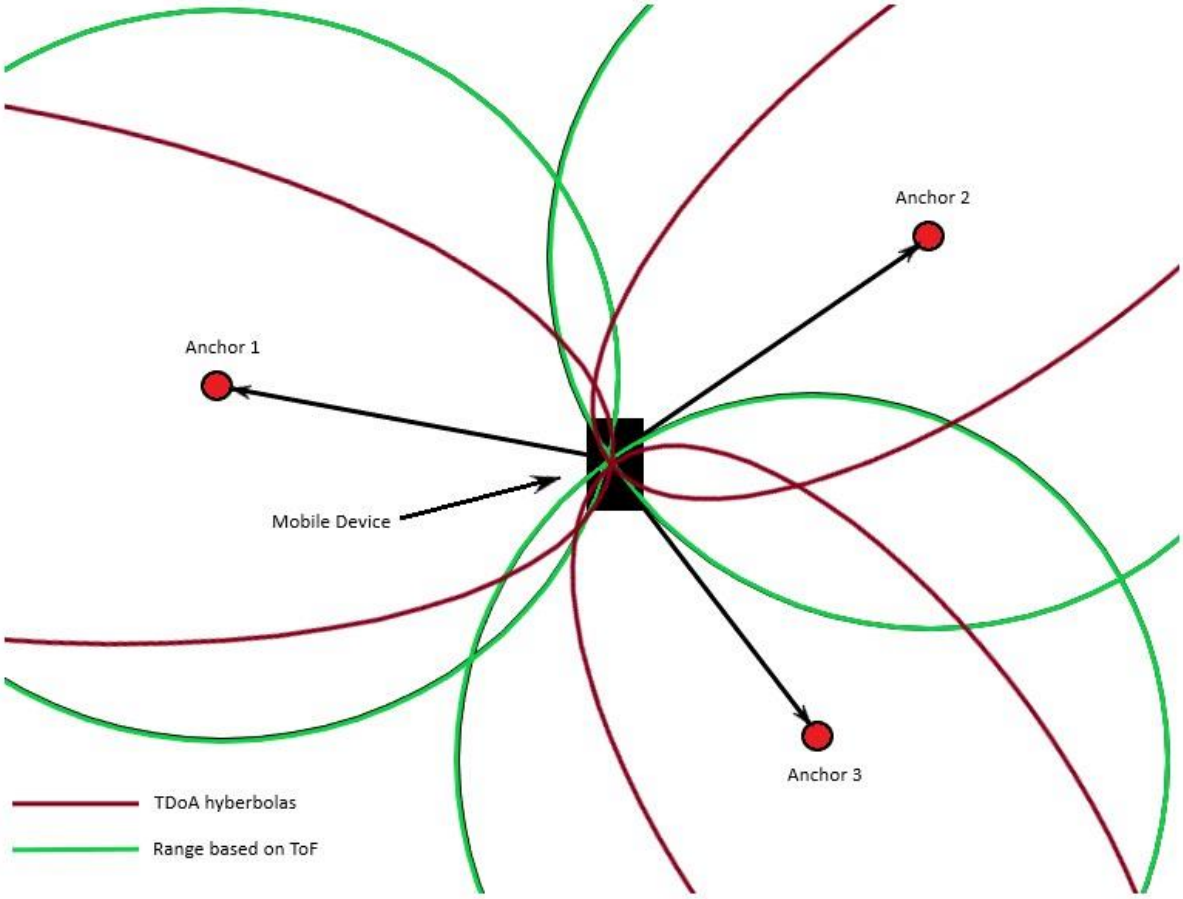

Figure 13. TDoA and ToF based methods for positioning. [23]

For accurate positioning to be successful, the anchors must be well synchronized with each other in these methods. If the device also needs to know its own location, depending on the use case, the information must be sent to the device via a separate message. For example, in the automotive industry, the key does not need to know its own location in order to open the doors; it is sufficient that the anchors installed in the vehicle track the location of the key and know when the key is near the vehicle. [3]

2.5.2 FiRa standard

The FiRa (Fine Ranging) Consortium is an organization which aims to promote the use of UWB technology and ensure the interoperability of UWB products through defined standards. The FiRa Consortium comprises more than one hundred members, such as NXP, Qorvo, Samsung, Apple, Bosch, and Google. Members include various device manufacturers, chip manufacturers, service providers, technology suppliers and testers. In 2020, FiRa published their first technical requirement specifications for the UWB PHY and MAC layers based on the IEEE 802.15.4z standard. [24]

In the same year 2020, the UWB Alliance, another organization promoting the use of UWB, began working together with FiRa to further accelerate the development and adoption of the technology [25]. The purpose of this cooperation is to share ideas and information and work towards a common goal, so that as many companies as possible support the use of UWB. They are working for possible improvements such as longer range, higher data throughput and better security, as well as desire to ensure interoperability and coexistence with UWB and other wireless technologies, without interference on the frequencies where both operate. The goal of the organizations is also to market UWB technology in general to make it well-known like other wireless technologies (BLE, Wi-Fi) and to promote UWB technology in areas where it is not yet known or allowed. [24]

FiRa announced its certification program in 2021, where compliance with the specifications is evaluated at independent authorized testing labs, and compatibility with other FiRa Certified devices is ensured. FiRa defined a common UWB command interface (UCI) for testing UWB devices, and the testing includes many different parameters, such as pulse mask verification, baseband impulse response, pulse timing verification, transmitted and received packet format verification, transmit signal quality, normalized root mean square error (NRMSE), packet reception sensitivity, first path dynamic range verification and test for dirty packet received. This testing is important to ensure that devices really are compatible and meet the regulations. [24][26][27]

In addition to the MAC and PHY layer specifications, FiRa has developed a completely new layer on top of them, the Common Service & Management Layer (CSML). This is relevant for UWB technology, because in order to establish a UWB connection between two devices, prior knowledge of the settings to be used is required. The CSML enables the operation of the FiRa compatible devices and includes the necessary mechanisms for device discovery, profile selection, the best parameter selection algorithm and establishing a UWB connection. In addition, the CSML also offers reference application programming interfaces (APIs) to support third-party application development, which can be used as a guide when developing operating system-based APIs. Unfortunately, without the FiRa membership it is not possible to learn more about these mechanisms, such as the algorithm used to select the best parameters for the UWB connection. [3][28]

Figure 14 shows the procedure that the FiRa standard presents for the device discovery, UWB connection establishment and ranging operation. First, the device discovery is performed by an out-of-band (OOB) mechanism, usually using Bluetooth low energy (BLE). The service discovery is performed to determine the services supported by the devices after the successful pairing of devices by BLE. After this, it is possible to create an alternative secure BLE connection, which can be used for the data exchange and to perform optional application data exchange. The fifth step is to exchange the UWB capabilities of the devices. This message contains information about the FiRa's PHY and MAC versions, the roles of the devices and the supported UWB parameters, such as the STS configuration support, ranging

methods and AoA support, MAC address support, PRF mode support, convolutional code length support and several other parameters. Once the capability information is exchanged, the parameters can be selected based on the algorithm developed for it, and then these selected settings can be exchanged with a message containing the UWB session ID, FiRa's PHY and MAC versions, device role, ranging method and the UWB parameters to be used. If a frame structure including the STS is used, its key is exchanged between the devices in step 7. After this, all the parameters needed to establish the connection have been changed and the UWB communication and ranging operation can be started. [2][3]

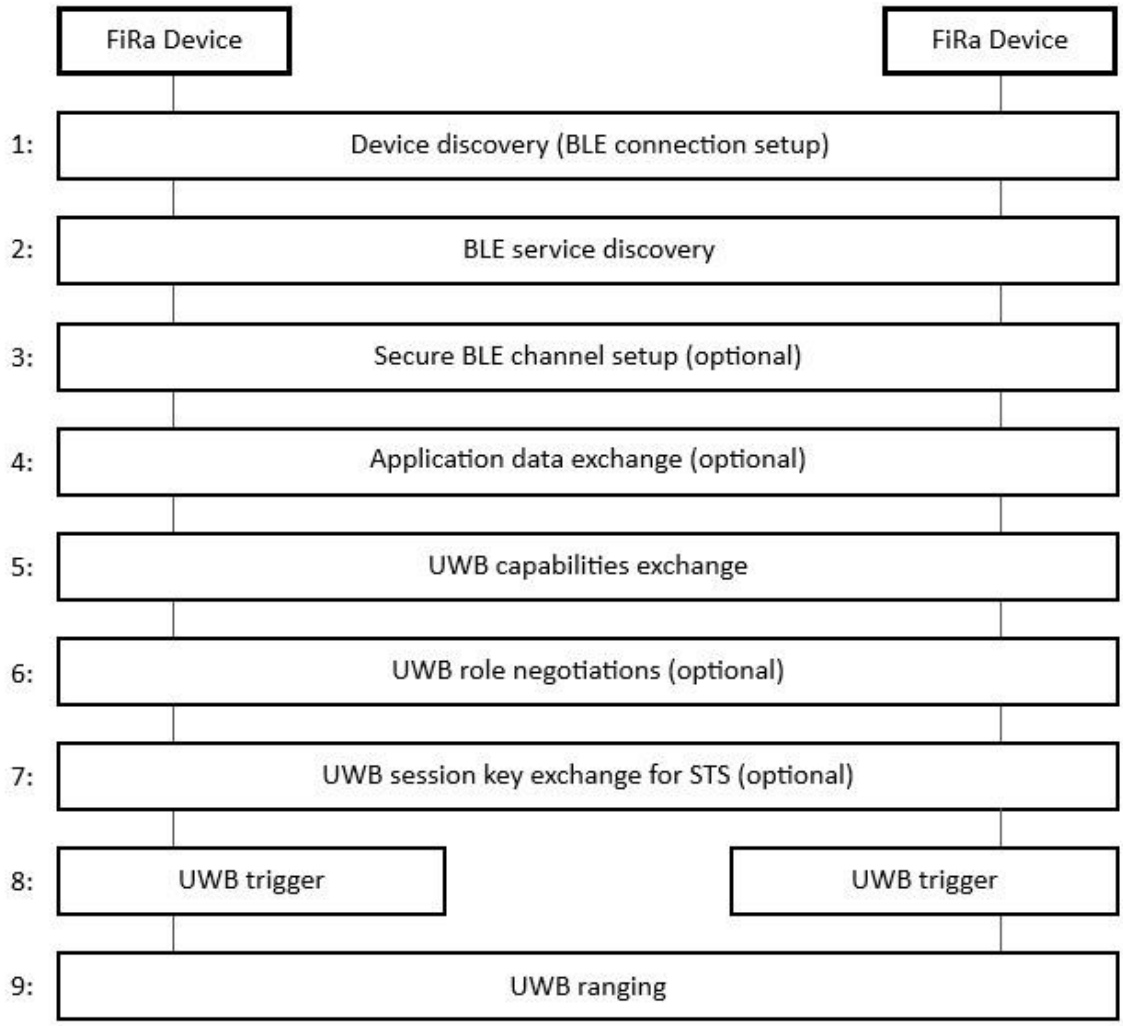

Figure 14. Establishing a connection and ranging operation for UWB in the FiRa standard. [3]

To guarantee compability, it is important that device manufacturers only use specifications according to one standard. For example, Apple has its own procedure for establishing a UWB connection, the structure of which is similar to FiRa, but the messages are not the same, which makes them incompatible. [3]

2.6 Use cases and comparison of other technologies

Due to its popularity and availability, many different industries are either adopting or have already adopted UWB technology to operate together with other technologies. The advantage of UWB is precise positioning and security that no other technology is capable of. These features are currently in great demand in many different use cases, and new possibilities are constantly being planned. For example, the FiRa Consortium defines an extensive list of different use cases, and they are divided into three main categories of use cases: hands-free access control, location-based services, and peer-to-peer services. Figure 15 shows these three main categories for UWB use cases. [24]

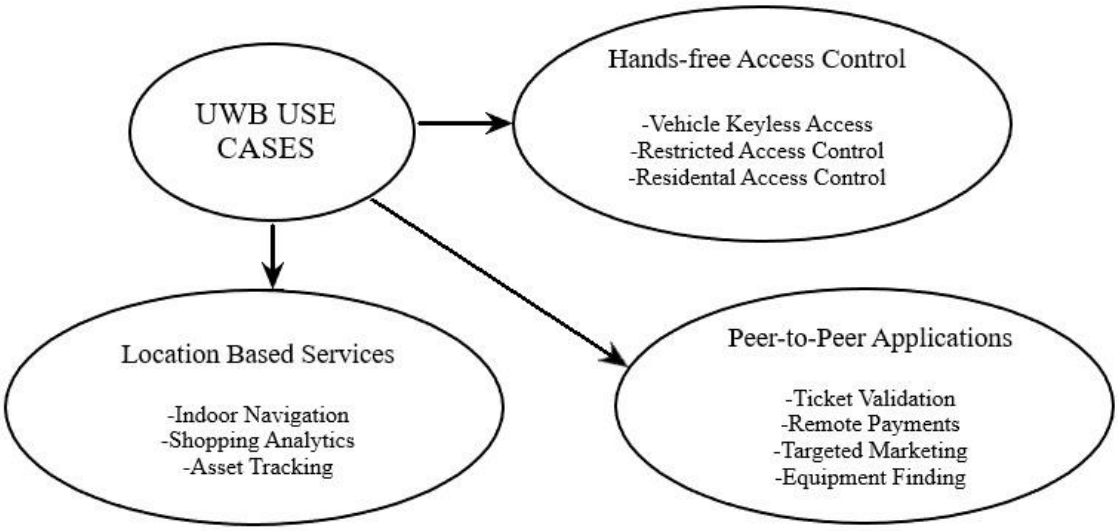

Figure 15. Example of UWB use cases categorized. [24]

Hands-free access control means accessing something or somewhere without keys, codes, or fingerprints, for example the door of a car or home, different areas of a factory/building or a home computer. UWB technology can be used to identify the user, the user's location and to grant access. Since the positioning accuracy of UWB is within a few centimeters, the desired distance to allow access can be defined very precisely. It is therefore easy to identify whether a person is entering or leaving the building, so the doors can be locked after exiting, which is challenging with other technologies due to imprecise and uncertain positioning. UWB is also immune to relay attacks, which have been a problem when using signal strength to determine distance. Additional security can be added, for example, by requesting fingerprint identification on the mobile phone, which can be used to ensure that the mobile phone has not been stolen but is in the possession of the rightful owner. [2][24]

Location-based services are another main category. They are intended for indoor positioning, where GPS (Global Positioning System) is not exactly accurate. In this category, people or objects can be located in a certain area using UWB, for example at home, in a shop or in a factory. With UWB, it is possible to operate in dense multipath environments and still provide accurate location, so it can also be used at, for example, public events and concerts. [24]

Peer-to-peer, or device-to-device, is the third of the main categories where UWB allows two devices to share their location information with each other, and thanks to the simple AoA technique, the devices can do it very precisely. This category offers a very wide range of possibilities, from locating a phone or an object to VR (virtual reality) gaming and smart

homes. It is possible to use the mobile phone as a key in various use cases at home, at work and in the city, such as obtaining a parking space and securely paying for a ticket. [24]

As seen in the use cases, they are related to the security and precise positioning provided by UWB technology, and in these areas UWB is unique. The comparison between UWB and other technologies in positioning is straightforward because most technologies are not designed for that. However, it must be kept in mind when comparing that UWB is just making its breakthrough, and it is constantly evolving to achieve the best features, which older technologies have mostly already done.

With UWB technology, the costs are slightly higher than those of BLE, because UWB is still relatively new and the production volumes are significantly lower than Bluetooth. It is possible to reach a range up to 100 meters in the LOS situations with the UWB, but the actual range depends on the used channel, the antenna design and the allowed power consumption. The UWB signal penetrates well through most building materials such as wood and brick, but not metal. Obtaining location information with the UWB is also much faster than other technologies, usually milliseconds at most, while some technologies can have a delay of up to several seconds. This means that UWB is an excellent technology for real-time positioning involving fast-moving objects. [5][24]

Bluetooth is not designed originally for positioning, and its ability to determine the location is based on the RSSI technique, i.e., the closer the device is, the stronger the signal is. The signal reflections and penetration losses can have an effect by increasing the error of the location by even meters. Bluetooth also offers a beacon-based positioning method, but dozens of beacons are needed to obtain a reliable and accurate location as receiving the LOS signals is essential. However, the use of Bluetooth technology is useful if only rough meter-level accuracy is required, as the technology is already available in all new smart devices. [5][29]

Wi-Fi has the same problem with positioning as Bluetooth because it also uses the RSSI technique to estimate location. Wi-Fi also consumes significantly more power than UWB, and Wi-Fi routers are expensive. The advantage of Wi-Fi over UWB is the same as Bluetooth: it is already used almost everywhere, both in public and private places, and all new smart devices already support Wi-Fi. [29]

GPS is still an excellent technology for positioning over long distances and when operating outdoors, but indoors positioning errors increase radically, and centimeter-level positioning is impossible. GPS also consumes more power than UWB technology. [29]

NFC (Near-Field Communication) technology has become popular due to its cheapness, small size and low power consumption, but it cannot be used for positioning. The range of short-range NFC is only a few centimeters, which is the most common implementation, and it can only be used to indicate if there are two NFC devices withing the range, not to estimate the distance. Passive NFC, which is used in credit cards and keys, for example, does not need a separate power source. NFC is mainly used for contactless payments, but the disadvantage of these unidentifiable payments is that their theft has become more common. With the UWB technology, these same features can be achieved with improved security and identification, but of course at slightly higher costs. [29]

Compared to other available technologies, it can be stated that UWB technology is the best choice if reliable and accurate location is needed. Additionally, it provides secure wireless access control, data transfer and contactless payment. There are numerous new possibilities and use cases as the capabilities of UWB are recognized. [29]

2.7 Future trends

As the need to know the real-time location of resources such as people, equipment or materials has grown, it has opened new doors for UWB technology to emerge. Smartphones act as pioneers in the development and growth of UWB technology, just as they once paved the way for Wi-Fi and Bluetooth. The work that FiRa does is also important to guarantee compatibility between these UWB devices and thus make expansion possible. Several articles estimate that the size of the UWB yearly market will grow to nearly 2 billion USD by 2030, and some indicate even close to 5 billion USD. [5][30][31][32][33]

Smart device manufacturers such as Apple, Samsung, Google, and Xiaomi have already added technology to their phones, and other device manufacturers will follow this trend as well. The comprehensive UWB support of smart devices is one of the key factors for the rapid growth and adoption of the technology. Other factors accelerating the growth of the UWB market are need of various RTLS applications, and the growing need for IoT (Internet of Things) technology, in both private and industrial applications. It has been estimated that by 2030, 1.8 billion UWB-supporting devices would be in use, more than half of which would be smartphones. Other major UWB device categories besides smart phones are consumer tags, consumer wearables, access control in the automotive industry and smart home devices as well as devices targeted for factory use. [34]

At technology side, the UWB has a lot of room to develop by reducing power consumption and increasing both accuracy and speed. If the growth rate follows predictions, by 2030 almost every new smart device will have UWB technology built in.

3 UWB UTILIZATION AND IMPLEMENTATION

Technology companies at various fields, like Apple, Samsung, Google, Audi, and BMW, have started to add UWB technology to their own products. It is predicted that the UWB will be as affordable as BLE technology in the near future due to increased popularity and associated competition, which decreases the cost of the technology. Accurately locating objects or people is pivotal to many different use cases, and as the UWB technology becomes common in the devices, it opens up opportunities for development, new use cases and third-party applications.

In this chapter, the utilization and implementation of UWB technology in a handheld device in parallel with other technologies is studied. The UWB must fulfill three main requirements on planned use: identify and authenticate the user, accurately locate the user, and enable secure payment. One target of the thesis is to map the suitability of the UWB technology for these use cases, and to find out the related potential challenges and advantages compared to other technologies. It is also necessary to find out applicable standards and other requirements for target geographical markets that must be considered and fulfilled when using UWB technology.

The current UWB component supply base is briefly introduced, and component selections for the evaluation platform of the thesis are made based on technical parameters and end-user features. A review of the factors affecting the selection process, which should be considered when choosing, e.g., antennas for the platform will be given. The measurement arrangements are designed after the selections of all the components to be studied have been made. The radio performance and platform measurement results provide essential information for the success of the project and identify possible ways to improve its performance even further.

3.1 UWB for mPOS device

Adding UWB technology to a handheld device is a growing trend, and thus such components are more widely available and cheaper than before. The major influential companies in the UWB market include Apple, Qorvo, NXP, Zebra, 5D Robotics, Pulse~LINK, Texas Instruments, Litepoint, Samsung, Sony, IMEC, Ubisense, Johansson Technology, Taiyo Yuden and Ignion. These companies either already use or plan to use UWB in their future products and intend to increase their presence in UWB technology. Decawave, which was a pioneer in UWB technology and proved the functionality of UWB, was bought by Qorvo in 2020 [35]. Since then, Apple has brought awareness to the UWB market by releasing its own smartphones and other products featuring UWB technology. [31][34]

A mobile Point-of-Sale (mPOS) is a smartphone, tablet or other wireless handheld device that works like a cash register as an electronic POS (Point-of-Sale) system. The POS system refers to the technology used by seller to accept payments, and POS refers to the physical location where the customer pays for services. Modern POS systems have become more common because they make it easier for the seller to analyze and develop the company's functions: sales monitoring, inventory management, personnel guidance, customer data and customer feedback collection. The mPOS is portable and convenient to take with one wherever a transaction needs to take place, unlike a traditional POS system, which usually consists of a stationary display, a cash register, a receipt printer, a card reader and a barcode scanner. This can speed up customer service and offer more payment options, and it is significantly more affordable for the seller than acquiring a traditional POS system. Battery life plays a vital role in these devices, as they should last as long as possible without the need

for charging. Increasing number of companies and industries have adopted mPOS systems due to the availability and affordability of the technology, and therefore mPOS payments are constantly being made in increasing numbers. [36][37]

When using the device as a means of payment, the goal is to ensure as safe and problem-free operation as possible. UWB offers two prominent features for this: an additional layer of security with the STS and precise location determination. UWB is the best of the available technologies for indoor accurate positioning due to its unique features and simple AoA technique that only requires a second antenna. It is already used in several smartphones from Apple and Samsung, both of which have also announced their own UWB tags [38][39]. Similarly, the aircraft manufacturer Boeing has said that it uses UWB technology to locate parts and tools in its own factories [29]. One challenge in using AoA technique is that it is not standardized, so it depends on the device manufacturer which method is used to obtain it. This may affect the guarantee of compatibility if there are several different methods in use. It would be advisable that the future IEEE 802.15.4ab standard defines common regulations for obtaining AoA. Unfortunately, it is also not known how the FiRa Consortium has considered the compatibility of the AoA data and results in its own standard and in the exchange of these messages between the devices. [3]

Another topic to be considered is the placement of the antennas in the integrated platform, in this case, inside of the tablet. It is necessary to find out the potential locations of the antennas and to investigate whether other technology or mechanical casing interferes or affects the quality of the UWB signals. It is also known that in the NLOS situations the accuracy can decrease, but by changing some of the channel parameters, it can be improved [40]. However, because neither FiRa nor Apple discloses more detailed information about their algorithms for selecting these parameters, the topic is excluded from this thesis. To obtain and operate with the best parameters, it would be important for the algorithm to be standardized as well, so that integration and debugging of the platform would be possible. [3]

User authentication is currently based on the CSML specification from FiRa, where user identification and establishing a UWB connection is performed using BLE technology. The use of this CSML also ensures interoperability with other FiRa devices to establish a UWB connection using a secure BLE channel if needed [3]. Currently, the FiRa CSML is therefore mandatory to be able to connect different UWB devices, as the IEEE standards do not define these higher layers. Apple and Omlox also offer their services for this purpose. It is not known at the time of writing whether there will be additions to this in the new IEEE 802.15.4ab standard and whether hybrid technology is the only possibility to establish a UWB connection. However, it must also be kept in mind here that UWB technology is still in the development stage and is certainly not yet in its final form.

Secure payment is mentioned in the most common use cases, and due to the precise positioning and the security provided by UWB, it should be suitable for this purpose [24]. A point & trigger type of option has been proposed, i.e., the payment could be handled by pointing the mobile phone towards the payment terminal, as well as a location-based remote payment, in which case line of sight to the payment terminal would not be required. Hybrid technologies, such as proposed UWB + NFC technology for secure payments, have also been introduced. If necessary, it is also possible to add other security measures, such as biometric identification or fingerprint, depending on the desired security for the application. Companies specializing in electronic payment have also started to investigate the use of UWB in paying for the services they offer. [2][41]

As early as 2020, NXP Semiconductors started cooperation with Japan's largest telecom operator DOCOMO and Sony to develop hands-free mobile payment and personalized

advertising using UWB technology. NXP has also started cooperation with ING bank and Samsung in a pilot project where a peer-to-peer payment application based on UWB technology is developed. Customers should be able to send money or pay a bill with the ING banking application available on their phone. When two Samsung phones equipped with UWB technology are close enough to each other, they could see each other through the app. Peer-to-peer payments have increased enormously, and money already moves through mobile transfers in many ways, such as with MobilePay. It is usually necessary to know the other person's profile in advance or to search for it using a username, an email address or a phone number. With UWB technology, this would not be necessary, as it would be enough for the smartphones to be within range. [41][42]

EMVCo is a group consisting of six of the world's largest payment service providers: MasterCard, Visa, Amex, Discover, JCB and UnionPay. EMVCo has established the Wireless Task Force whose task is to investigate the suitability of various wireless technologies (BLE, Wi-Fi, UWB) for secure payment and how they could improve payment experiences. EMVCo plans to release an updated version of the EMV Secure Remote Commerce (SRC) specifications and the SRC testing program. Testing ensures that the devices used to accept payments, often smartphones, offer reliable and consistent payment experiences. The EMV specifications play a vital role in creating a flexible and common basis for new payment methods, so that consumers can pay for goods and services the way they want. EMVCo works with technical bodies and its community around the world to develop support for wireless payments and remote commerce. [43][44][45]

In positioning, UWB is already used more than other use cases, and its use in secure payments is also being studied in several different cooperation projects. UWB technology is the most promising choice for our project, at least based on the use cases and the availability of the essential components. A UWB chip, UWB antennas and the FiRa's CSML are required to establish a connection between two UWB devices. In order to support UWB in ready-made mPOS devices, the obtained data must be processed with software as well. It requires programming for the software and there are already some available UWB libraries for different operating systems that can be used.

Google added the UWB API (Application Programming Interface) to Android 12, but it was only intended for its own use, leading to speculation that Google is intentionally limiting the adoption of UWB. Since then, Google announced that it was developing a separate public API for UWB that would be open to third parties. The preliminary version can already be found in the Jetpack library and can be used on UWB-supported devices. It is still in the alpha stage, and thus it does not yet have all the necessary functions that developers would need. Opening the API to everyone will certainly benefit the development of the library and speed up its completion, as software developers can familiarize themselves with the UWB technology and create new features and applications. [3][46][47]

Apple has also announced its own Nearby Interaction API for third parties to add technology and software compatibility with Apple products to their devices. However, achieving full compatibility between device manufacturers will be problematic if several different APIs are used. [3][20]

The UWB handheld device with Wi-Fi 6E potentially has co-channel interferences between the systems. According to FiRa, interference on the upper UWB channels is reasonable, and for this reason, the usage of UWB channel 9 is recommended by them [24]. The most common frequency range worldwide for UWB is 6.0 – 8.5 GHz based on Table 1. So, if the interference level of Wi-Fi 6E is too challenging at the frequencies from 6 to 7 GHz, there are still UWB channels available on the higher frequencies for the operation.

3.2 Comparison and selection of UWB chips

The growing interest towards UWB technology has increased both the demand and the supply for the UWB chip market. The leading manufacturers of the UWB chips are Qorvo, NXP, IMEC and Apple. The first two are the most interesting for the project, since the chip must support the UWB channels 5 and 9, AoA technique, and be IEEE 802.15.4z compliant with support for the STS frame format. The challenge of comparison is that more detailed technical information about the parameters or datasheets for all these chips are not publicly available.

Qorvo has a DW1000 chip based on the previous IEEE 802.15.4-2015 standard, which has been used the most in UWB research. The newer Qorvo DW3000 generation is designed towards the IEEE 802.15.4-2015 and IEEE 802.15.4z standards. It includes support for the new 64 MHz BPRF mode as well as support for the AoA technique, channels 5 and 9, and all frame formats including the STS. It also supports all ranging methods: SS-TWR, DS-TWR, TDoA and PDoA. It supports the payload length up to a maximum of 1023 bits, PRF 16 or 64 MHz, and data rates 0.85 or 6.81 Mbps. It has been stated to meet all global UWB radio requirements, and it is FiRa compliant. The chip promises ranging accuracy of ±6 cm and PDoA accuracy of ±10 degrees in the LOS condition. For example, Google uses Qorvo's DW3720 UWB chip in their Pixel 6 Pro smartphones. [48][49]

NXP has announced the Trimension series, including the SR040 and SR150 UWB chips for IoT use, the NCJ29D5 UWB chip for automotive use, and the SR100T UWB chip for mobile use. At least the SR040, SR150 and NCJ29D5 are IEEE 802.15.4z compatible, but unfortunately no public technical information is available for the SR100T. The SR100T is aimed at secure ranging use cases for Android mobile phones and is FiRa certified, based on information from the NXP website. The NXP SR150 chip for the IoT environment supports frequencies from 6.24 to 8.24 GHz (UWB channels 5, 6, 8 and 9), and 64 MHz and 128 MHz PRF modes, ranging techniques SS-TWR, DS-TWR and TDoA as well as AoA measurement. In addition, the STS usage is possible and the FiRa's MAC and PHY layers are already installed, and there is an option to update the firmware. The SR150 promises ±10 cm accuracy in ranging use and ±3 degrees accuracy in AoA measurements. Although no technical information has been found on the SR100T chip, it is likely to be similar to other Trimension series UWB chips. Thus, it would support the IEEE 802.15.4z standard and AoA technique. However, this assumption is not enough to be included into the comparison. At least smartphones Samsung Galaxy Note 20 and Xiaomi MIX4 have implemented these NXP's SR100T UWB chips. [3][50]

Apple has announced its own UWB chip, the U1, which is IEEE 802.15.4z compliant, and supports the UWB channels 5 and 9, but otherwise there is not much information about the U1 chip. Both Qorvo and NXP have announced that their products are compatible with the Apple's U1 chip, and all three companies are members of FiRa. [48][50]

The IMEC's IR-UWB chip supports the IEEE 802.15.4z standard and operates in the band from 6 to 9 GHz. Unfortunately, no public technical datasheet is available, and thus exact support of the IEEE 802.15.4z standard is unknown [51].

All IEEE 802.15.4z standard compliant chips support the mandatory requirements for the non-HRP-ERDEVs, such as at least the one segment STS support. The chips from Qorvo and NXP support all the different ranging methods introduced in the IEEE 802.15.4z standard. However, this means that the new preamble codes of length 91 may not be supported, nor the new HPRF modes for 128 MHz and 256 MHz. It would be possible to shorten the on-air time, and thus reduce the power consumption in the device by using the HPRF mode, as well as

improve accuracy with these new preamble codes. Support for the HPRF mode is not found in the Qorvo DW3000 chip, according to the datasheet, and there is no information about other manufacturers [48]. Otherwise, the Qorvo DW3000 chip is an excellent option for UWB implementation, and it is included into the Murata Type2AB UWB module.

The Murata's Type2AB module has been selected for the UWB implementation in the thesis and a photo of the evaluation board is shown in Figure 16. Two of these evaluation boards are needed to establish a UWB connection and study its accuracy with different antennas and channel parameters.

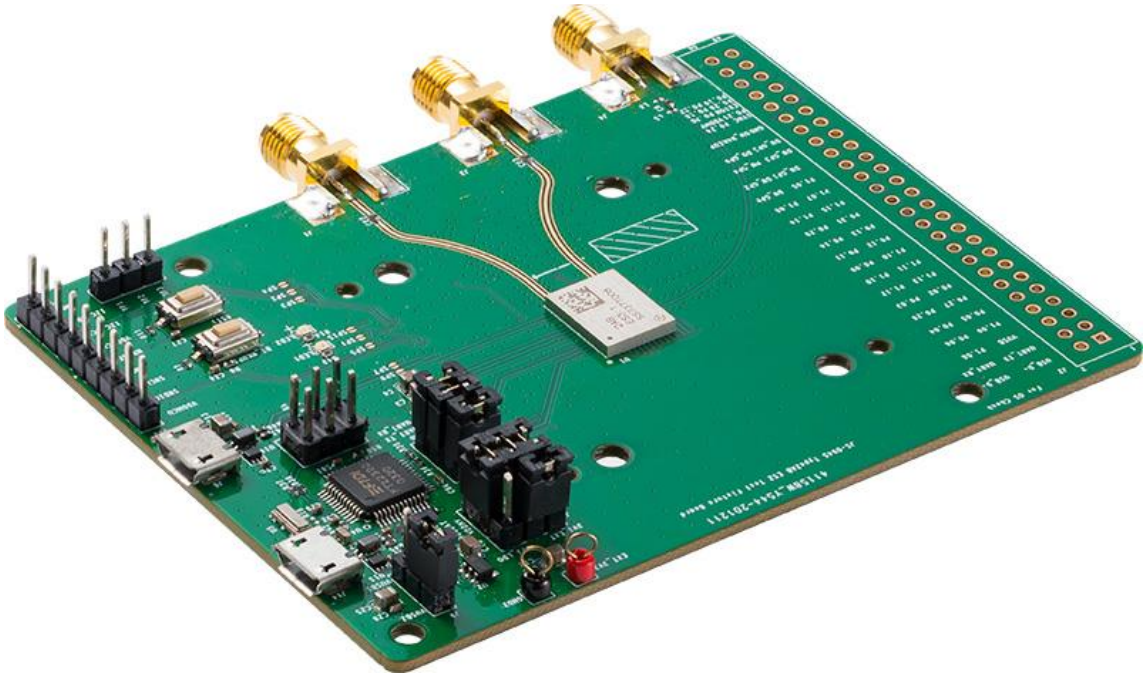

Figure 16. Murata Type2AB Evaluation Board. [52]

The Murata's 2AB module has a compact size and low power consumption, making it therefore ideal for a battery-powered device. The module includes a UWB chip from the Qorvo's DW3000 family and a nRF52840 BLE chip from Nordic IC. Additionally, it has an internal reference clock for both chips. The evaluation board has USB ports for data transfer and power connection, SMA connectors for UWB and BLE antennas, programmable buttons, pins for adjusting board settings, and a connection for programming and updating the firmware. The current consumption of the module is only 560 nA in sleep mode, 4.0 µA when BLE is enabled, 4.4 to 8.4 mA when UWB is enabled and 50 to 60 mA in TX/RX situations. The size of the module is 10.5 x 8.3 x 1.44 mm, and its operating temperature is from -40 to 85 °C. [52]

Murata offers a user interface and instructions for setting the UWB channel parameters as desired with a computer. The study of the UWB chip with different channels, different frame formats and different frame lengths can be performed with this user interface and firmware that can be programmed on the evaluation board. In this way, the effects of the channel parameters in distance and angle of arrival measurements can be studied.

Qorvo's DW3000 uses the PDoA technique to obtain the AoA information, where the PDoA calculation is performed during the TWR response [48]. An estimate for the angle from which direction the signal arrived can be calculated from the phase difference of the arriving signals at the two antennas. In general, everything starts from the assumption that the distance between two UWB devices is much greater than the separation between the double antennas

on the device where the phase difference is calculated. Figure 17 illustrates the situation for calculating the position of a UWB tag when the UWB signal arrives at the two antennas of the UWB anchor at various times.

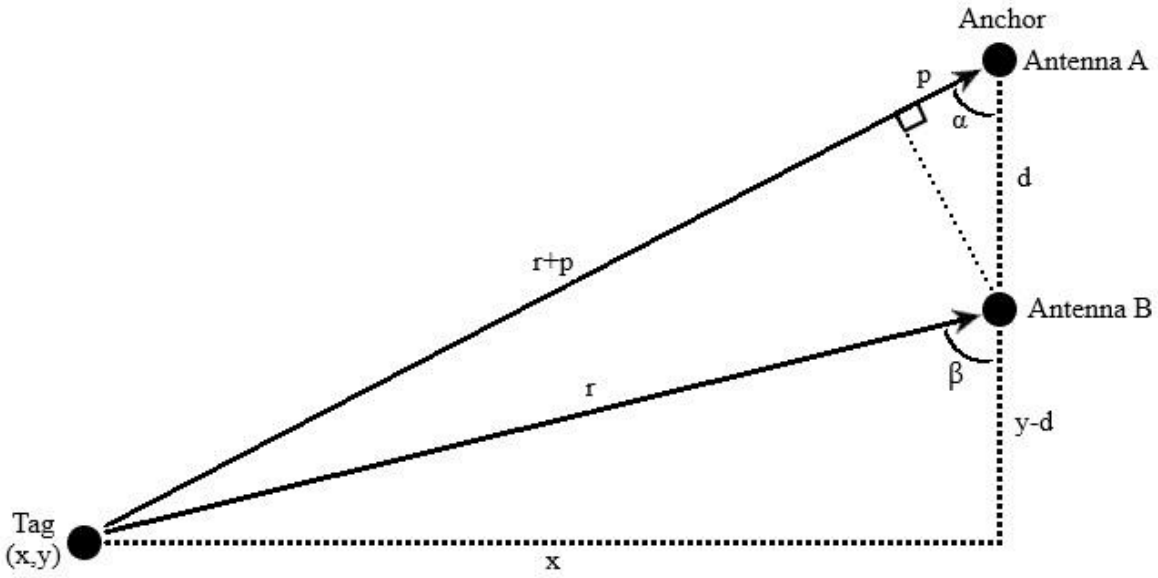

Figure 17. UWB signal arrival at two UWB anchor antennas separated by *d*. [53]

Figure 17 illustrates a case where the UWB tag is located at (*x*,*y*) and the coordinates of *x* and *y* need to be determined. The separation *d* between antennas A and B in the UWB anchor is known, and the distance *r* can be calculated using the ToF, for example from the tag to antenna B. The distance from the tag to antenna A is then *r*+*p*, where *p* is the distance difference of the arrived signal between antennas A and B. The distance difference is obtained from the time difference t_p, which is the difference in the arrival times of the signal to antennas A and B. The time difference can be calculated in at least two different ways: either by separately calculating the ToFs of the signal to both antennas and taking their difference, or by counting the time between the arrival of the signal at antennas B and A. Using the time difference t_p, the distance difference *p* can now be calculated by multiplying it by the speed of light. Assuming that the distance between the devices *r* is much greater than the separation between the double antennas *d*, which is less than 20 mm on the UWB channel 9, two trigonometric cosine formulas can be defined:

$$\cos(\alpha) = \frac{p}{d} \;\&\; \cos(\alpha) = \frac{y}{r} \quad \rightarrow \quad \frac{p}{d} = \frac{y}{r} \quad \rightarrow \quad y = \frac{p * r}{d}. \tag{6}$$

The first coordinate *y* of the tag's location can be derived based on the cosine formulas. The second necessary coordinate *x* can be calculated using the Pythagorean theorem:

$$x^2 + y^2 = r^2 \quad \rightarrow \quad x = \sqrt{r^2 - y^2}. \tag{7}$$

Both coordinates (*x*,*y*) of the tag's location can be determined by using equations (6) and (7) [53]. With the help of the cosine theorem, it is also possible to determine the angles α and β, which are almost the same for both antennas when *r* is much greater than *d*. This is called the TDoA method [7]:

$$\cos(\alpha) = \frac{p}{d} \quad \rightarrow \quad \alpha = \arccos\left(\frac{p}{d}\right) = \arccos\left(\frac{t_p * c}{d}\right). \tag{8}$$

The same angle α is also obtained by using the phase difference $\Delta\varphi$ of the signals arriving at the two antennas. This is called the PDoA method and can be written [7]:

$$\begin{aligned} \Delta\varphi = \varphi_A - \varphi_B &= 2\pi * f * t_p = 2\pi * f * \frac{p}{c} = 2\pi * \frac{d * \cos(\alpha)}{\lambda} \\ \rightarrow \quad \alpha &= arccos\left(\frac{\Delta\varphi * \lambda}{2\pi * d}\right) = arccos\left(\frac{\Delta\varphi * \lambda}{360° * d}\right) \approx arccos\left(\frac{\Delta\varphi}{180°}\right), \end{aligned} \tag{9}$$

where λ is the signal wavelength. In other words, several different methods have been presented to obtain the position, either with the help of the AoA technique or without the need for angle calculation, and it depends on the manufacturer which method is used, because it is not standardized in any way [3].

3.3 Comparison and selection of UWB antennas

In the UWB communication, the transmitter and the receiver must have a broadband antenna suitable for UWB use. Antennas are fundamental components of all communication systems, and their selection depends on the project requirements and constraints, such as the desired frequency range, performance, and physical size. In the selection of UWB antennas, the challenges are increased by the large bandwidth and its RF performance over the entire frequency range, such as radiation pattern, antenna gain and efficiency as well as impedance matching. Antennas are usually the largest components of wireless communication systems, so a small size is usually the main goal along with the best possible performance. Over the past few years, several different manufacturers have offered a wide range of antennas for the UWB purpose, varying in size, features, and prices. Manufacturers of the UWB antennas include at least Johansson Technology, Ignion, Taoglas, Kyocera/Ethertronics, Taiyo Yuden and Molex. [54]

When selecting an antenna based on specifications, it is important to understand all the technical data so that they meet all the requirements. Some of the UWB antennas were directly left out due to their size or because they were intended to operate at frequencies below 6 GHz. Some antennas support frequencies ending at 8 GHz, so they are not ideal for the UWB channel 9, the center frequency of which is slightly below 8 GHz. Since the peak gains, return losses and efficiencies for the antennas are remarkably similar to each other, antennas manufactured with different techniques can be considered.

Four different types of the UWB antennas are studied in the thesis: ceramic, PCB (printed circuit board), FPC (flexible printed circuit) and chip antenna. Figure 18 shows the illustrative designs of the selected antenna types. The polarizations of all selected antennas are linear, and the radiation patterns are omnidirectional, meaning that they radiate in all directions without significant directivity. The specified peak gains for these antennas are between 2.5 and 6.0 dBi, and efficiencies between 70 and 85% according to the technical datasheets. The sizes of the antenna radiators themselves vary from a few millimeters to a few centimeters, but with the evaluation boards, all antenna modules are approximately the same size.

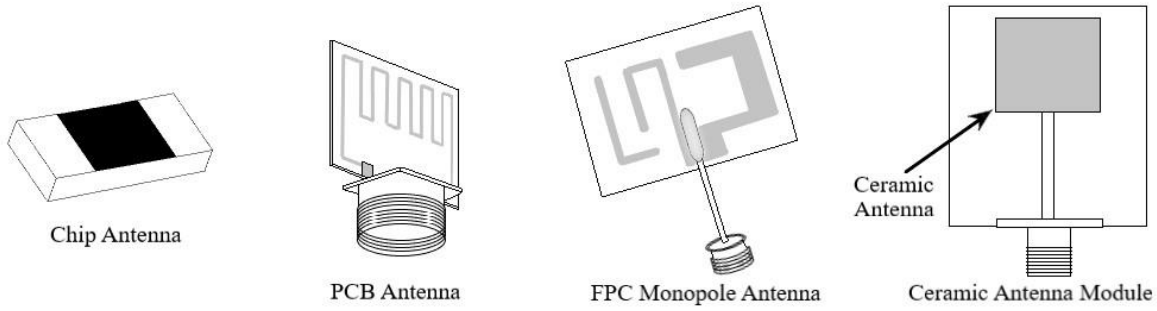

Figure 18. Illustrative designs of chip, PCB, FPC and ceramic antennas.

The standalone chip antennas are the smallest in size and are therefore an interesting option for the project. The other antennas are slightly larger, and thus require more space in the device, which may not be available.

As mentioned earlier, the AoA technique requires two antennas to calculate the phase difference between the antennas. Therefore, it is necessary to order two pieces of the selected antennas to perform the desired measurements. The separation d between the two receiving antennas should be less than $\lambda/2$. The signal wavelength and separation are related to each other following as:

$$\lambda = {}^{c}/_{f_c} \quad \rightarrow \quad d = {}^{c}/_{2f_c}, \tag{10}$$

where c is the speed of light and f_c is the center frequency of the UWB channel. The needed separations between the two antennas are $d \approx 18.78$ mm at channel 9, and $d \approx 23.11$ mm at channel 5. Thus, the separation between the two antennas is selected according to the UWB channel 9, so that the condition is met on both channels. [5][7]

The design of UWB antenna systems should focus on ensuring the best performance in the intended use, considering the effects of the environment and the integration platform. An unsuitable antenna leads to both pulse distortion and center frequency shift, and thus affects the operation and performance of the entire system. It is therefore important to study the performances of the selected state-of-art UWB antennas in their proper intended usage simultaneously with other wireless technologies. [3]

Similarly, the effects of the position, orientation and placement of the antenna need to be studied based on the performance of the entire system. However, the placement of the antennas in the device depends mostly on the possible and available free places within the device. Two UWB antennas close to each other are needed for AoA measurement, so there may not be many possible places available. In addition, the openings for the antennas are mandatory in the metal frame of the device. Although the UWB signals penetrate almost all materials well, they do not penetrate metal.

4 MEASUREMENTS

The measurements were performed for the UWB module, the UWB antennas and the entire UWB system. The focus was to investigate the operation of the UWB module on the UWB channels 5 and 9, with the center frequencies of 6489.6 MHz and 7987.2 MHz, which were rounded to 6500 MHz and 8000 MHz to simplify the measurements. The measurements were performed to verify pulse shape requirements for the PSD mask and the main and side lobe levels, and to test the functionality by changing channel parameters.

Conducted S-parameter measurements were completed to obtain S11 parameters for the studied antennas, both without the prototype device and attached to the protype device. In addition, radiation measurements were performed for the studied antennas as well without and with the prototype device. The antenna efficiency, gain and radiation pattern could be determined from the radiation measurements. The antenna measurements were conducted so that one device was disassembled and reassembled as a measuring platform (prototype device). The antennas could be placed in different suitable places on this prototype device, and it enabled modelling how the case and other technology affect the results and the performance of the studied antennas.

Finally, the operation and accuracy of the entire UWB system with the different antennas, different channels and different channel parameters was studied. For this, a new measuring platform was prepared, with which the distance of the UWB modules remains the same when the antennas are changed and the operation is studied. For angle measurement, the other UWB module must be able to move either around its axis, or alternatively around the circumference of a circle, so that the distance between the modules remains unchanged.

4.1 UWB module measurements

Some firmware can be installed on the UWB evaluation boards, and a computer can be used to execute commands to adjust the desired channel parameters or operating method for them. Frequency domain measurements were performed with a spectrum analyzer and time domain measurements with an oscilloscope. The individual pulses and pulse bursts are so fast that there was no spectrum analyzer available that would be able to scan the entire pulse. The whole image needs to be composed by collecting samples from several pulses. A useful feature of the UWB module for this purpose was a continuous frame transmission mode, which enabled spectral testing and assembly of the full image. However, spectrum analyzer-based measurements are not presented due to data transfer problem. The spectrum analyzer had only a floppy diskette for this and a computer with a floppy drive was not available. So, another alternative for frequency domain measurements was found and the advanced Keysight DSA91204A digital signal analyzer was used for the purpose. It supports the time domain measurements up to 12 GHz bandwidth and frequency domain analysis can be performed by using the FFT (Fast Fourier Transform). It is fast enough to measure these short UWB pulses, and it was used to verify the correct pulse shape and the effect of different channel parameters in the time domain, as well as determine the behavior of the pulse in the frequency domain on both relevant UWB channels. The channel parameter tests, such as increasing the PRF and changing the length of the preamble or payload data of UWB module, confirmed that the module worked as expected. Channel selection itself had no effect on the time domain measurements unless other channel parameters were changed. An example of a complete BPRF frame recorded with an oscilloscope showing the SYNC and SFD fields (M1 to M2), the PHR field (M2 to M3) and the PHY payload field (M3 to M4) is shown in Figure 19.

Figure 19. An example of a complete BPRF frame where SYNC and SFD fields M1-M2, PHR field M2-M3 and payload field M3-M4 can be seen.

Figure 20. As an example, a part of the zoomed preamble, to which the polarities of the pulses (-1, 0, 1) have been added with blue numbers.

A part of preamble is zoomed in Figure 20. The signal coding consisting of positive pulses (+1), negative pulses (-1) and non-sent pulses (0) is clearly visible in the figure above, and corresponding logical values were added to the figure with blue numbers. The used ternary code sequence can be changed as desired from the options presented in the standard, as well as the number of code repetitions in the SYNC field, and thus the length of the preamble can also be altered. For example, if a ternary code with a length of 91 pulses is selected and it is repeated 32 times, there would be 2912 pulses in the SYNC field. The pulse shape and the small sidelobes after them can also be observed from Figure 20, where sidelobes do not exceed the limit value of 0.3 of the maximum pulse amplitude, which is required in the IEEE 802.15.4z standard.

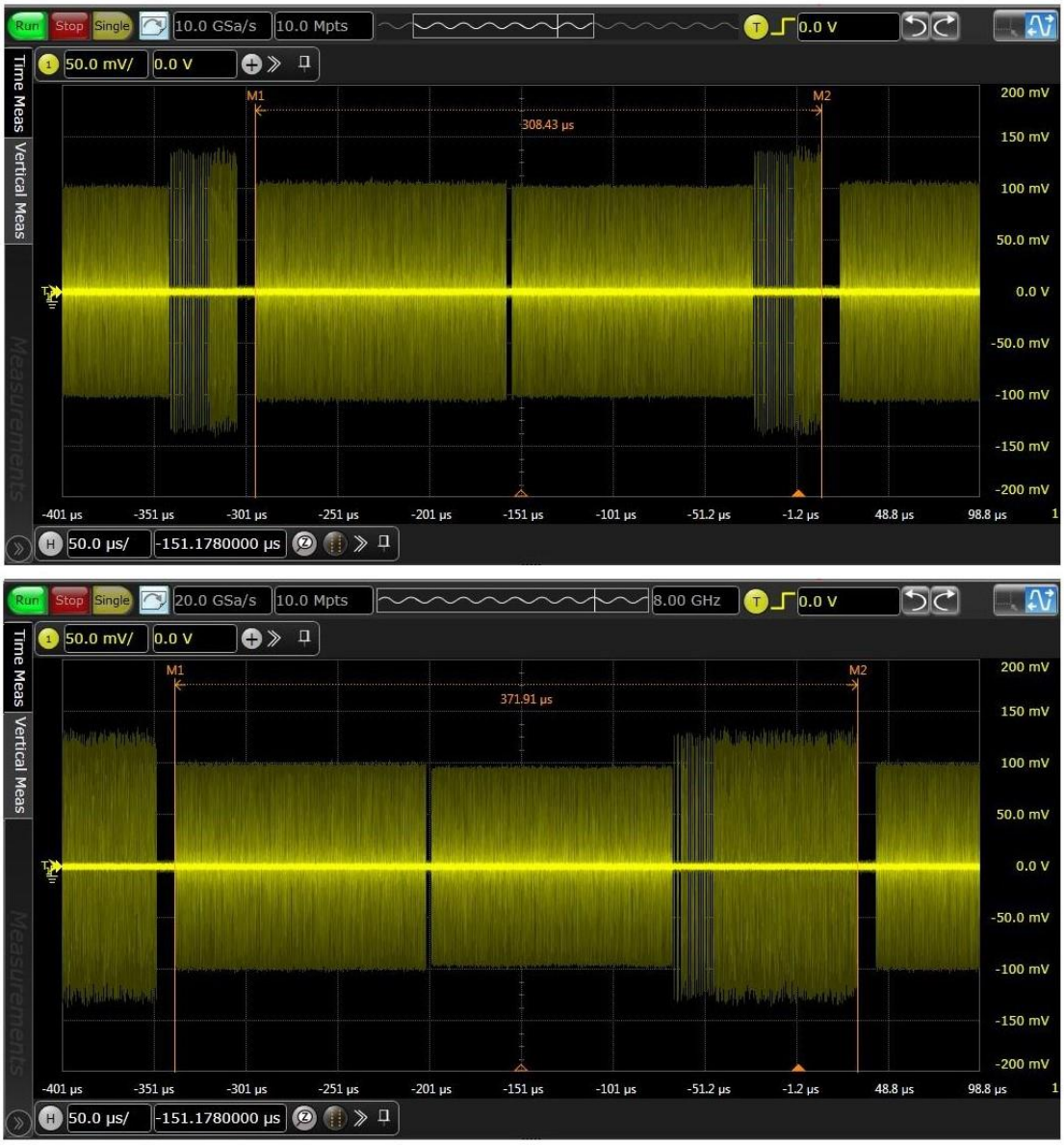

Figure 21. Effect in the BPRF frame when the payload length is increased.

The effect in the BPRF frame is shown in Figure 21 when the length of the payload was increased from 8 bits to 64 bits by changing the channel parameter for the UWB module. The length of the payload increased eight times in the lower image compared to the one above, which verified the correct operation of this channel parameter.

A section of the UWB module in the continuous frame transmission mode is shown Figure 22. Different time spans were used to zoom in the signal, and those show the composition of the pulse burst and the shape of the individual pulses in details. The pulses behaved nicely, and there was no big ringing occurring after them.

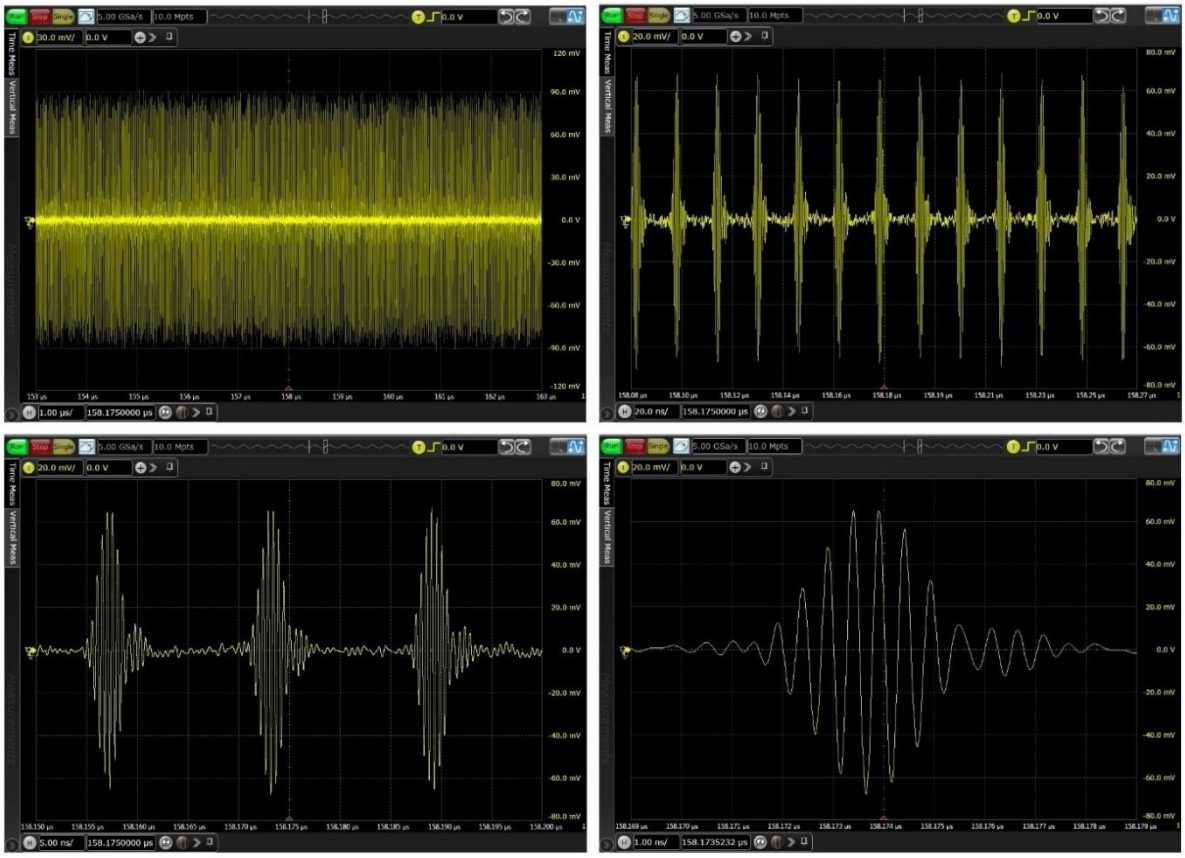

Figure 22. A part of the continuous frame transmission mode and zoom from it.

The power spectral density can be studied in the continuous frame transmission mode from the frequency domain graphs. The number of samples affects the accuracy of the spectrum plot, since they are created with a FFT, and those are not necessarily as accurate as the one obtained with a spectrum analyzer. It can be seen from Figure 23 that the pulse passed the PSD requirements defined by FCC and ETSI on both studied channels, i.e., the maximum transmission power level did not exceed -41.3 dBm/MHz. In addition to this, in order to coexist with the adjacent UWB channels without interference, the requirements defined in the IEEE802.15.4z standard for the pulse mask require -10 dB attenuation at the frequencies $f_c \pm 0.65/T_p = f_c \pm 325$ MHz and -18 dB attenuation at the frequencies $f_c \pm 0.8/T_p = f_c \pm 400$ MHz [17]. The pulse duration T_p is defined as 2.0 nanoseconds in the IEEE802.15.4z standard for both studied UWB channels 5 and 9, when the channel bandwidth is 500 MHz and f_c is the center frequency of the channel. These frequencies of interest are marked in red, and the transmission power attenuations of interest are marked with red lines in Figure 23. At channel 5, at the frequencies 6175 MHz and 6825 MHz the attenuation was about 15 dB, and at the frequencies 6100 MHz and 6900 MHz the attenuation was even more than 30 dB. On channel 9, at the frequencies 7675 MHz and 8325 MHz the attenuation was about 12-15 dB, and at the frequencies 7600 MHz and 8400 MHz the attenuation was more than 30 dB as well. As a conclusion, measured values indicate that in these conditions the IEEE802.15.4z standard requirements are fulfilled on both studied UWB channels.

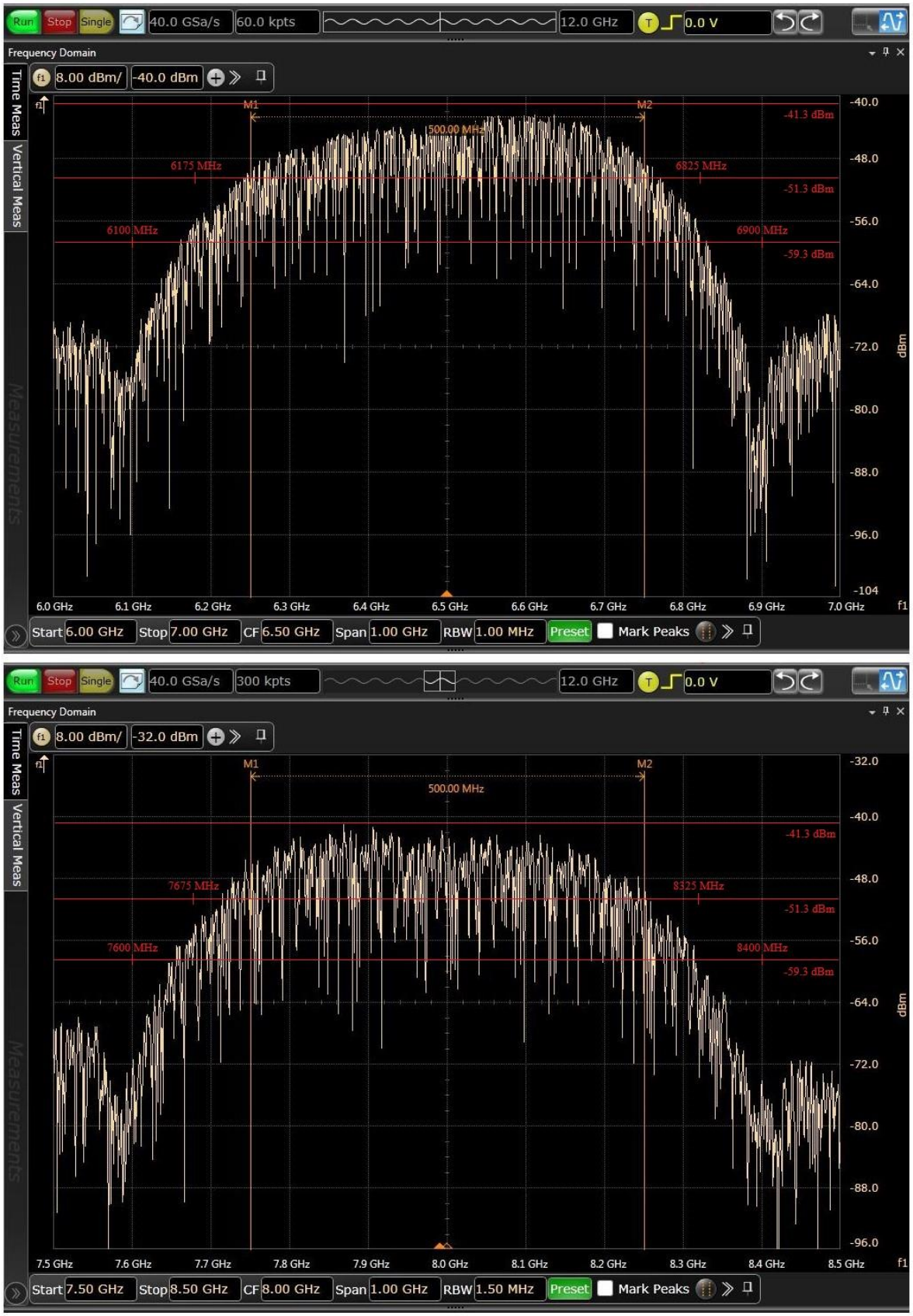

Figure 23. Power spectral density graphs on the UWB channels 5 and 9, as well as the frequencies of interest marked in red, for which the limits according to the IEEE802.15.4z standard have been defined.

4.2 Measurements of UWB antennas

Accurate and efficient measurement of UWB antennas can be challenging due to the wide frequency band, in contrast to measuring a narrow band antenna intended for a specific frequency only. The scattering parameter S11 is usually similar when repeating measurements for the antenna, but the radiation parameters (gain, efficiency and radiation pattern) may have significant differences. Conducted parameter measurements are more repeatable than radiated parameter measurements which are more time-consuming and typically complex to measure accurately. [55]

Four different types of the antennas were measured and two of each were needed for AoA measurements. All the studied antennas were not available with an SMA connector, but those were added to all to enable easier and faster measurements. The SMA connectors ensured that no additional adapters were needed, and thus possible errors caused by them was avoided. The purpose of the measurements was to find out how the performance of the antennas changes when they are attached to the prototype device, and how these results could be improved. Passive mechanical objects located near the antenna affect the characteristics of the antenna, such as impedance matching and radiation patterns. The final location for the antennas in the ready-made device has not been chosen, and by studying potential locations, information can be obtained about the factors to be considered.

A measurement platform must be designed so that the antennas are as close as possible to the locations where they are placed in the final product. The used measurement platform was done by removing the back cover, battery, main circuit board and other protection mechanics from the handheld device. The prototype device included only a large display, a part of the plastic protective cover, required internal wires, and a metal frame. The remaining parts in this platform are the main contributors needed to analyze loading effects of the antennas. There were no places for the studied antennas in the metal frame, thus new suitable openings for the antennas were made with a miller. Additionally, spaces for the SMA connectors were added for measurement purposes, which are not needed for the final product. It was ensured that the antennas with SMA connectors fit and can be attached firmly in the desired position on the platform. The edges of the openings and spaces were coated to make sure that unwanted ground contacts do not occur if the measurement cable moves during the measurement. The attachment of the antennas was done with a thin double-sided tape, strong enough to hold the antennas in the desired position during the measurements. Using the tape allowed for an easier removal of the antennas after measurements compared to using hot glue. An illustration of the back side of the measurement platform or the prototype device under test (DUT) is presented in Figure 24. The locations of the antennas and the metal frame including milled spaces for the antennas and SMA connectors are clearly shown in the figure.

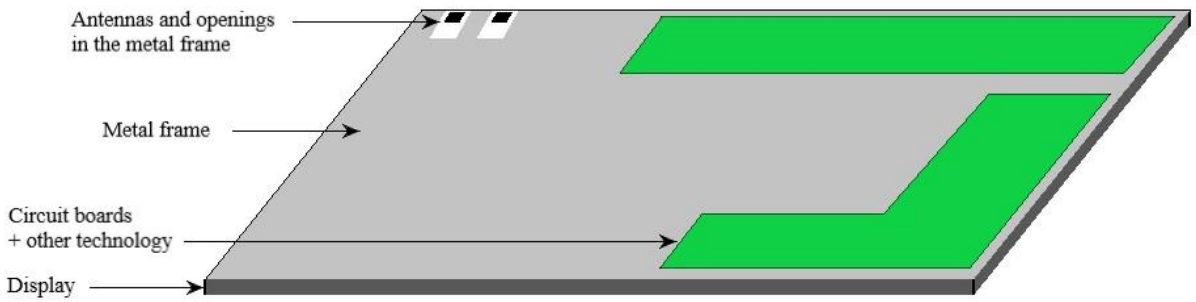

Figure 24. Model drawing of the back side of the prototype DUT, showing the locations of the antennas with openings in the metal frame and other technology components.

The S-parameter measurements (S11, S21, S12 and S22) were performed for the antennas using Copper Mountain's S5085 Vector Network Analyzer. The results were plotted on the frequency scale and on the Smith chart. The single-port reflection coefficient S11 measurement of the antenna indicates the amount of power reflection from the antenna [56]. It is desirable to minimize the S11 value so that all transmission power is radiated from the antenna. First, measurements were done for the antennas as standalone or not attached to the device under test. Then these results were used as reference values when the antennas were attached to the DUT. The frequency ranges of interest in the antenna measurements are at the band from 6250 to 6750 MHz (UWB channel 5) and at the band from 7750 to 8250 MHz (UWB channel 9). The ceramic and chip antenna also had their own evaluation boards from the antenna vendors, where they were attached during the measurements.

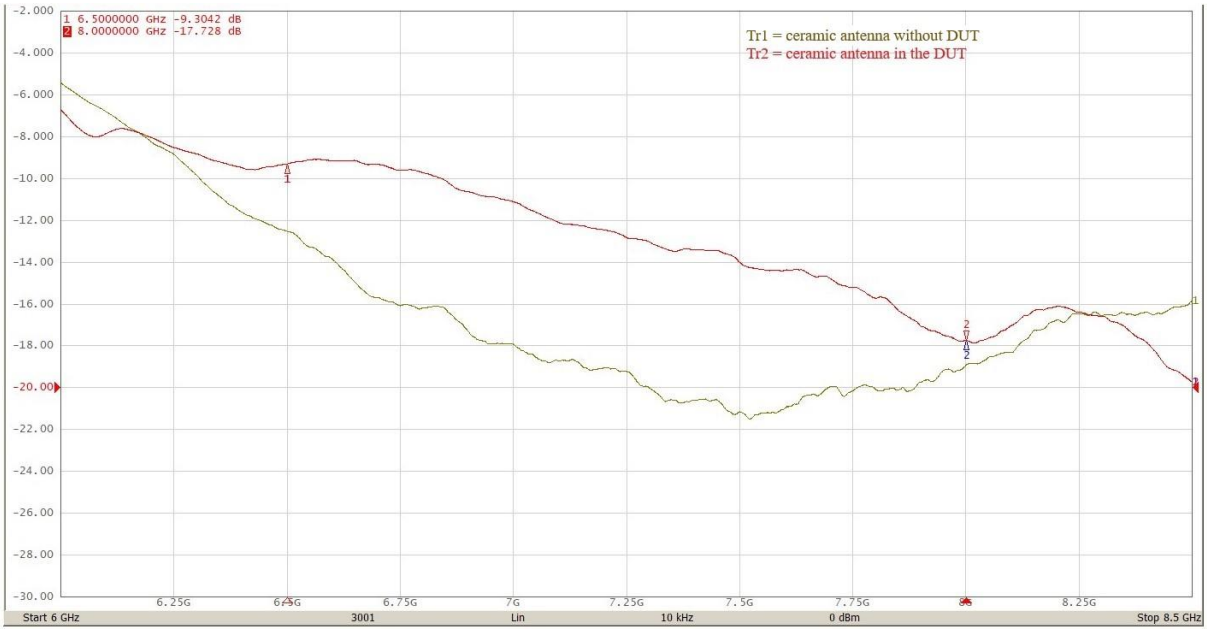

Figure 25. Measured S11 results of the ceramic antenna standalone on its evaluation board and attached to the DUT.

Figure 25 shows the measured S11 results of the ceramic antenna standalone on the evaluation board and attached to the DUT. It could be observed that the S11 values of the ceramic antenna were worse on almost the entire frequency range of 6 – 8.5 GHz when it was attached to the DUT. The difference was about 3 dB at the center frequency of 6.5 GHz (UWB channel 5) and the maximum deviation on channel 5 was 6 dB. The difference was about 1 dB at the center frequency of 8.0 GHz (UWB channel 9), and the maximum deviation on channel 9 was about 5 dB. The S11 values of the ceramic antenna when attached to the DUT were -9.3 dB at the center frequency of the lower UWB channel, and -17.7 dB at the center frequency of the upper UWB channel.

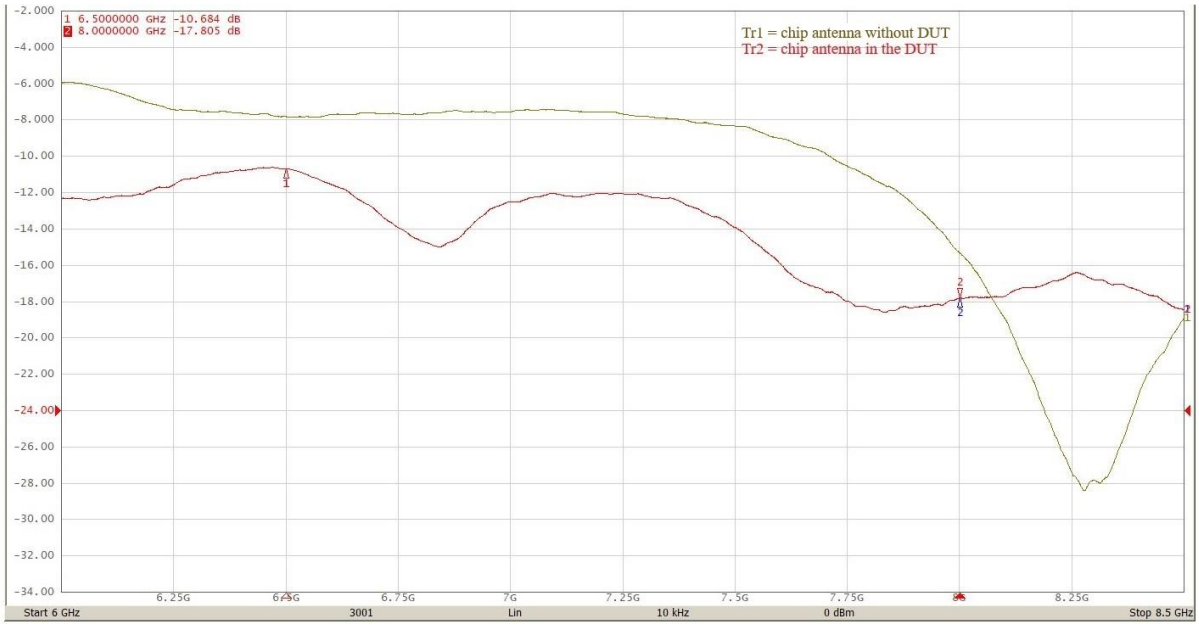

Figure 26. Measured S11 results for the chip antenna standalone on its evaluation board and attached to DUT.

The measurement results of S11 for the chip antenna standalone on the evaluation board and attached to the DUT are presented in Figure 26. The S11 values of the chip antenna were improved when it was attached to the DUT. The S11 result in the DUT was 3 dB better at the center frequency of channel 9 but decreased at the higher edge of the channel. The S11 was 2.5 dB better in the DUT at the center frequency of channel 5 and the maximum deviation on the channel was 6 dB. The S11 value of the chip antenna attached to the DUT was -10.7 dB at the center frequency of the lower UWB channel, and -17.8 dB at the center frequency of the upper UWB channel.

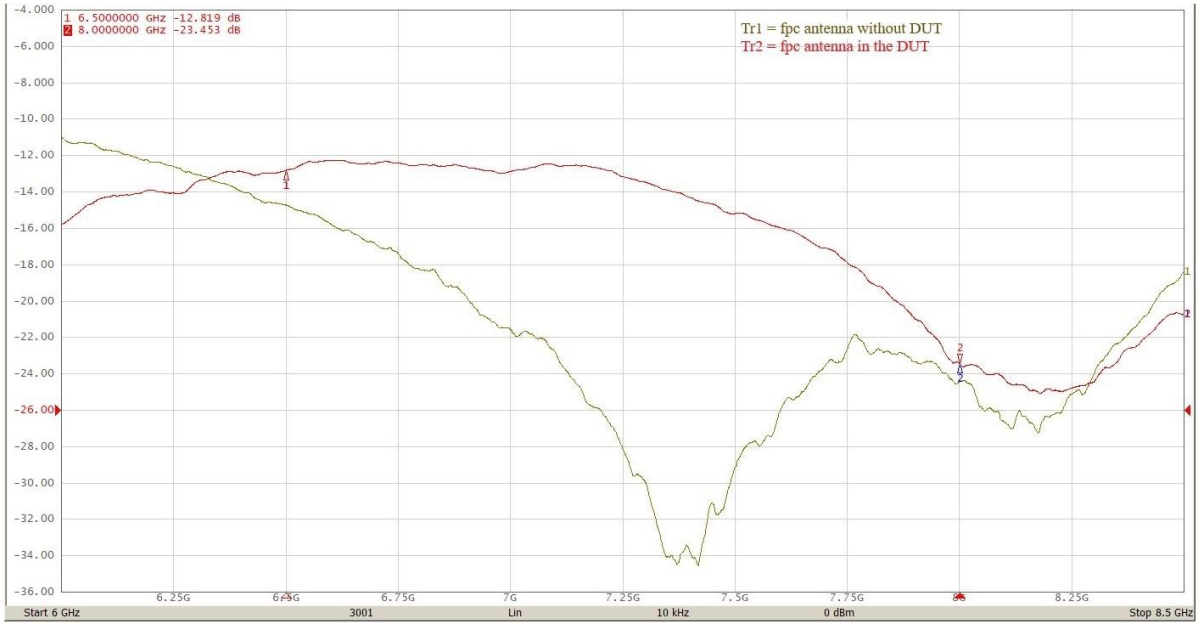

Figure 27. Measured S11 results for the FPC antenna standalone and attached to DUT.

The measured S11 results of the FPC antenna without and with the DUT are presented in Figure 27. The S11 values of FPC antenna were worse when attached to the DUT at the entire studied frequency band. The difference between standalone and the DUT case was 2 dB at the center frequency of channel 5, and 5 dB at the higher edge of the channel. The results of channel 9 were almost equal since the difference was only about 1 dB between cases. The S11 value of the FPC antenna attached to the DUT was –12.8 dB at the center frequency of the lower UWB channel, and -23.5 dB at the center frequency of the upper UWB channel.

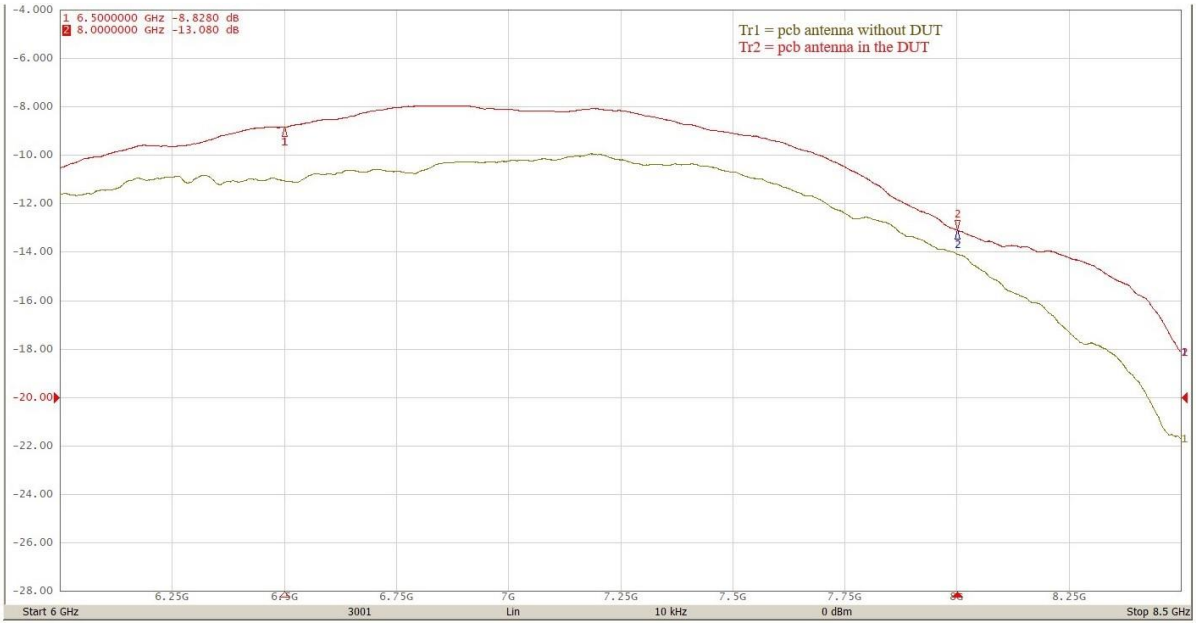

Figure 28. Measured S11 results for the PCB antenna standalone and attached to DUT.

Figure 28 shows the measured S11 results for the PCB antenna standalone and attached to the DUT. The S11 values of the PCB antenna were constantly 1 to 3 dB worse in the entire investigated frequency band when attached to the DUT. The S11 values of the PCB antenna attached to the DUT was -8.8 dB at the center frequency of the lower UWB channel, and -13.1 dB at the center frequency of the upper UWB channel.

As a summary, a clear effect to the S11 values from Figures 25 to 28 could be observed when the studied antennas were attached to the DUT. The chip antenna had a clear matching improvement at lower frequencies when it was attached to the DUT. The target for the antenna matching is -10 dB which is considered good enough for an internal small antenna. However, the PCB and ceramic antenna at lower frequencies did not meet this target. It should be noted that the sizes of the antennas and their modules vary, thus the openings of the metal frame were not exactly the same size for all, and this may have contributed to the results. The ceramic and chip antenna were attached on top of their own evaluation boards, and thus the antenna radiators themselves were located slightly higher from the prototype device than the FPC and PCB antennas. A minor movement of the cable or the position of the antenna during the measurements affected the results, but to minimize the effect the positions of the cable and antennas remained the same in each measurement.

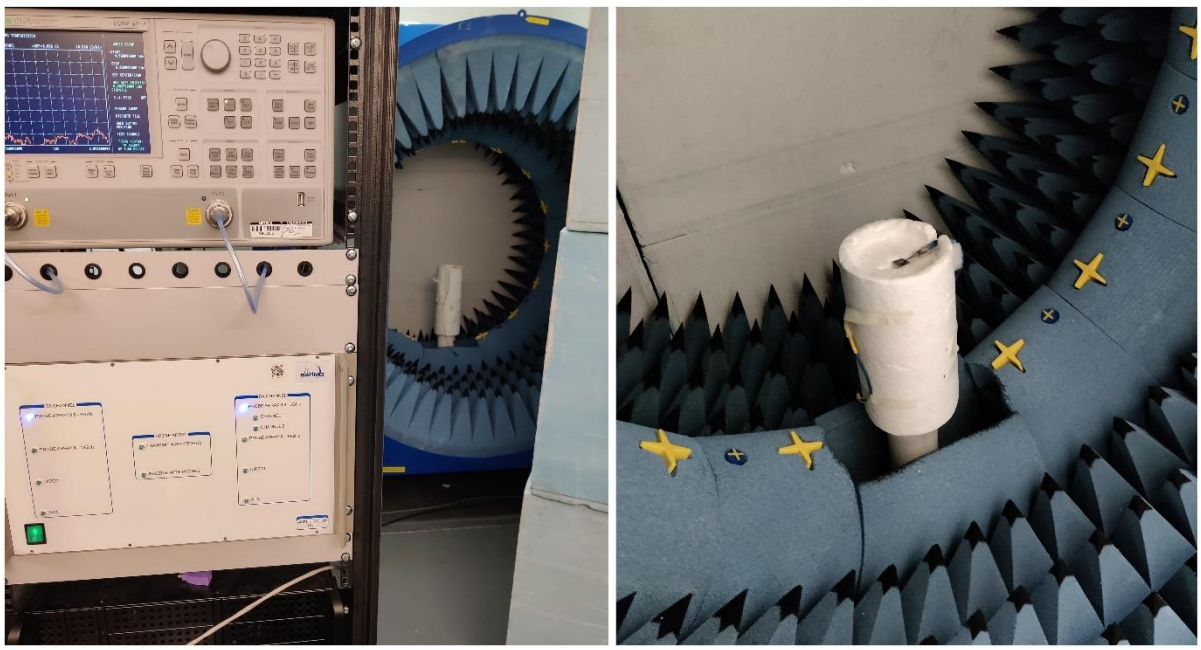

Figure 29. Satimo Starlab 18 measurement system and its antenna chamber.

Radiated measurements were performed on the selected antennas at the University of Oulu radio laboratory, where the antenna measurement system Satimo Starlab 18, which is shown in Figure 29, was used. The Starlab is an excellent tool for measuring antennas, and it consists of a network signal analyzer, an antenna chamber and a control unit to run dedicated software. Several antenna probes are placed in the antenna chamber controlled by the control unit, as shown on the right side of Figure 29. The control unit revolves a mast where the DUT is placed. Starlab collects a certain number of samples from the near-field with its sensors to calculate the far-field response with the FFT. The software calculates the gain, directivity, radiation patterns (in 1D, 2D and 3D), and radiation efficiency based on results. The Starlab 18 supports frequencies from 800 MHz up to 18 GHz and thus the studied frequency range 6000 – 8500 MHz is conveniently located in the middle of it. [57]

All the studied antennas are omnidirectional style and the Satimo system was calibrated to match this kind of environment by using the Satimo's reference antenna. The calibration software corrects systematics errors from the measurements. The measurement system was calibrated to cover 6000 – 8500 MHz with steps of 50 MHz, resulting in 50 measurement points, which is sufficient for creating a far-field response. The control software can perform the near-field to far-field conversion for the measurement results and for plotting gains, efficiencies and radiation patterns.

A total of eight radiation measurements were performed with the Satimo system: four antennas as standalone and four when attached to the DUT. The goal for analysis was to understand magnitude of the passive loading of the prototype device to the radiation performance of the antennas. Each measurement arrangement was photographed before the chamber was closed, and the images were used to confirm the position of the antenna, and thus ensured that the placement accuracy was in the order of a centimeter at most. The inaccuracies caused by the position of the antenna and the movement of the cable were therefore considered minimal in the measurement results.

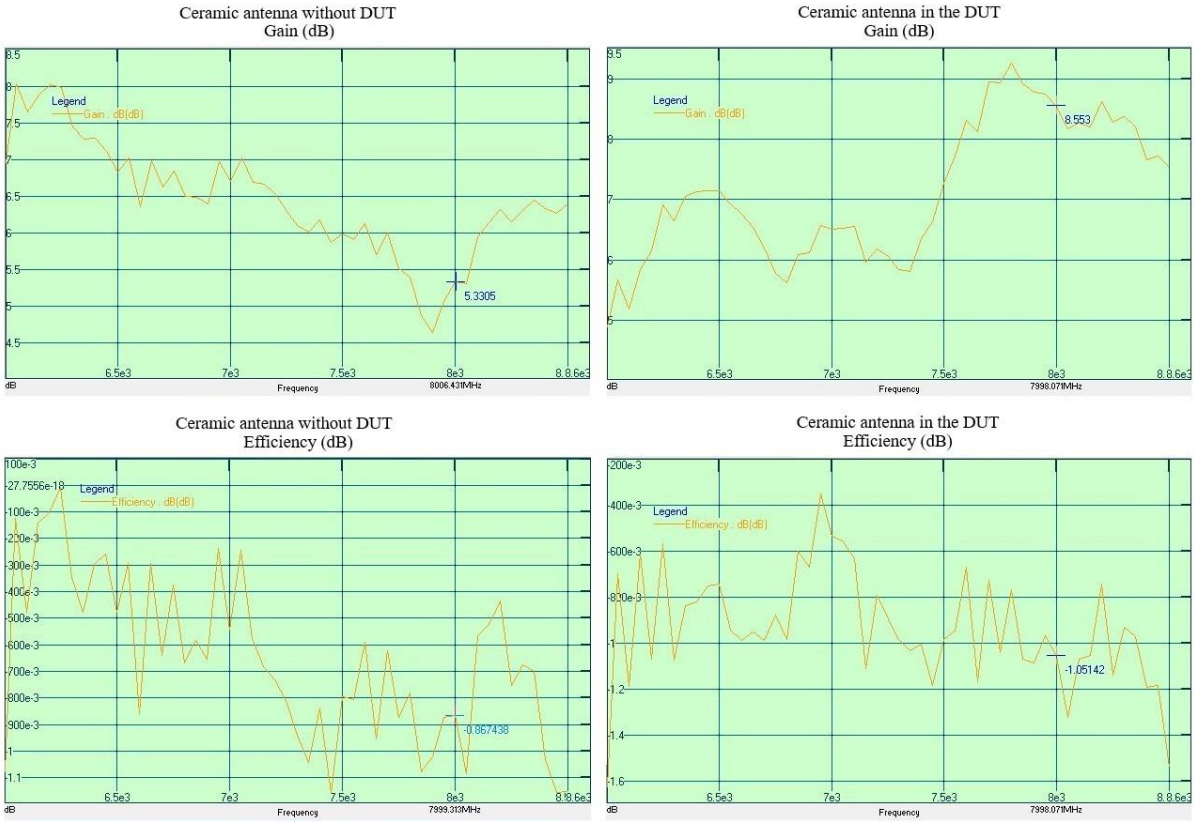

Figure 30. Gain and efficiency of the ceramic antenna at frequencies 6 – 8.5 GHz standalone on its evaluation board and attached to the DUT.

Figure 30 presents the gain and radiation efficiency of the ceramic antenna without and with the DUT. It can be observed that the gain was higher in the upper band when the antenna was attached to the DUT, and at the center frequency of the upper UWB channel at 8 GHz the difference was about 3.2 dB. The efficiency was slightly worse at lower frequencies when the antenna was attached to the DUT, but at higher frequencies there was no significant difference.

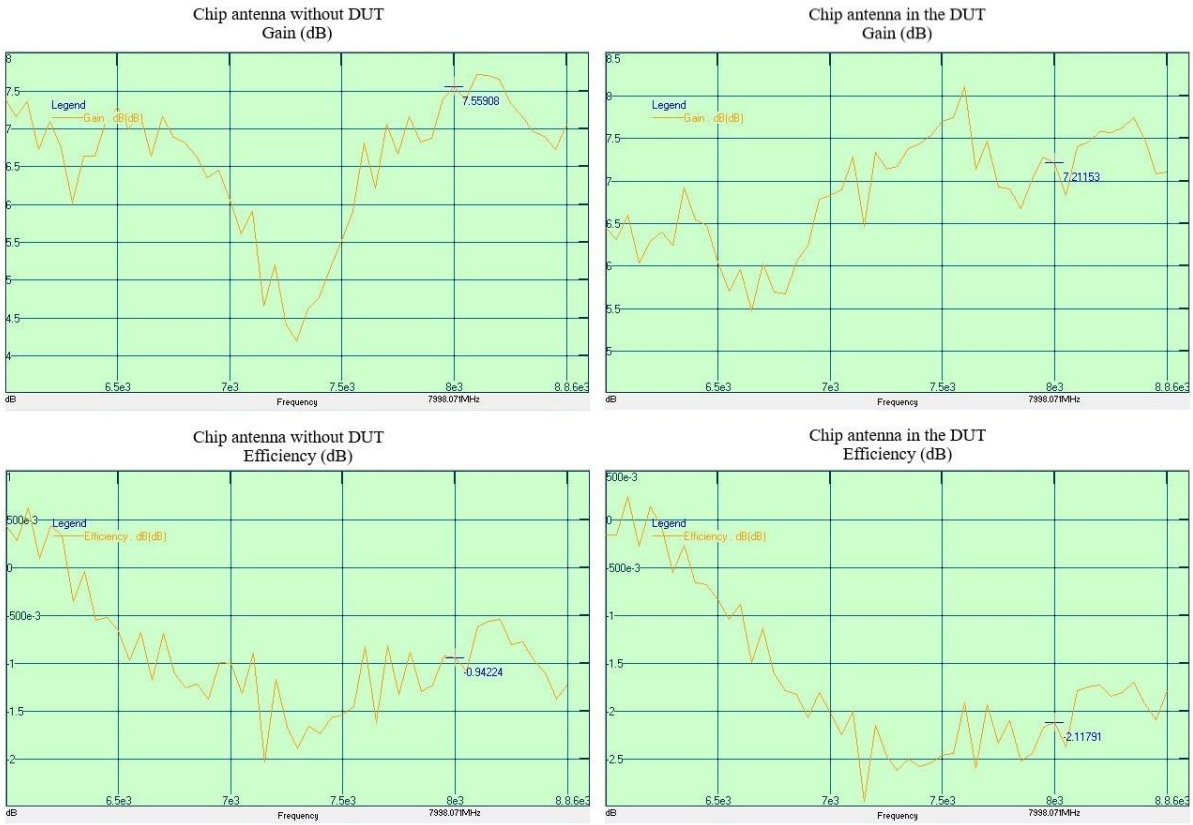

Figure 31. Gain and efficiency of the chip antenna at frequencies 6 – 8.5 GHz standalone on its evaluation board and attached to the DUT.

Figure 31 shows the gain and efficiency of the chip antenna standalone on the evaluation board and when attached to the DUT. The gain was slightly lower on the UWB channel 5 when the antenna was attached to the DUT, but at higher frequencies there were minor differences. The efficiency, on the other hand, deteriorated a little over the entire investigated band when the chip antenna was attached to the DUT.

The antenna gains and efficiencies without the DUT and when attached to the DUT are presented in Figure 32 for the FPC antenna and in Figure 33 for the PCB antenna. When the FPC antenna was attached to the DUT compared to standalone, the gain was lower on the UWB channel 5 and higher on the UWB channel 9. The efficiency of the FPC antenna with the DUT was slightly weaker in the entire investigated frequency band. When the PCB antenna was attached to the DUT, the gain was lower on the UWB channel 5 and higher on the UWB channel 9, and the efficiency was also somewhat worse in the entire studied band, as was the case with the FPC antenna.

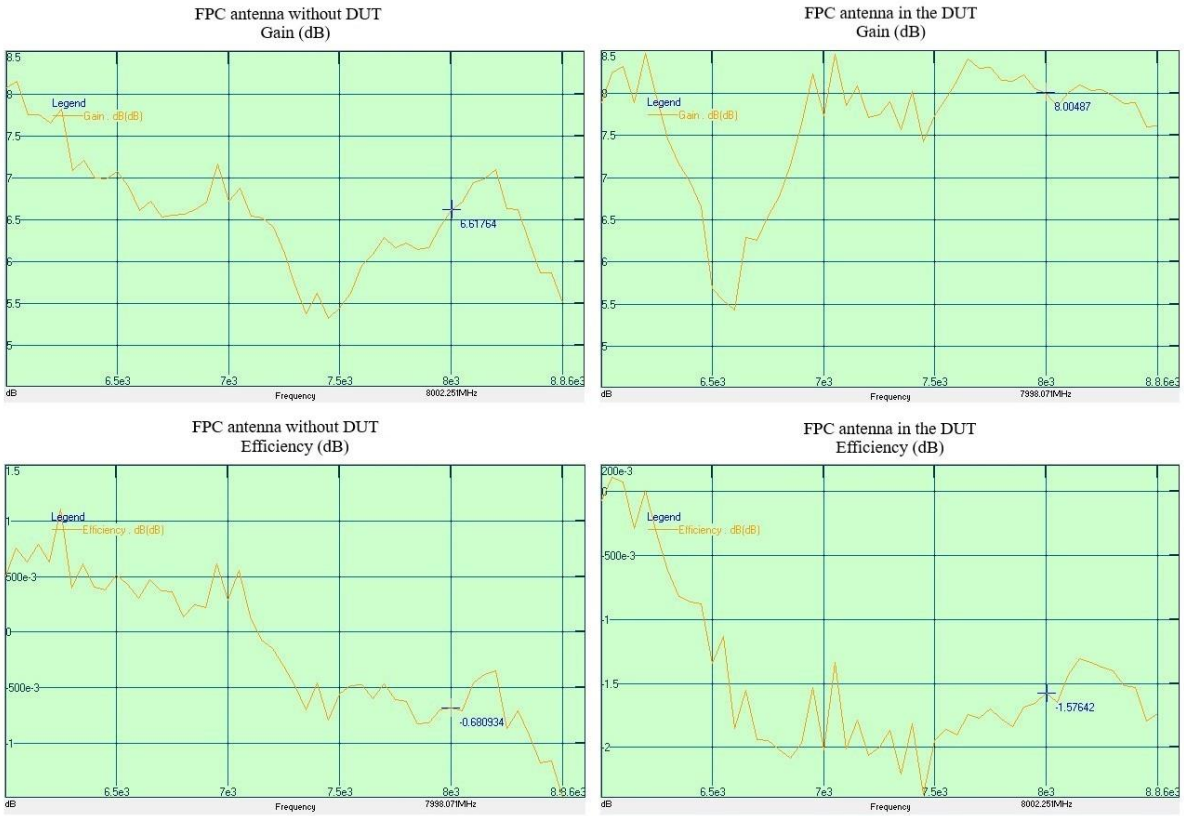

Figure 32. Gain and efficiency of the FPC antenna at frequencies 6 – 8.5 GHz standalone and attached to the DUT.

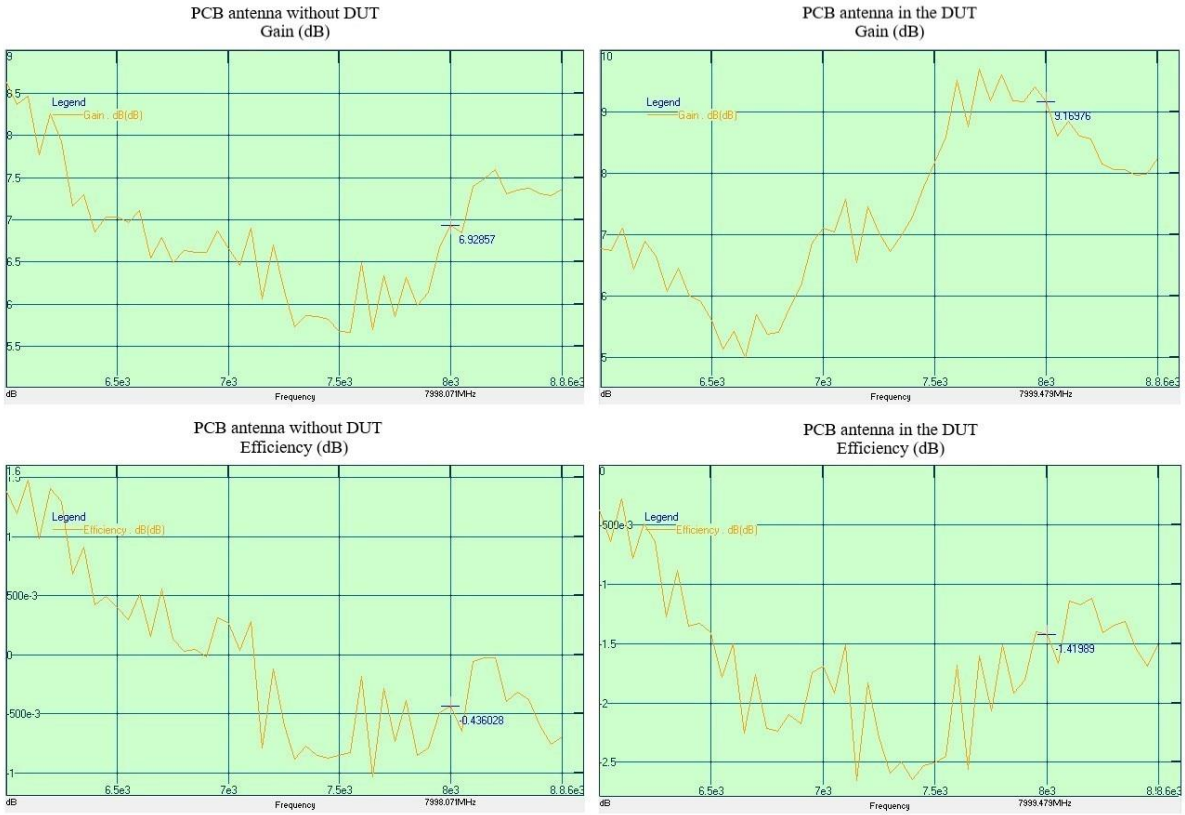

Figure 33. Gain and efficiency of the PCB antenna at frequencies 6 – 8.5 GHz standalone and attached to the DUT.

It should be noted that in some of the results the efficiency was more than 0 dB, in other words more than 100%, which would mean that the antenna radiated more power than was fed into it. This is hardly true, so it can be assumed that there were some uncertainties in these measurement results, possibly due to an error in calibration or sampling. The efficiency of an antenna indicates the ratio of the power radiated from the antenna and the power fed into it. It is usually expressed in percentages or decibels, for example: 100% corresponds 0 dB, while 80% is -1 dB, 50% is -3 dB, 10% is -10 dB and so on [56].

In all conductive and radiated measurements, the openings in the metal frame were not the same size for all the studied antennas, because the sizes of the antennas and their modules vary slightly. Antenna gains are quite low in portable devices, due to the small size and omnidirectional nature of the antenna, usually in the range of 2 to 7 dB. In this application, as well, the antenna is wanted to radiate power as evenly as possible in all directions, and not just in a certain direction. In portable devices, for example, the efficiencies of the Wi-Fi antennas are typically in the range of -6 dB to -2 dB [56]. The results of gains and efficiencies are therefore in line with typical values, since the measured gains range from 5 to 9 dB and the efficiencies were better than -3 dB.

The radiation pattern of the antenna defines how much the antenna radiates in each direction. An omnidirectional pattern is required for the antennas in the mPOS application since the locations of the receiver and the transmitter can vary considerably, and the antennas must transmit and receive signals from all directions. Figure 34 shows the used three-dimensional coordinate system for the antenna measurement, and the position of the antenna in this system. [56][58]

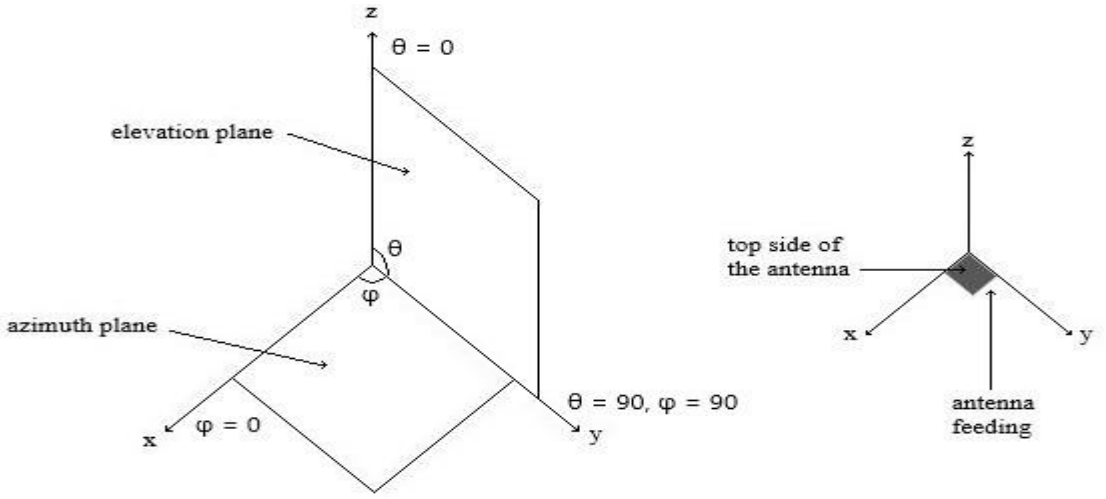

Figure 34. Three-dimensional coordinate system for the antenna measurement and antenna position in the measurement system.

The 3D antenna pattern is plotted on two principal planes: the horizontal plane which is also called the azimuth plane, and the vertical plane which is also called the elevation plane, as illustrated in Figure 34 [58]. The antenna was placed on the azimuth plane as shown in the Figure 34, where the top side points parallel to the z-axis, at angle $\theta = 0°$. The radiation power of the antenna must be calculated with all values of θ and φ to construct the 3D radiation pattern. The benefit of the 3D radiation pattern is that it is easy to read and thus understand how the antenna radiates into different directions. The radiation patterns of all the studied antennas are presented in the 3D coordinate system at the center frequencies of the UWB channels 5 and 9 in the figures below. The radiation patterns were also measured for both the

standalone antenna configuration and when attached to the DUT. The radiation patterns were plotted with the Satimo system, where the red and orange correspond the high radiation level, the yellow and green the medium radiation, and the blue means low radiation in Figures 35 to 38.

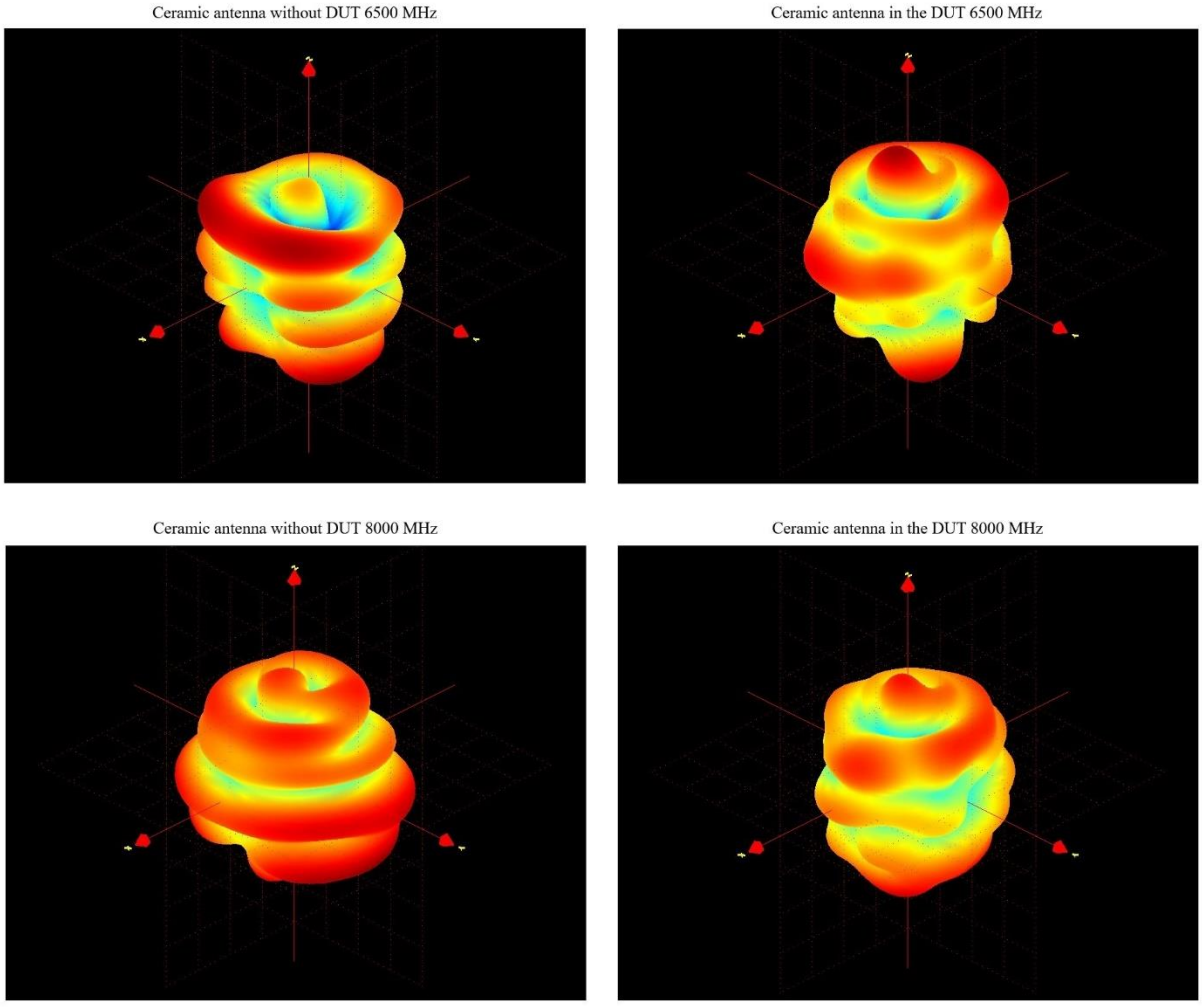

Figure 35. 3D radiation patterns of the ceramic antenna standalone on its evaluation board and attached to the DUT at the center frequencies of UWB channels 5 and 9.

Figure 35 shows the 3D radiation patterns of the ceramic antenna on the left standalone on its evaluation board and on the right attached to the DUT at the center frequencies of the UWB channels 5 and 9. A slightly reduced radiation power was observed on the lower channel with the DUT, which can be partially explained by the reduced efficiency. In the upper channel, the radiation power deteriorated even more, the most obvious reason being the reduced efficiency and the increased gain when the ceramic antenna was attached to the DUT. Although the radiation power has reduced, the radiation pattern has remained omnidirectional, which is the most important aspect in this case.

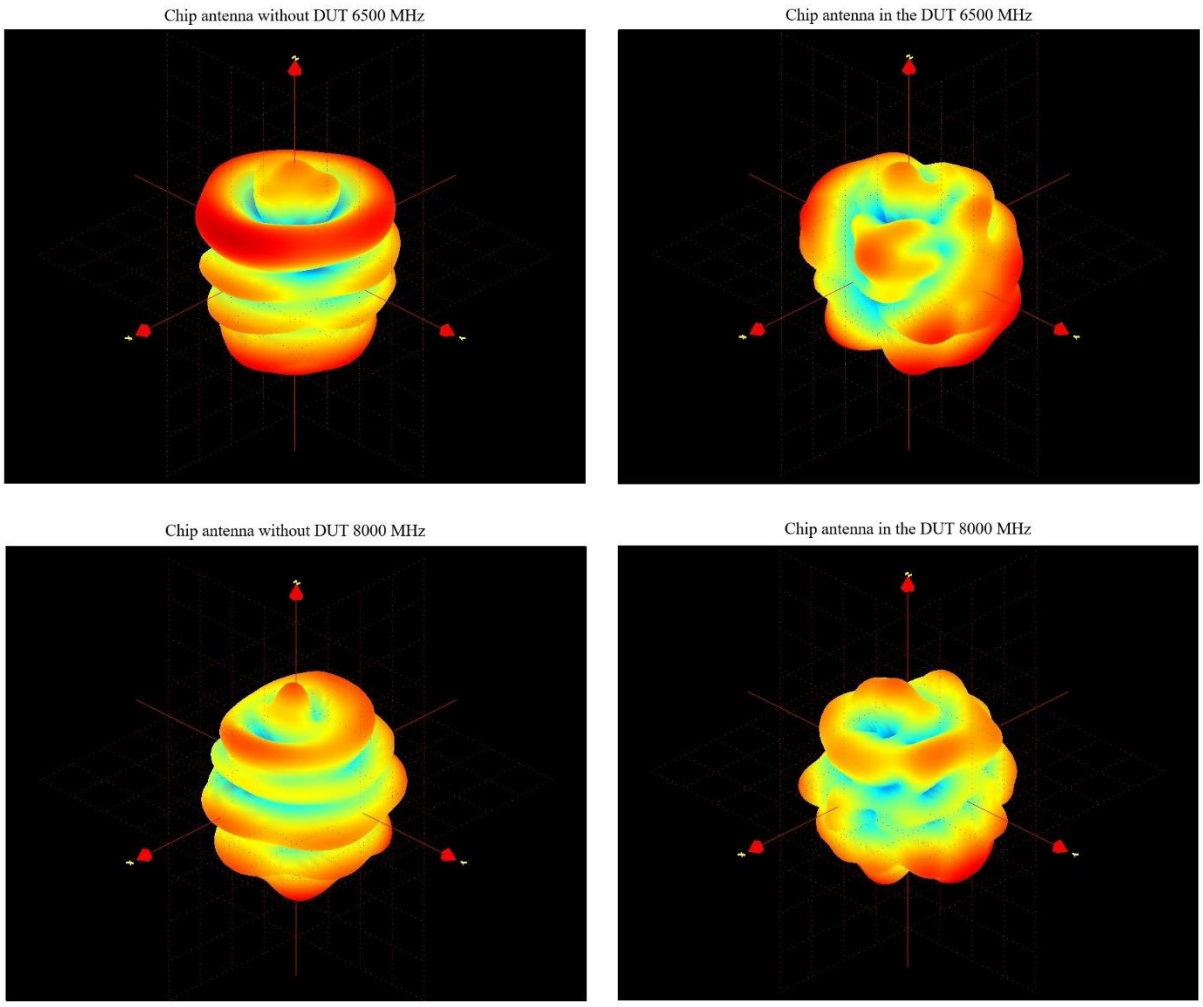

Figure 36. 3D radiation patterns of the chip antenna standalone on its evaluation board and attached to the DUT at the center frequencies of UWB channels 5 and 9.

Figure 36 shows the 3D radiation patterns of the chip antenna on the left without the DUT and on the right attached to the DUT at the center frequencies of the UWB channels 5 and 9. A clear change in the radiation patterns and radiation power on both channels can be seen when the chip antenna was attached to the DUT. In the upper channel the radiation power was quite low even without the DUT, and when attached to the DUT the additionally degradation can be partially explained by the reduced efficiency and increased gain. However, the radiation pattern has remained somewhat omnidirectional, and the radiation power is expected to cover a short-range operation at least.

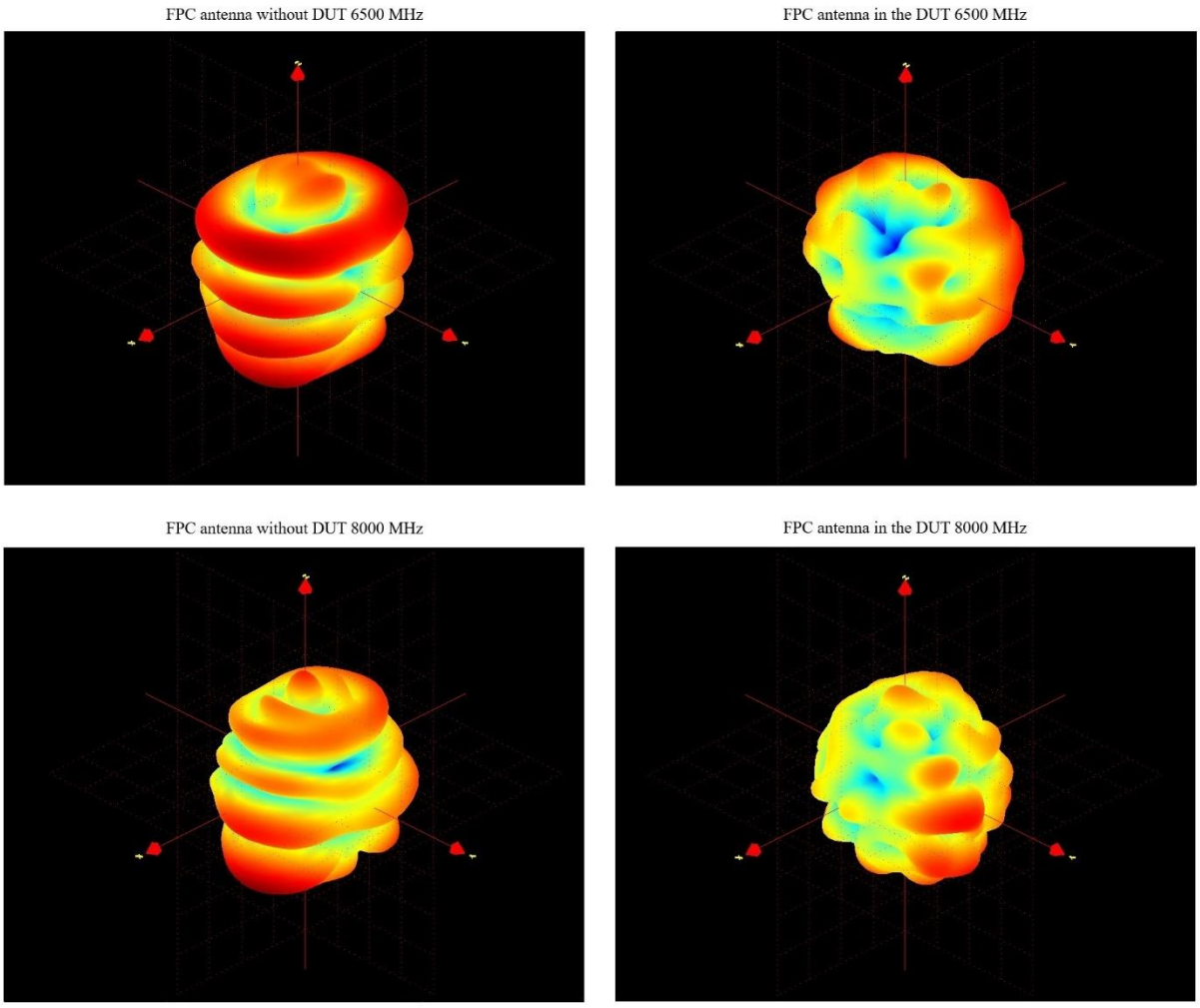

Figure 37. 3D radiation patterns of the FPC antenna standalone and attached to the DUT at the center frequencies of UWB channels 5 and 9.

Figure 37 shows the 3D radiation patterns of the FPC antenna on the left standalone and on the right attached to the DUT at the center frequencies of the UWB channels 5 and 9. Now a clear change in the radiation patterns of the FPC antenna when attached to the DUT and a degradation of the radiation power could be observed, mostly in the positive direction of the x-axis. This can be partly explained by the fact that this thin FPC antenna was located slightly more inside the DUT than the previously measured antennas, which were located on the top of thicker evaluation boards. Thus, the metal frame located around the FPC antenna was preventing more radiation. Additionally, the efficiency was also reduced when the FPC antenna was attached to the DUT. Although the radiation power with the DUT in certain directions was weaker on both studied frequencies, the patterns remained omnidirectional.

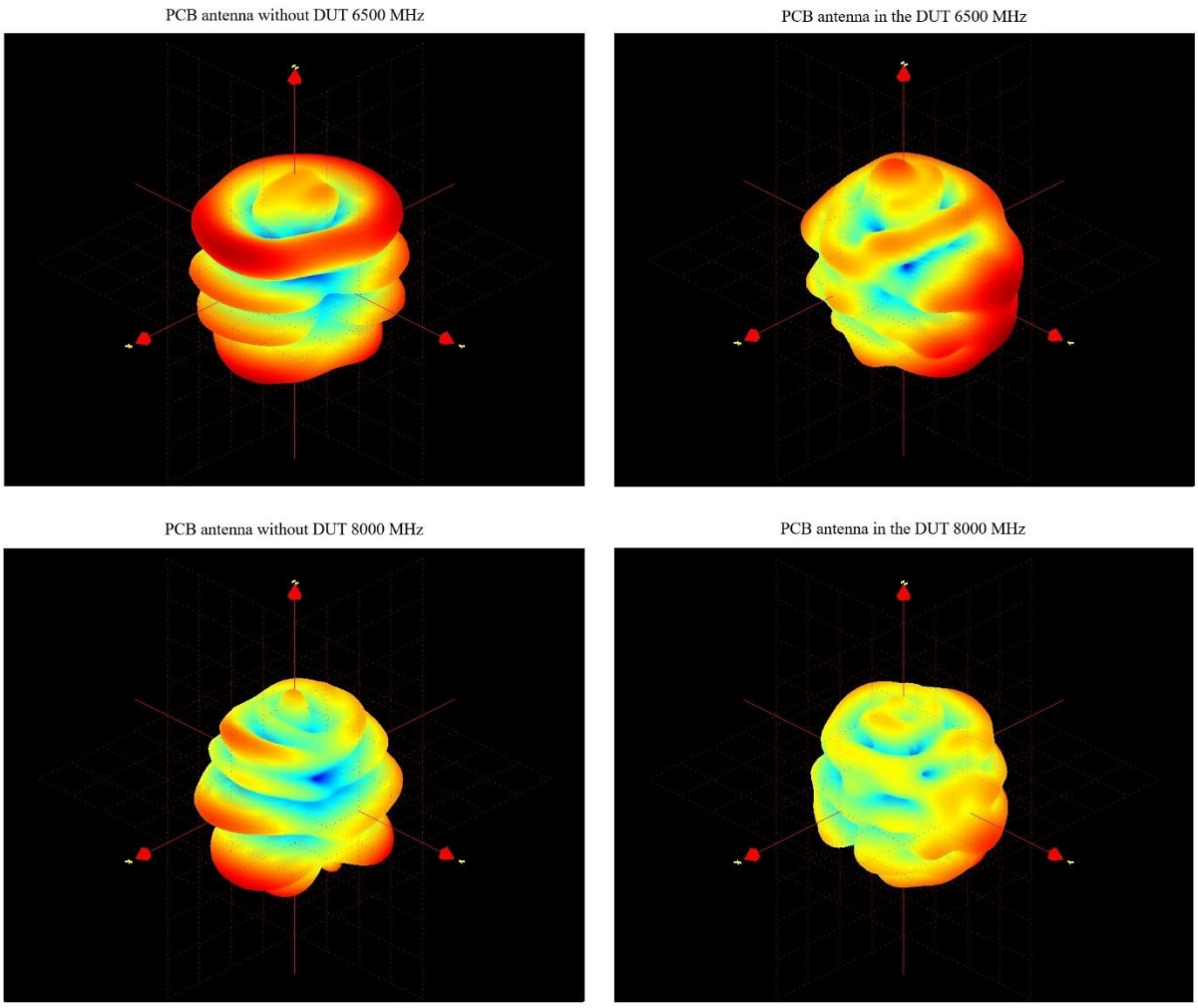

Figure 38. 3D radiation patterns of the PCB antenna standalone and attached to the DUT at the center frequencies of UWB channels 5 and 9.

Figure 38 shows the 3D radiation patterns of the PCB antenna on the left without the DUT and on the right attached to the DUT at the center frequencies of the UWB channels 5 and 9. It could be noticed that the radiation power was reduced, and the radiation pattern changed for the PCB antenna with the DUT at both frequencies. The degradation of the radiation power on the upper channel can be partly explained by the decreased efficiency and increased gain. The PCB antenna also did not have a separate evaluation board, so it was located a little deeper in the DUT like the FPC antenna, and similarly the radiation was weakest to the positive x-axis direction. However, the omnidirectional radiation pattern was still visible when the PCB antenna was attached to the DUT.

The radiation patterns of all antennas changed when the antennas were attached to the DUT based on the results from Figures 35 to 38. As a summary, the radiation power of all the studied antennas decreased at the center frequencies of the UWB channels 5 and 9 when they were attached to the DUT. The ceramic antenna worked best, while the performance of the FPC antenna was most impacted when attached to the DUT. The results were partly affected by the openings made in the metal frame of the DUT, where the antennas were placed for the measurements. The openings were not identically sized for all measured antennas due to the differences in the sizes of the antenna modules or their evaluation boards. Similarly, the

antennas that did not have separate evaluation boards were located a little deeper in the DUT, so the effects of the surrounding metal frame were probably greater.

The distance from the antenna to the closest mechanical part of the DUT affects the matching and radiation results. Additionally, the metal parts close to the radiator may act as an additional radiator alongside antennas and have a significant effect on the operation and performance of the antenna. Thus, the size of the opening in the metal frame has an effect on the antenna and therefore it was also studied.

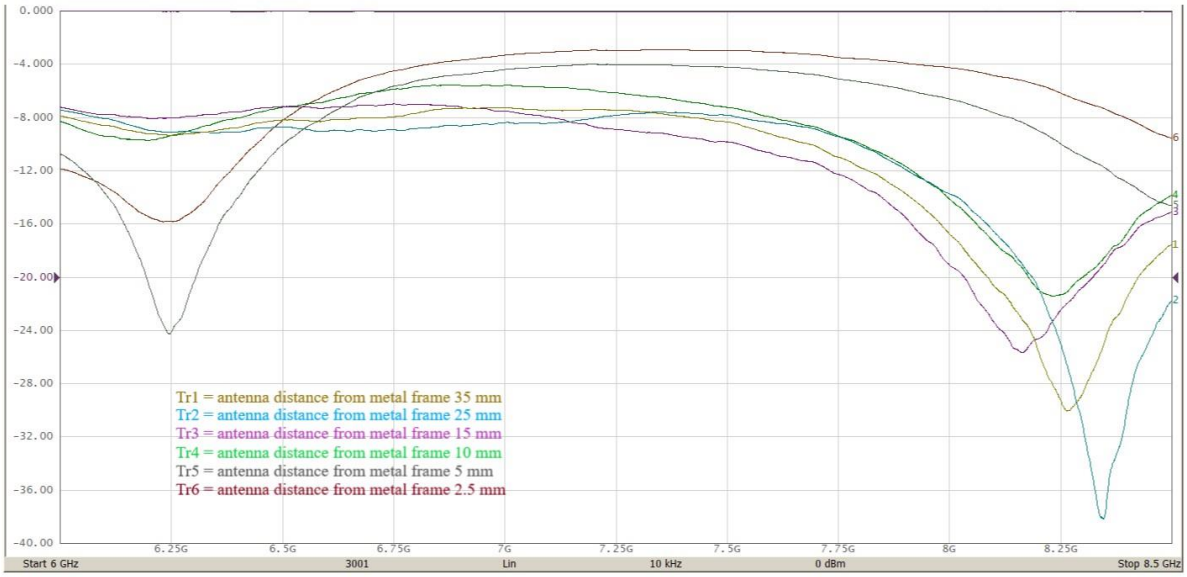

Figure 39. Measured S11 results for the standalone chip antenna on its evaluation board with different distances from the metal frame.

The effect of the distance from the standalone chip antenna on its evaluation board to the metal frame is shown in Figure 39 expressed by the S11 results. At 35 mm from the metal frame, the S11 value was basically the same as the standalone chip antenna, but at 25 mm, a slight degradation was seen in the upper band and a shift of the notch to a higher frequency. When the distance was reduced to 15 mm, the notch weakened and moved to a lower frequency, but at the center frequency of the UWB channel 9 at 8 GHz, the S11 value was slightly better than without the metal frame. At distance of 10 mm, it could be observed that the notch had become even smaller and moved to 8.25 GHz. By further reducing the distance, the notch moved towards 8.5 GHz until it went out of the measurement range and a new notch appeared at lower frequencies. By reducing the distance to 5 mm, the notch was now at 6.25 GHz and the S11 value had deteriorated in the entire upper frequency band. When the distance between the antenna and the metal frame was only 2.5 mm, the S11 values and the notch decreased even more.

The antenna performance can be tuned slightly better at the studied frequencies by changing the distance of the antenna to the metal frame, i.e., by changing the size of the opening in the metal frame. It is possible to find the ideal size for the opening, optimizing the best S11 value for both UWB channels 5 and 9 or only for one channel. It was observed that there was an improvement in the lower channel when the distance of the antenna to the metal frame was about 5 mm, and in the upper channel there was an improvement at distances of 10 to 15 mm.

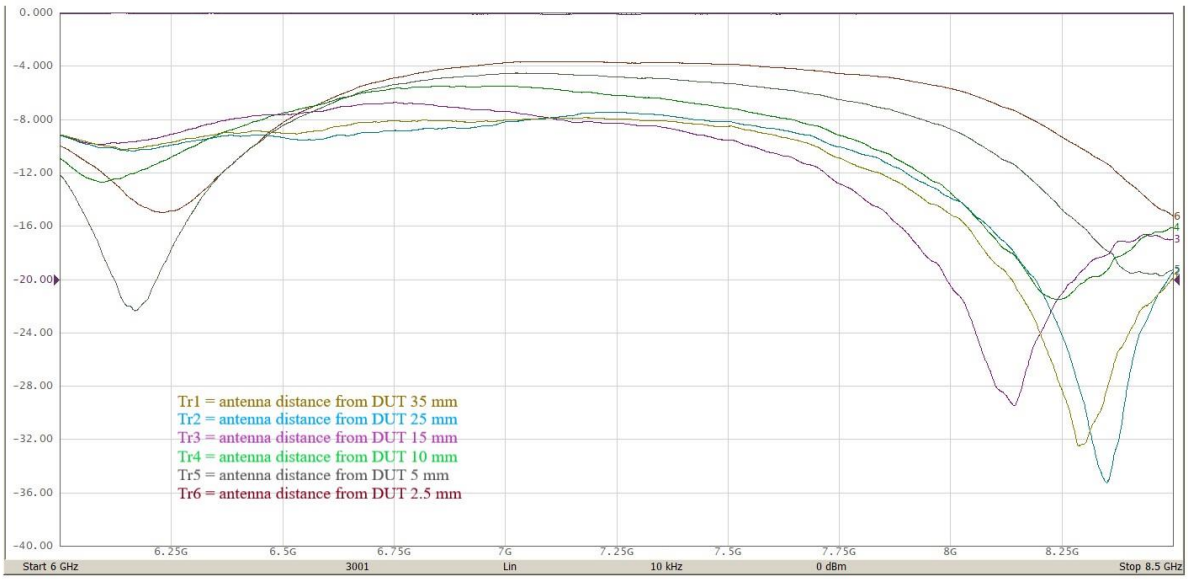

Figure 40. Measured S11 results for the standalone chip antenna on its evaluation board with different distances from the DUT.

In Figure 40, the measurements for the S11 parameter have been performed for the chip antenna on its evaluation board, when the distance of the antenna to the prototype DUT was changed. It could be noticed that the S11 results were similar to the previous measurement with just the metal frame, although now other passive loads of the DUT were also included. This proves that the biggest individual passive contributor to the antenna performance in the prototype DUT is the metal frame.

4.3 UWB system measurements

The UWB system measurements were performed to verify the operation of two UWB modules and their location accuracy against the manufacturer's specifications. A new measurement setup was needed so that the distance and angle measurements could be accurately performed and to enable the exchange of the studied antennas between the measurements. There were two alternatives for the measurement system: the first, where the UWB modules are located at stationary points and the UWB module equipped with a double antenna can rotate to examine the angle, and the second, where the UWB module equipped with the one antenna would go around the circumference of a circle, and the UWB module equipped with the two antennas would be in the center of the circle. However, the second system would require a large space for the measurements and the possibility of distance errors would be greater. Therefore, it was decided to create a platform where the UWB evaluation boards are located in fixed positions exactly two meters apart from each other. Other aspect of the platform was that the UWB evaluation board with the double antennas must be able to rotate so that the distance remains unchanged when the angle is changed. An illustration of the measurement platform from the top and from the side, as well as the locations of the UWB evaluation boards with their antennas is shown in Figure 41. All system level measurements were performed only for the UWB modules and antennas without the prototype device.

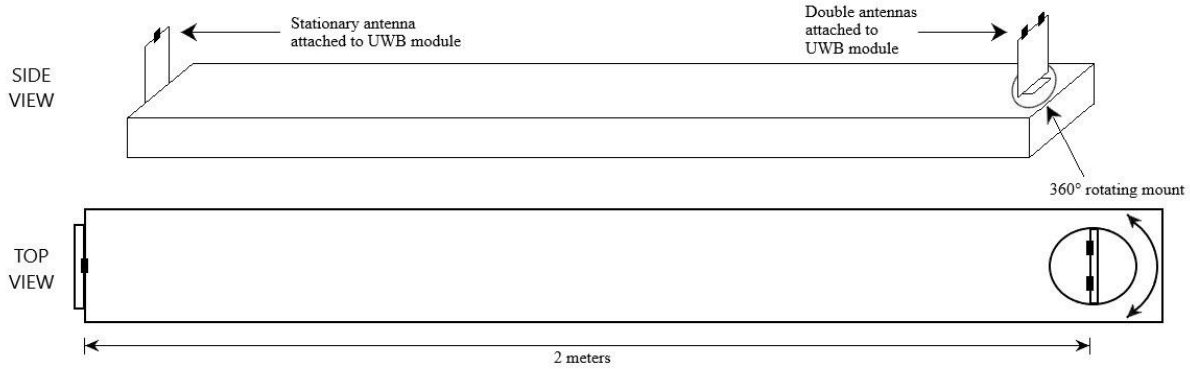

Figure 41. Illustration of the measurement platform from above and from the side, as well as the location of the UWB modules with antennas.

The measuring platform was made from a wooden plank and bases for the UWB modules were added to it. A photograph of the final measuring platform for measuring the distances and angles of the UWB modules as well as for the antenna calibration is showed in Figure 42. The single-antenna UWB module with a stationary base acts as a tag in the system. The double antenna UWB module acts as an anchor and has a 360-degree rotating base that can be adjusted in 15-degree steps. The specifications for the DW3000 chip in the LOS situations are ranging accuracy of ±6 cm and angle accuracy of ±10 degrees. In addition, if the angle is greater than ±60°, the measurement accuracy is no longer that reliable according to the manufacturer. Therefore, the angles were only examined to ±60° on the UWB channels 5 and 9 with all studied antennas. The ranging accuracy was measured for all four antennas in the LOS situations at distances of 2, 5, 10, 15 and 20 meters on the UWB channels 5 and 9.

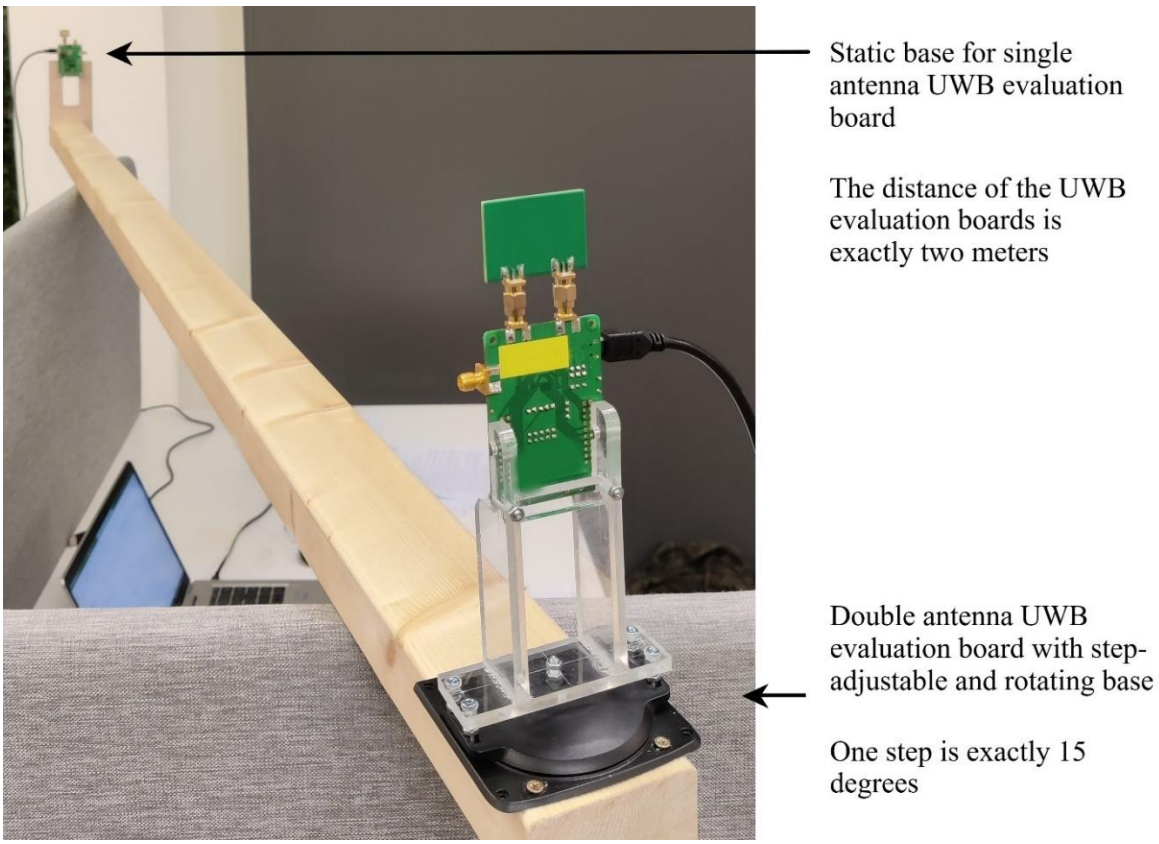

Figure 42. A measurement platform created to study the UWB operation.

The antenna distance can be accurately calibrated to two meters by modifying the delay parameter of the modules. By adding or subtracting one nanosecond of the delay to the flight time, a 30-centimeter change in distance is obtained. The measurements were performed using the three-message two-way ranging method. The UWB modules came with computer software that can configure one module as an anchor and the other as a tag. The double antenna module (anchor) listens the incoming messages from the single antenna module (tag) and responds to them. When the final message, containing the necessary timestamps, arrives from the tag to the anchor, the distance and the angle can be calculated. Channel parameters can be changed but those must be the same on both modules to establish the connection and perform communication successfully.

Before pairing, both UWB modules are in the search mode and listen for Blink messages. When the tag is turned on, it starts sending these Blink messages that contain its address. If the selected channel parameters are the same on the modules, the other UWB module can now receive these Blink messages. The anchor operation can be started, and the user must accept permission for the anchor to connect with the tag based on the address. After this, the anchor-tag pair switches to ranging mode and starts exchanging TWR messages and calculating PDoA if the PDoA mode is on. On the computer, the software calculates the average and standard deviation of the distances and PDoA values. The program also reports with an error code if there are errors in transmission or reception.

The measurements were started by examining the accuracy of the angles with the help of the measurement system as presented in Figure 42. Two antennas less than 20 millimeters apart were needed for the angle measurement, and due to the physical size of the antennas, it was a challenge. This physical size can also limit the choice of the final antenna if there is not enough space for the antennas and their required openings in the device. Another factor that had to be considered when measuring the angle was that the two antennas of the UWB module were quite overlapping after 60 degrees, so this could affect the inaccuracies of the measurement results.

The antennas were calibrated by modifying the delay parameter to match the distance of two meters, and the measurements were performed with the following channel parameters: UWB channel 5 or 9, preamble length 128, preamble code 9, PRF 64 MHz, data rate of 6.81 Mbit/s, STS field before PHR and Payload fields, STS length 128, standard PHR mode with 850 kbit/s data rate and PDoA mode on. The measurement results on the UWB channel 5 including five different antennas as well as their results for the distances and PDoA values for angles from 0° to ±45° with 15-degree steps, are presented in Table 3. Now the measurement also included the original double antenna that came with the UWB modules, and its results can be used as a reference for the results of the other studied antennas. In each measurement, 50 TWRs were performed from which the average and standard deviation were calculated for the distance and PDoA value. In addition, the measurements were repeated 3 times to ensure the reliability and repeatability of the results.

Table 3. Distances and PDoA results for angles from 0° to ±45° obtained with the different antennas on the UWB channel 5. The value above is the average and below in parentheses is the standard deviation of 50 TWR results. Orig is the double antenna that came with the UWB modules.

Antenna	**Distance**	**Angle 0°**	**Angle -15°**	**Angle -30°**	**Angle -45°**	**Angle 15°**	**Angle 30°**	**Angle 45°**
Orig1	1.9958m	-7.7°	41.5°	83.4°	134.6°	-65.6°	-102.9°	-142.1°

	(3.5cm)	(11.5°)	(8.0°)	(9.1°)	(6.9°)	(9.0°)	(7.5°)	(8.2°)
Orig2	2.0177m (2.8cm)	-1.5° (9.4°)	45.8° (9.5°)	86.5° (10.1°)	135.8° (5.6°)	-66.7° (9.0°)	-103.0° (9.0°)	-135.1° (8.1°)
Orig3	1.9944m (2.4cm)	-5.1° (7.3°)	41.2° (8.3°)	87.3° (8.1°)	139.9° (6.7°)	-64.7° (9.2°)	-100.3° (7.8°)	-139.0° (7.8°)
Cera1	2.0016m (6.7cm)	-52.4° (11.5°)	-21.6° (6.6°)	35.2° (10.1°)	124.7° (11.0°)	-74.3° (13.2°)	-109.6° (8.7°)	-156.5° (6.3°)
Cera2	2.0200m (3.5cm)	-54.2° (10.4°)	-16.3° (7.5°)	33.6° (10.2°)	122.2° (10.9°)	-72.7° (11.6°)	-110.6° (7.2°)	-153.1° (6.4°)
Cera3	2.0040m (4.8cm)	-50.2° (9.4°)	-20.0° (6.9°)	34.1° (10.3°)	123.9° (7.8°)	-76.8° (12.8°)	-110.7° (7.7°)	-153.1° (6.4°)
Chip1	2.0151m (2.6cm)	-2.8° (6.9°)	72.4° (8.5°)	101.8° (7.8°)	133.1° (5.7°)	-86.0° (6.3°)	-116.0° (8.4°)	-114.3° (7.0°)
Chip2	2.0021m (3.2cm)	-6.6° (8.2°)	73.4° (9.8°)	106.1° (6.8°)	132.0° (7.8°)	-90.0° (7.7°)	-119.1° (6.7°)	-118.2° (9.0°)
Chip3	2.0143m (3.6cm)	-3.9° (8.5°)	70.4° (9.6°)	107.9° (8.1°)	131.8° (6.1°)	-85.4° (6.9°)	-116.7° (8.9°)	-114.7° (9.1°)
FPC1	2.0153m (2.7cm)	-17.9° (6.5°)	32.0° (8.4°)	67.8° (9.7°)	90.6° (8.3°)	-69.1° (6.3°)	-109.4° (7.6°)	-152.8° (6.2°)
FPC2	1.9967m (3.8cm)	-14.5° (6.7°)	33.1° (8.1°)	65.9° (8.8°)	92.4° (10.2°)	-72.6° (6.8°)	-110.3° (6.7°)	-151.7° (5.9°)
FPC3	2.0039m (3.4cm)	-21.5° (8.6°)	34.8° (9.8°)	66.1° (9.7°)	87.6° (9.4°)	-69.8° (7.1°)	-115.3° (6.9°)	149.0° (6.4°)
PCB1	2.0190m (1.9cm)	44.1° (9.2°)	100.5° (10.4°)	--- (179.0°)	-104.2° (18.0°)	2.6° (9.4°)	-33.4° (7.2°)	-63.5° (7.8°)
PCB2	2.0106m (2.8cm)	46.1° (7.7°)	102.8° (12.0°)	--- (169.5°)	-108.8° (17.7°)	-1.8° (8.5°)	-36.2° (6.2°)	-60.6° (8.0°)
PCB3	2.0054m (2.7cm)	44.5° (7.4°)	95.9° (11.2°)	--- (168.9°)	-99.7° (20.7°)	-2.2° (7.3°)	-41.1° (8.0°)	-63.4° (7.3°)

It can be seen from Table 3 that the distance results are remarkably accurate based on 50 TWRs. The average values were at most a few centimeters away from the actual 2-meter distance, and the standard deviations for the distances marked in parentheses remained within a few centimeters for all studied antennas.

With the used software, it was not possible to set the offset for the angles to 0°, but it is possible to adjust it with a command if this software is not used or it can be manually calculated afterwards. Since the interest in the measurement was the angle accuracy when the physical angle of the double antenna UWB module was changed in 15-degree steps, it did not matter if the offset could not be set correctly in these results. The possible PDoA scale is ±180°, meaning that when the result exceeds +180°, the result moves to the negative side. This distorts some of the averages and standard deviations obtained, as the PDoA results vary between negative and positive values.

Table 3 shows the change in the PDoA results when the physical angle of the double antenna UWB module was changed. The average phase differences increased or decreased from around 30° to 60° when the physical angle was changed in 15-degree steps, depending on the antennas. The standard deviations for the PDoA were mostly within 10°, slightly more with the ceramic and PCB antennas. With the PCB antennas, the PDoA results increased in one step over 80°, so the results drifted to the edge of the PDoA scale ±180° and beyond.

Therefore, the PDoA values of the PCB antennas at angle -30° vary between negative and positive, messing up both the average and standard deviation. The same happened with almost all studied antennas when the physical angle was changed to ±60°, so those results were not useful for studying accuracy and were not recorded in Table 3. However, the obtained results showed that it was possible to measure the PDoA when the physical angle was ±60°, as the PDoA results were similar in each measurement. If the physical angle was set to ±75°, the antennas overlapped each other too much, which generated errors in the transmission and the results were not obtained accurately.

The angle of arrival had to be calculated manually from the obtained data using one of the equations (6), (8) or (9) presented earlier. Table 4 shows the calculated angles of arrival for all studied antennas on the UWB channel 5. The equation (9) and the average PDoA results obtained from Table 3 were used for the calculation. In addition, the offset has been added separately to the calculations, so that the zero angles of all studied antennas would be close to zero and thus simplify the comparison of the arrival angle results.

Table 4. The angles of arrival for all studied antennas on the UWB channel 5.

Antenna	**Angle 0°**	**Angle -15°**	**Angle -30°**	**Angle -45°**	**Angle 15°**	**Angle 30°**	**Angle 45°**
Orig1	1.4°	-14.3°	-28.6°	-49.4°	20.4°	33.9°	51.1°
Orig2	-0.5°	-15.7°	-29.7°	-50.0°	20.7°	33.9°	47.6°
Orig3	0.6°	-14.2°	-30.0°	-52.0°	20.1°	32.9°	49.6°
Cera1	-0.1°	-10.1°	-28.3°	-60.9°	7.4°	20.5°	43.4°
Cera2	0.5°	-11.8°	-27.8°	-59.8°	6.8°	20.9°	41.6°
Cera3	-0.8°	-10.6°	-27.9°	-60.5°	8.3°	21.0°	41.3°
Chip1	-0.1°	-24.7°	-35.4°	-48.7°	27.5°	39.1°	38.4°
Chip2	1.1°	-25.1°	-37.1°	-48.2°	29.0°	40.4°	40.0°
Chip3	0.2°	-24.0°	-37.8°	-48.1°	27.3°	39.4°	38.6°
FPC1	0.7°	-15.2°	-27.1°	-35.2°	17.6°	32.4°	53.1°
FPC2	-0.4°	-15.6°	-26.5°	-35.9°	18.8°	32.8°	52.4°
FPC3	1.8°	-16.1°	-26.5°	-34.1°	17.8°	34.8°	50.9°
PCB1	0.8°	-18.9°	---	50.4°	14.2°	25.7°	35.7°
PCB2	0.2°	-19.8°	---	52.2°	15.6°	26.6°	34.7°
PCB3	0.7°	-17.2°	---	48.6°	15.7°	28.2°	35.6°

From the results of the angles of arrival in Table 4, it can be observed that all studied antennas achieved the right kind of results when the physical angle of the double antenna UWB module was changed. Clearly the best results were obtained with the original double antenna, with which all the arrival angles differed from the actual angle by ±7 degrees at most. The results of the FPC antennas for the arrival angles were also quite accurate, except for the angle of -45°. The biggest exceptions were the PCB antennas with the angles of -30° and -45°, which produced incorrect results, as well as the chip antennas with angles of 30° and 45°, which produced the similar results on both angles.

However, the repeatability was reliable for the most of these angle measurements because similar results were obtained, deviating by a few degrees at most, except for a few cases. Although the arrival angles in Table 4 do not completely correspond to the real angles, their accuracy can possibly be improved, for example, by using antenna-specific look-up tables. Pre-measured results of the angles of arrival with different PDoA values could be stored in

these look-up tables. The values from the look-up table could then be compared to the obtained results and thus to determine the correct angles for the measurements.

To study the operation of the UWB modules on channel 9, the measurements were repeated keeping the other channel parameters the same as in the previous measurement. Table 5 shows the measurement results on the UWB channel 9 for all studied antennas and the distance and PDoA results obtained with the angles from 0° to ±45°. The measurements were repeated twice and in each measurement 50 TWRs were performed, from which the averages and standard deviations were calculated.

Table 5. Distances and PDoA results from 0° to ±45° obtained with the different antennas on the UWB channel 9. The value above is the average and below in parentheses is the standard deviation of 50 TWR results.

Antenna	**Distance**	**Angle -0°**	**Angle -15°**	**Angle -30°**	**Angle -45°**	**Angle 15°**	**Angle 30°**	**Angle 45°**
Orig1	2.0260m (2.3cm)	-1.4° (5.8°)	40.9° (9.3°)	77.1° (7.9°)	108.1° (8.9°)	-55.5° (9.7°)	-130.3° (8.1°)	163.1° (7.2°)
Orig2	2.0194m (2.2cm)	-0.4° (7.4°)	38.1° (8.3°)	76.6° (8.6°)	113.7° (6.8°)	-47.2° (9.3°)	-134.7° (6.0°)	162.7° (6.3°)
Cera1	2.0139m (2.5cm)	7.0° (6.3°)	30.7° (8.7°)	72.0° (8.7°)	157.6° (6.5°)	-21.4° (8.3°)	-66.1° (9.0°)	--- (134.8°)
Cera2	2.0192m (2.3cm)	5.4° (7.1°)	28.9° (6.3°)	77.3° (7.1°)	159.2° (6.2°)	-18.2° (6.3°)	-68.4° (8.7°)	--- (128.6°)
Chip1	2.0063m (2.1cm)	-122.8° (7.1°)	-81.5° (9.6°)	-85.1° (6.4°)	-153.2° (7.5°)	-21.8° (7.2°)	66.3° (10.5°)	136.0° (4.4°)
Chip2	2.0115m (2.2cm)	-129.5° (6.3°)	-72.5° (9.6°)	-84.8° (5.7°)	-150.3° (6.5°)	-20.5° (6.0°)	70.4° (8.6°)	133.9° (5.2°)
FPC1	1.9987m (6.2cm)	-73.4° (12.7°)	0.6° (19.0°)	139.6° (12.0°)	165.8° (9.1°)	-86.6° (8.8°)	26.4° (17.5°)	-2.8° (10.4°)
FPC2	2.0104m (4.8cm)	-84.4° (10.8°)	-10.1° (22.4°)	128.5° (8.5°)	163.3° (7.2°)	-87.7° (8.3°)	14.8° (12.6°)	-8.7° (8.9°)
PCB1	2.0272m (2.1cm)	6.0° (6.5°)	53.0° (5.3°)	96.3° (7.5°)	128.5° (7.1°)	-66.9° (6.7°)	-77.8° (6.4°)	-96.2° (7.4°)
PCB2	2.0181m (2.6cm)	6.2° (6.2°)	55.9° (6.2°)	93.7° (6.2°)	129.6° (7.1°)	-61.2° (7.4°)	-77.0° (7.1°)	-90.2° (7.0°)

From Table 5 it can be observed that the average distances were remarkably accurate, but the average PDoA results now varied significantly more than the previous results obtained on the UWB channel 5. The standard deviations of the PDoA results were mostly within 10°, except for the FPC antennas whose standard deviations of the PDoA were larger than with the other studied antennas. At the angle of -45°, the PDoA results of the ceramic antennas drifted to the edge of the measurement scale, so those PDoA results were not comparable. The PDoA results of the chip antennas for the different angles were strange: apparently the measurement scale was exceeded several times during the measurements, and thus, the only conclusion from these results is that they were repeatable. The same overextending of the measurement scale occurred when examining the FPC antennas.

Table 6 shows the calculated angles of arrival for all studied antennas on the UWB channel 9 with the physical angles from 0° to ±45°, using the equation (9) and the average PDoA

results obtained from Table 5. To facilitate the comparison, the offset has also been separately added to the calculations so that the zero angles of all studied antennas would be close to zero.

Table 6. The angles of arrival for all studied antennas on the UWB channel 9.

Antenna	Angle 0°	Angle -15°	Angle -30°	Angle -45°	Angle 15°	Angle 30°	Angle 45°
Orig1	0.4°	-13.1°	-25.4°	-36.9°	18.0°	46.4°	-65.0°
Orig2	0.1°	-12.2°	-25.2°	-39.2°	15.2°	48.4°	-64.7°
Cera1	-0.2°	-7.8°	-21.6°	-59.2°	8.8°	23.5°	---
Cera2	0.3°	-7.2°	-23.4°	-60.2°	7.8°	24.3°	---
Chip1	0.0°	-16.1°	-14.8°	15.3°	-36.0°	-64.6°	-92.1°
Chip2	3.0°	-19.2°	-14.9°	13.6°	-36.5°	-66.0°	-91.1°
FPC1	-0.9°	-25.2°	-75.9°	-92.1°	3.8°	-33.4°	-24.1°
FPC2	3.0°	-21.8°	-70.6°	-90.1°	4.2°	-29.7°	-22.2°
PCB1	0.1°	-15.1°	-30.3°	-43.6°	23.8°	27.6°	34.3°
PCB2	0.0°	-16.1°	-29.4°	-44.1°	21.9°	27.0°	32.1°

It can be seen from Table 6 that the results for the angles of arrival with almost all studied antennas on the UWB channel 9 were significantly less accurate than the previous results obtained on channel 5. The inaccuracies of the original double antenna also increased when positive angles were measured. The arrival angles of the FPC and chip antennas were the most distorted due to the peculiar PDoA results from which the arrival angles were calculated. The best results on channel 9 were obtained with the PCB antenna, although the results of the arrival angles were poor when the physical angle of the double antenna UWB module was turned to the positive direction.

As a summary, these measurements gave excellent results for the distances with all studied antennas on both UWB channels. The results remained similar with the high accuracy of a few centimeters when the measurements were repeated. However, the accuracies of the angles of arrival require further research. Based on the obtained results, it is difficult to conclude the true accuracy for the angles, especially on channel 9. On the UWB channel 5, reasonably good results were obtained for the arrival angles, with a few exceptions. From the results in Table 3 and Table 5, it can be observed that the average PDoA results were similar to each other when the measurements were repeated and the standard deviations for PDoA were mostly within 10 degrees. Thus, certainty can be obtained at least for the reliability and repeatability of the PDoA results. One of the problems with the PDoA results was also their drifting to the edge of the measurement scale at larger physical angles, so the obtained averages were not practical for calculating the arrival angles.

In retrospect, calculating the angles of arrival using the PDoA results was not necessarily the best option. Firstly, the PDoA results reported by the software has already been calculated from the obtained raw data and its calculation method is not exactly known, so there is no certainty whether it may contain possible errors. Secondly, in the equation (9) used to calculate the angles of arrival from the phase differences, it is assumed that $\lambda/2$ is the exactly same as the gap d between the two antennas. However, this is not always the case, because the gap d could vary slightly between different antennas, and it was also difficult to place two antennas on the antenna outputs in the UWB evaluation board at the same exact distance. Because of this, it would have been more reasonable to calculate the angles of arrival directly from the raw data using the equation (6), which could have produced better results than calculating from the PDoA results.

Unfortunately, the raw data that would contain the necessary values to use the equation (6) could not be saved directly from the used software, and new measurements for all antennas could no longer be performed for this thesis. Therefore, studying the angles of arrival in this regard requires further research and new measurements. Examining larger angles using a different calculation method is also possible, since the PDoA results were distorted for them. The angles of arrival also need to be investigated further on the UWB channel 9, as the results obtained were particularly inaccurate and strange. This may require collaboration with the manufacturer of the UWB modules, in addition to changing the calculating method for the angles of arrival, because the original double antenna also showed large errors in the angle results on channel 9. In addition, the possibility of using the look-up tables for the obtained results should also be studied, since those could further improve the accuracies of the angles of arrival and the reliability of the results.

The operation of the UWB modules with the different antennas at varied distances were studied to validate functionality in the LOS situations. The long-range measurement required that the original measuring platform was cut in the middle into two parts, and thus no new platform was needed. The measurements were started by calibrating all studied antennas when the UWB modules were two meters apart, and after that the distance was increased. The measurements also include the original double antenna from the manufacturer of the UWB modules, whose results can be used for the comparison.

Table 7. The results of the distance measurements at 2, 5, 10, 15 and 20 meters for all studied antennas on the UWB channels 5 and 9. The value above is the average and below in parentheses is the standard deviation of the distance from 50 TWRs.

Distance	**Original**	**Ceramic**	**Chip**	**FPC**	**PCB**
CHAN 5					
2m	1.9991m (3.9cm)	1.9941m (3.0cm)	2.0082m (3.0cm)	2.0215m (2.9cm)	2.0114m (2.3cm)
5m	5.0146m (3.0cm)	5.2013m (4.4cm)	5.0164m (2.7cm)	4.9919m (2.0cm)	4.9843m (3.4cm)
10m	10.0156m (2.9cm)	10.2090m (2.9cm)	10.0112m (3.5cm)	10.0343m (2.7cm)	10.0330m (2.9cm)
15m	15.0395m (3.3cm)	15.2686m (4.8cm)	15.0114m (4.6cm)	15.0538m (4.6cm)	15.0166m (2.8cm)
20m	20.0634m (3.8cm)	20.2874m (3.5cm)	20.0288m (3.7cm)	20.0316m (2.3cm)	20.0565m (3.3cm)
CHAN 9					
2m	2.0029m (3.8cm)	2.0163m (6.0cm)	2.0123m (4.8cm)	2.0380m (3.9cm)	2.0109m (3.5cm)
5m	5.0245m (4.0cm)	5.0751m (6.5cm)	4.9943m (4.3cm)	4.9662m (3.3cm)	4.9956m (2.7cm)
10m	10.0699m (2.7cm)	10.1424m (2.4cm)	10.0064m (4.5cm)	9.9495m (3.7cm)	10.0529m (3.3cm)
15m	15.0652m (2.6cm)	15.0730m (4.7cm)	15.0237m (3.3cm)	14.9037m (6.5cm)	15.0285m (2.4cm)
20m	20.0716m (2.0cm)	20.1484m (3.0cm)	20.1196m (5.6cm)	19.9131m (10.3cm)	20.0754m (5.0cm)

Table 7 shows the results at the distances of 2, 5, 10, 15 and 20 meters for all studied antennas on the UWB channels 5 and 9. It can be seen from the measurement results that all antennas can operate precisely up to a distance of at least 20 meters in the LOS situations without errors in the transmission. This distance is sufficient for the intended use in the project, but it must be noted, that the NLOS situations are actually more common. The standard deviations were mostly small, but slightly larger on the UWB channel 9 than on channel 5. Potentially, the results could also be improved if the calibration of the antennas was done at five or ten meters.

Since the results were excellent up to 20 meters, the maximum range was studied as well. The maximum distance measurement cannot be done indoors, so the only option was to perform the measurement outdoors. Due to the strong wind and light drizzle, the maximum-range measurement execution was difficult since the UWB modules must be connected to the laptops during the communication. The original and the chip antennas were used for the maximum-range study on the UWB channels 5 and 9 in the LOS situation. The original antenna reached the range of 71 meters where it was able to successfully perform TWR on channel 5. However, the Reed-Solomon decoding errors (RSE) and the Cyclic redundancy check errors (CRCE) started appearing after about 30 meters, and the communication between the modules was intermittent. A successful TWR achieved 25 meters with the original antenna on the UWB channel 9. This result indicates that the original antennas are optimized for the usage on the UWB channel 5. The chip antenna successfully achieved the range of 44 meters on channel 5, but the RSE and CRCE errors occurred after 25 meters and the communication was intermittent. The maximum range of 37 meters was achieved with the chip antenna when operating on channel 9. The same errors appeared in the transmission after 25 meters. However, considering the small size of the chip antennas, the maximum achieved range was a positive surprise.

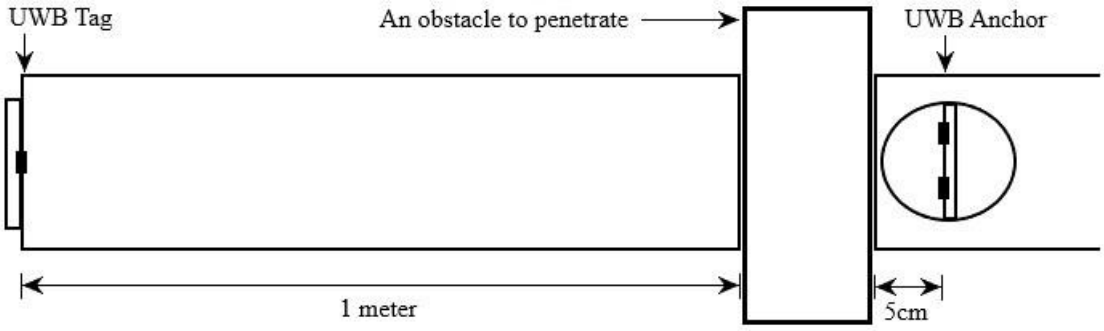

Figure 43. An illustration of the measurement setup used to study obstacle penetration.

Finally, a few measurements were performed with the original double antenna through various obstacles emulating the real operational NLOS environment. These measurements can be used to show how much the penetration of the different material obstacles affects the accuracy of the distance measurements. The measurements were performed so that the module acting as a tag was placed one meter away from the obstacle and the module acting as an anchor was placed approximately 5 centimeters away on the other side of the obstacle as shown in Figure 43. The distance without an obstacle was 1.05m and the thickness of the obstacle must be added to this value separately.

Table 8. Penetration ability and the effect of obstacles on the range accuracy performed twice with the original double antenna on the UWB channels 5 and 9. Above is the average distance and below in parentheses is the standard deviation from 50 TWRs.

	CHAN 5	**CHAN 5**	**CHAN 9**	**CHAN 9**
Without any obstacle	1.0581m (4.1cm)	1.0624m (4.5cm)	1.0458m (3.0cm)	1.0455m (2.8cm)
Concrete wall thickness 50cm	2.2071m (17.9cm)	2.1217m (11.2cm)	2.7596m (---)	Error (---)
Wooden door thickness 5cm	1.1242m (2.7cm)	1.1380m (3.3cm)	1.1205m (3.4cm)	1.1171m (2.8cm)
Steel door thickness 5cm	---	---	---	---
Glass window thickness 0.4cm	1.1113m (2.9cm)	1.1248m (3.5cm)	1.0841m (3.4cm)	1.0789m (3.4cm)
Chipboard wall thickness 13cm	1.1901m (4.2cm)	1.2001m (3.6cm)	1.2065m (3.0cm)	1.1959m (2.8cm)
Human thickness 30cm	1.4880m (12.7cm)	1.4787m (14.9cm)	1.5899m (23.7cm)	1.4969m (18.0cm)

The effects of a wooden door, a glass window and a normal chipboard wall were minimal to the distance accuracy on both UWB channels, which can be seen from the results in Table 8. However, the thin window glass distorted the distance by a few centimeters. The steel door signal did not pass through on either channel, but it was previously known that the UWB pulses penetrate through metal poorly. The signal penetrated a 50 cm thick concrete wall on the UWB channel 5, 50 TWRs were completed even though the communication between the UWB modules was intermittent due to the RSE and CRCE errors. However, the result was more than half a meter wrong, as the actual distance between the UWB modules was about 1.55m. On the UWB channel 9, after several errors in the transmission, a significantly less accurate result was obtained. In the second measurement on channel 9, 50 successful TWRs could not be performed, even though several attempts were made. Based on this result and the result of the maximum range, it seems that the original antennas are optimized for the UWB channel 5, which can partly explain the poorer penetration on channel 9. In addition, penetration directly through my chest, the thickness of which was estimated to be about 30 cm, was also examined. The averages of these results were more than 10cm from the actual distance between the UWB modules and the standard deviation was quite large. The individual TWR results varied by a few tens of centimeters during the measurement, slightly more on channel 9, but there were no errors in the transmission. The results show the effect of individual obstacles, and it can be concluded that the accuracy of the results deteriorates the more objects the signal must pass through.

However, looking at the overall results in this section, there is strong evidence that the UWB technology can accurately determine the distance, at least indoors in the LOS situations. All studied antennas achieved exceptionally accurate results up to 20 meters. However, in the NLOS situations, determining the distance accurately can be more challenging and possible cause errors in the transmission. It is important to study the operation of the UWB in a real environment, where there can be many people and other obstacles between the UWB devices. The angles of arrival also require further research, because based on the results obtained in the thesis, it is difficult to assess their true accuracy. However, this requires new measurements to be made so that the necessary data can be

collected and the angles can be calculated using a different calculation method. Unfortunately, there was no time left to perform new measurements for this thesis, but I am optimistic that the angles can be collected with the accuracy that the UWB module manufacturer has stated, and possibly by using the look-up tables their accuracy and reliability could be improved even further. Obtaining precise and correct angles is crucial in the project, so that UWB technology could be utilized for the desired use case to locate the user. As always, one must keep in mind that the UWB technology is still in development phase and improvements are possible – they just need to be discovered.

5 DISCUSSION

In this thesis, the implementation and utilization of current state-of-the-art UWB technology into a portable mPOS device was investigated and verified. The topic was first studied in theory, after which the use cases and the comparison of advantages and drawbacks with other technologies were introduced. This posed a challenge at the beginning of writing the thesis, because there were a lot of contradictions and differences between the sources, and it took time to ensure the correctness of the data. The standards and requirements from the regulatory bodies were clarified both regionally and globally to consider all the relevant regulations concerning the use of the UWB technology. The availability of UWB components on the market was examined and their selection was carried out for the thesis to ensure the actual implementation. Measurements were planned and implemented for the UWB chip standalone as well as for the UWB antennas separately, and finally the functionality of the components and technology in the entire UWB system was validated.

The UWB technology is a very strong candidate for real-time indoor positioning because the studied material shows that it is accurate and fast compared to other technologies. Several large technology companies have already UWB technology in their own products for this purpose. In addition to this, UWB technology consumes little power and offers high security, both of which are prominent features when implementing this technology to the handheld device functioning as a part of the payment system.

There are slightly different requirements for UWB technology that must be followed in different regions. On behalf of the regulatory bodies, in most areas UWB can operate on frequencies from 6 to 8.5 GHz without the need for mitigation techniques, i.e., on the UWB channels 5, 6, 8 and 9 defined in the IEEE 802.15.4 standard. The IEEE 802.15.4z is the current main standard for the UWB that improves the security and accuracy of the technology from previous versions, and on which current manufacturers of UWB components and devices rely on in their products. The IEEE 802.15.4z standard provides a comprehensive basis for the UWB technology, but it lacks an upper layer to perform device discovery and channel parameter selection and exchange, as well as standardized methods for AoA and PDoA techniques. It would be advisable to address these matters in the future IEEE 802.15.4ab standard, in addition to other improvements for the UWB technology. These standardizations could secure broad interoperability for UWB devices worldwide, just as Wi-Fi or USB are compatible regardless of device manufacturers.

Based on the studied materials, the biggest challenges at the moment are the possible compatibility problems between different device manufacturers and the possible interference of other technologies on the UWB operating frequencies. The FiRa consortium is an important committee for the development of UWB technology, and it strives to ensure compatibility through its own standards and certifications. At the time of writing, FiRa, Apple, and Omlox are the only ones that offer, in addition to the MAC and PHY layers, upper layers that allow UWB devices to connect (device discovery) and communicate (parameter exchange) with each other. This means that there must be support for one of these, to connect ready-made UWB devices. The UWB operates on top of licensed and unlicensed frequency bands, so it must be able to work at the background of other legacy technologies without interfering with them. The effects of strong Wi-Fi 6E transmission have been studied, and they have been shown to cause interference on the UWB channels operating in the 6 and 7 GHz range. This could not be verified with the help of measurements in the thesis, but according to the literature, if the interference occurs on the UWB channel 5, the UWB operation should be performed on the upper UWB channels to avoid the potential problem.

UWB components are available from several different manufacturers, and some were selected for the thesis based on the required characteristics. The comparison of UWB chips, however, was difficult because the datasheets of all manufacturers were not publicly available, and thus more detailed information about the characteristics of the UWB chips could not be obtained. This thesis focused on Murata's 2AB module which contains, in addition to the BLE chip, the Qorvo DW3000 family UWB chip.

The comparison of the UWB antennas was simpler because their datasheets were available on the manufacturer's website and the selections were easy to make based on this information. Since the antenna parameters reported by the manufacturers were similar to each other, it was decided to choose the antennas according to different manufacturing techniques.

The measurement arrangements were planned and implemented successfully, and all the desired measurements for the thesis were completed as intended. The design and construction of the measuring platforms for the measurements were also successful and they functioned as planned. The downside of the built prototype device to which the antennas were attached during the antenna measurements was that the openings in the metal frame were not completely ideally sized for all studied antennas due to differences between their modules and evaluation boards.

The UWB module measurements were used to investigate the effect of changing the channel parameters on the pulse burst, and their functionality was verified with the measurement results. At the same time, it was possible to demonstrate that the requirements of the IEEE 802.15.4z standard were met, both for the pulse shape in the time domain and for the power spectral density in the frequency domain.

With the measurements of the UWB antennas, the effects on the performance of the studied antennas were found out when they were implemented in the prototype device. Antenna parameter verifications were done to check the correctness of the manufacturer’s specifications and to investigate how other passive components of the device would load the antennas. As a summary, the results were quite good in terms of S11 parameters, gains and efficiencies, but the degradations when attached to the device were noticeable. However, the results for these were in line with small internal antennas from other technologies. In the radiation pattern measurements of all studied antennas, changes and degradations of the radiation power were noticeable when they were attached to the device. The degradation of the radiation power certainly shortens the maximum range, but hopefully there are no effects on the operation at shorter distances. It is possible to improve the radiation patterns and radiation power slightly by modifying the size of the opening in the metal frame of the device. The measurements showed that the distance of the antenna, especially to the metal frame, affected its performance, so this way the antenna can be tuned somewhat better.

Based on the measurement results of the UWB system, getting the distance indoors in the LOS situations was really accurate up to 20 meters with the studied antennas. The achieved range and accuracy for the UWB system is sufficient in the planned use, but the NLOS situations should be investigated further, because they are probably more likely in the real operating environment of the device. The measurements showed the effect of the penetration of different materials and obstacles on the accuracy of the ranging operation. It can be concluded that the penetrations of thick barriers and people increase the inaccuracy of the results. The metal door was a special case since the UWB pulses were not penetrated at all. On the other hand, penetrating through a normal thin wall, door and window had only a small effect on the accuracy of the distance. It would be interesting to study how many people, for example, would have to be in a row to stop the UWB signal from passing through.

The angles of arrival require further research and new measurements, as it is difficult to estimate their true accuracy from the results of this thesis. All studied antennas on the UWB channel 5 achieved appropriate results for the angles of arrival, but some of them also had large inaccuracies, which may be due to the equation with which they were calculated. The results for the angles of arrival were much more inaccurate on the UWB channel 9, and based on them, only the similarity of the results when repeated at different physical angles with all studied antennas can be concluded. By using a different calculation method to obtain the angle, new measurements must be performed to gather the necessary information for the calculation. Unfortunately, there was no time left to complete them for the thesis, but I believe that obtaining angles with reasonable accuracy is possible, as the manufacturer of the UWB modules has announced. By creating the look-up tables from the performed measurements and their results, potentially more reliable and accurate angles could be achieved. In the desired use case, obtaining accurate and correct angles is necessary to precisely locate the user.

The future looks promising for UWB technology because accurate real-time indoor positioning is necessary in many different applications, both for the needs of consumers and companies. Although UWB technology still has a few stumbling blocks in its development, it is on its way to its enhanced and perfected form. It is very likely that the usage of the UWB will increase in the future in all smart devices once common regulations and standards guarantee broad interoperability between the device manufacturers.

6 SUMMARY

The thesis studied the current situation of UWB technology, as well as its possible utilization and implementation in an mPOS device.

At first, the possibility of utilization and implementation in general was begun by studying the basics of UWB, as well as the benefits and potential challenges of the technology. With the help of the regulations, an understanding was gained of what must be taken into consideration regionally and globally when implementing UWB technology. Additional information about the utilization of UWB technology and its current state was obtained by studying the standards defined for it. The study revealed that in addition to the MAC and PHY layers of the IEEE 802.15.4z standard for the UWB, an upper layer is needed to enable UWB devices to exchange the necessary information for communication. Therefore, compliance with the FiRa's standard is mandatory at the time of writing, so that UWB communication can be created between two UWB devices. The main use cases intended for UWB technology were clarified and the differences were compared to other available technologies. Through this, it was possible to demonstrate the superiority of UWB technology in terms of accurate positioning and security.

Secondly, the possibility of utilization and implementation in the mPOS device was confirmed based on the collected information and consequently an understanding of the suitability of UWB technology for the project was obtained. The UWB was an excellent technology for the required use cases, and this was demonstrated in the thesis. The availability of the UWB components for implementation was achieved by comparing off-the-shelf components. Comparing the UWB chips from different manufacturers was challenging without datasheets, unlike the comparison of UWB antennas, for which datasheets were easily available from the manufacturers. The UWB components selected for the thesis were presented and the choices were justified.

Finally, measurements were performed for the UWB module, the UWB antennas and the entire UWB system. With the measurements of the UWB module, it was possible to ensure both the functionality of the modules and the fulfillment of the requirements for UWB pulses. The effects on the performance of the antennas when there are other technologies and passive elements around them were studied with the UWB antenna measurements. It was possible to verify the functionality of the antennas in the assembled prototype device to which the studied antennas were attached during the measurements. The operation of the entire UWB system was investigated to determine its performance and accuracy. The measurements confirmed excellent accuracy up to 20 meters for the distance results in the LOS situations with all studied antennas, which is a sufficient distance for the planned use. In the NLOS situations, the accuracy and maximum range are reduced, and these situations should be further studied in addition to the individual obstacle penetrations performed in this thesis.

New measurements of the angles of arrival should be performed to ensure their accuracy, as the obtained results did not provide enough information for the best possible accuracy. There was no time left to perform these new measurements for this thesis, so that it would have been possible to study the arrival angles using a different calculation method. However, I am certain that obtaining the angles with the accuracy stated by the UWB module manufacturer is possible, but it requires further research. Obtaining precise and correct angles is necessary so that UWB technology can be utilized in the desired use case to precisely locate the user.

7 REFERENCES

[1] Negookar F. (2005) Ultra-Wideband Communications: Fundamentals and Applications. Book Publisher: Pearson

[2] Pirch H-J. & Leong F. (2020) Introduction to Impulse Radio UWB Seamless Access Systems. URL: https://www.firaconsortium.org/sites/default/files/2020-10/introduction-to-impulse-radio-uwb-seamless-access-systems-102820.pdf

[3] Coppens D., De Pooter E., Shadid A., Lemey S. & Marshall C. (2022) An Overview of Ultra-WideBand (UWB) Standards (IEEE 802.15.4, FiRa, Apple): Interoperability Aspects and Future Research Directions. IEEE Article.

[4] Hauk A. (accessed on 2.8.2022) UWB "Key experience": How the iPhone becomes a car key. URL: https://www.nextpit.com/uwb-key-experience-iphone-car-key

[5] Viot M., Seegars J., Dwyer K., Connell C., Pittenger D., Schnaufer D., Bizalion A. & Mariani A. (2021) Qorvo Special Edition: Ultra-Wideband for dummies. A Wiley Brand.

[6] What is Ultra-Wide Band (UWB) Technology? (accessed on 17.6.2022) URL: https://www.everythingrf.com/community/what-is-ultra-wide-band-uwb-technology

[7] Al-Kadi R. & Zorn C. (2020) Ultra Wideband – How It Works and Its Web of Potential. Article at ATZ electronics worldwide, 03/2020.

[8] Singh M., Roeschlin M., Zalzala E., Leu P. & Čapkun S. (2021) Security Analysis of IEEE 802.15.4z/HRP UWB Time-of-Flight Distance Measurement. In 14th ACM Conference on Security and Privacy in Wireless and Mobile Networks (WiSec 21), June 28-July 2, Abu Dhabi, United Arab Emirates.

[9] Stocker M., Brunner H., Schuh M., Boano C.A. & Römer K. (2022) On the Performance of IEEE 802.15.4z-Compliant Ultra-Wideband Devices. Institute of Technical Informatics, Graz University of Technology, Austria.

[10] Brunner H., Stocker M., Schuh M., Schuß M., Boano C.A. & Römer K. (2022) Understanding and Mitigating the Impact of Wi-Fi 6E Interference on Ultra-Wideband Communications and Ranging.

[11] Niemelä V., Haapola J., Hämäläinen M. & Iinatti J. (2016) An Ultra Wideband Survey: Global Regulations and Impulse Radio Research Based on Standards. All the authors are with the Centre for Wireless Communications (CWC), University of Oulu, Oulu, Finland.

[12] Sharma P.S., Vijay S. & Shukla M. (2020) Ultra-Wideband Technology: Standards, Characteristics, Applications. Helix E-ISSN: 2319-5592; P-ISSN: 2277-3495.

[13] ETSI (2019) Short Range Devices (SRD) using Ultra Wide Band (UWB); Part 3: Worldwide UWB regulations between 3,1 and 10,6 GHz. ETSI TR 103 181-3 V2.1.1

[14] Japan: MIC has recently published updates for Ultra Wide Band and mmWave radar regulations (accessed on 4.8.2022) URL: https://www.cetecom.com/en/news/japan-mic-published-updates-for-ultra-wide-band-and-mmwave-radar/

[15] Wikipedia (accessed on 5.7.2022) Section: IEEE 802.15.3: High Rate WPAN https://en.wikipedia.org/wiki/IEEE_802.15#Task_Group_4:_Low_Rate_WPAN

[16] Wikipedia (accessed on 5.7.2020) IEEE 802.15.4 https://en.wikipedia.org/wiki/IEEE_802.15.4

[17] IEEE Standard for Low-Rate Wireless Networks Amendment 1: Enhanced Ultra Wideband (UWB) Physical Layers (PHYs) and Associated Ranging Techniques. IEEE Std 802.15.4z™-2020 (Amendment to IEEE Std 802.15.4™-2020)

[18] Omlox – an open standard for precise real-time indoor locating system (accessed on 7.7.2022) URL: https://omlox.com/home

[19] The Car Connectivity Consortium – Digital Key (accessed on 9.8.2022) URL: https://carconnectivity.org/

[20] Apple Nearby Interaction (accessed on 9.8.2022) URL: https://developer.apple.com/documentation/nearbyinteraction/

[21] IEEE 802.15 WSN™ Task Group 4ab (TG4ab) 802.15.4 UWB Next Generation (accessed on 17.8.2022) URL: https://www.ieee802.org/15/pub/TG4ab.html

[22] IEEE Standard for Low-Rate Wireless Networks. IEEE Std 802.15.4™-2020 (Revision of IEEE Std 802.15.4-2015)

[23] Alarafi A., Al-Salman A., Alsaleh M., Alnafessah A., Al-Hadhrami S., Al-Ammar M. A. & Al-Khalifa H. S. (2016) UltraWideband Indoor Positioning Technologies: Analysis and Recent Advances. Sensors 2016, 16, 707.

[24] FiRa Consortium (accessed on 9.8.2022) URL: https://www.firaconsortium.org/

[25] UWB Alliance (accessed on 10.8.2022) URL: https://uwballiance.org/

[26] Litepoint (accessed on 15.8.2022) URLs: https://www.litepoint.com/knowledgebase/fira-consortium-ultra-wideband-uwb-phy-conformance-test-solution-with-iqgig-uwb-and-iqfact/ & https://www.litepoint.com/blog/uwb-certification-why-it-matters-and-how-its-tested-2/

[27] Koepp J. & Serdar N. (accessed on 22.9.2022) UWB Reloaded: Test and Certification of UWB devices according to IEEE802.15.4z. URL: https://www.microwavejournal.com/articles/36765-uwb-reloaded-test-and-certification-of-uwb-devices-according-to-ieee802154z?page=2

[28] Keum J. & Bansal A. (accessed on 11.7.2022) FiRa Consortium Releases Common Service & Management Layer and Physical Access Control System Specifications v1.0 URL: https://research.samsung.com/blog/FiRa-Consortium-Releases-Common-Service-Management-Layer-and-Physical-Access-Control-System-Specifications-v1-0

[29] Ultra-Wideband (UWB) Here's everything you need to know. (accessed on 21.6.2022) Internet article URL: https://bleesk.com/uwb.html

[30] Insight Partners (accessed on 24.8.2022) UWB Chipsets Market. URL: https://www.globenewswire.com/en/news-release/2022/02/11/2383657/0/en/Ultra-Wideband-Chipset-Market-Size-Worth-1-906-46-Mn-Globally-by-2028-at-21-1-CAGR-Exclusive-Report-by-The-Insight-Partners.html

[31] Data Bridge Market Research (accessed on 24.8.2022) Global UWB Market – Industry Trends and Forecast to 2029. URL: https://www.databridgemarketresearch.com/reports/global-ultra-wideband-uwb-market

[32] Markets and Markets (accessed on 24.8.2022) UWB Market by Application – Global Forecast to 2025. URL: https://www.marketsandmarkets.com/Market-Reports/ultra-wideband-market-200905786.html

[33] Market Research Future (accessed on 4.11.2022) Ultra-Wideband Market. URL: https://www.marketresearchfuture.com/reports/ultra-wideband-market-2367

[34] Zanella G. (accessed on 24.8.2022) Global UWB Market Shipment to Reach 317 Million Units in 2022. Article in EE Times Asia. URL: https://www.eetasia.com/global-uwb-market-shipment-to-reach-317-million-units-in-2022/

[35] Qorvo (accessed on 8.7.2022) Ultra-Wideband URL: https://www.qorvo.com/innovation/ultra-wideband

[36] Techtarget (accessed on 26.7.2022) mPOS (mobile point of sale). URL: https://www.techtarget.com/searchcio/definition/mPOS-mobile-point-of-sale

[37] Monei (accessed on 26.7.2022) Mobile POS Systems (mPOS): A Comprehensive Guide. URL: https://monei.com/blog/mobile-pos-system-mpos/

[38] Apple press release (accessed on 22.6.2022) Apple introduces AirTag. URL: https://www.apple.com/newsroom/2021/04/apple-introduces-airtag/

[39] Samsung news (accessed on 22.6.2022) Introducing the New Galaxy SmartTag+: The Smart Way to Find Lost Items. URL: https://news.samsung.com/us/introducing-the-new-galaxy-smarttag-plus/

[40] Tiemann J., Friedrich J. & Wietfeld C (2022) Experimental Evaluation of IEEE 802.15.4z UWB Ranging Performance under Interference. Sensors 2022, 22, 1643. URL: https://doi.org/10.3390/s22041643

[41] Balaban D. (accessed on 25.7.2022) Faster and More Accurate than Bluetooth and Wi-Fi, Can Ultra-Wideband Deliver on Promise of Hands-Free Ticketing? Article at Mobily Payments. URL: https://www.mobility-payments.com/2022/01/17/faster-and-more-accurate-than-bluetooth-and-wi-fi-can-ultra-wideband-deliver-on-the-promise-of-hands-free-ticketing/

[42] NXP Semiconductors news (accessed on 25.7.2022) NXP Collaborates with ING and Samsung to Pilot Industry's First UWB-Based Peer-to-Peer Payment Application. URL: https://www.nxp.com/company/about-nxp/nxp-collaborates-with-ing-and-samsung-to-pilot-industrys-first-uwb-based-peer-to-peer-payment-application:NW-NXP-COLLABORATES-WITH-ING-AND-SAMSUNG-TO

[43] Wikipedia (accessed on 20.7.2022) EMV. URL: https://en.wikipedia.org/wiki/EMV

[44] EMVCo Annual Report 2020 (accessed on 20.7.2022) URL: https://www.emvco.com/wp-content/uploads/documents/EMVCo-Annual-Report-2020.pdf

[45] Philips T (accessed on 20.7.2022) EMVCo reveals plans to extend specifications and testing programmes. Article at NFCW. URL: https://www.nfcw.com/whats-new-in-payments/emvco-reveals-plans-to-extend-specifications-and-testing-programmes/

[46] Conway A. (accessed on 2.8.2022) Developers can now implement Ultra-Wideband (UWB) support in apps with Android Jetpack. Article at XDA. URL: https://www.xda-developers.com/developers-ultra-wideband-uwb-android-jetpack/

[47] Developers Android (accessed on 2.8.2022) Core Ultra Wideband (UWB). URL: https://developer.android.com/jetpack/androidx/releases/core-uwb

[48] Qorvo DWM3000 Datasheet (accessed on 13.6.2022) URL: https://www.qorvo.com/products/p/DWM3000

[49] Qorvo (accessed on 14.6.2022) Qorvo® Delivers Ultra-Wideband in Google® Pixel 6 Pro. Article at Microwave Journal. URL: https://www.microwavejournal.com/articles/37369-qorvo-delivers-ultra-wideband-in-google-pixel-6-pro

[50] NXP Products (accessed on 15.6.2022) Secure Ultra-Wideband (UWB) Trimension Products. URL: https://www.nxp.com/products/wireless/secure-ultra-wideband-uwb:UWB-TRIMENSION

[51] Imec press release (accessed on 16.6.2022) Imec Showcases World's First Sub-5mW, IEEE 802.15.4z Ultra-Wideband Transmitter Chip. URL: https://www.imec-int.com/en/press/imec-showcases-worlds-first-sub-5mw-ieee-802154z-ultra-wideband-transmitter-chip

[52] Murata Type 2AB UWB Modules (accessed on 15.6.2022) URL: https://www.murata.com/en-us/products/connectivitymodule/ultra-wide-band/qorvo

[53] Zhang Y. & Duan L. (2020) Towards Elderly Care: A Phase-Difference-of-Arrival Assisted Ultra-Wideband Positioning Method in Smart Home. IEEE Access, Vol 8, 2020.

[54] Matin M.A. (2012) Ultra-Wideband RF Transceiver. Chapter 1, 7. UWB Antennas.

[55] Huang Y., Loh T. H., Foged L. J., Lu Y., Boyes S. & Chattha H. (2010) Broadband antenna measurement comparison. URL: https://www.researchgate.net/publication/224153997_Broadband_antenna_measurement_comparisons

[56] Antenna Theory (accessed on 5.9.2022) URL: https://www.antenna-theory.com/

[57] Satimo Starlab 18 Datasheet (2010) URL: https://www.pro-mac.sg/assets/files/Product-sheet_StarLab_2010.pdf

[58] Cisco (accessed on 15.9.2022) Antenna Patterns and Their Meaning. URL: https://www.industrialnetworking.com/pdf/Antenna-Patterns.pdf